Superscaling predictions for NC and CC Quasi-elastic Neutrino-Nucleus Scattering

Jose Enrique Amaro

Departamento de FÍSICA ATÓMICA, MOLECULAR Y NUCLEAR

ugr Universidad de Granada

NuFact 10

Overview - SuSA

- General formalism for neutrino scattering
- The Relativistic Fermi Gas (RFG)
- Super-Scaling Analysis (SuSA)
- The semi-relativistic shell model (SRSM)
- The relativistic mean field (RMF)
- Neutrino excitation of the Δ peak
- Neutral Current neutrino reactions
- SuSA predictions for the MiniBooNE QE cross section

1 General formalism

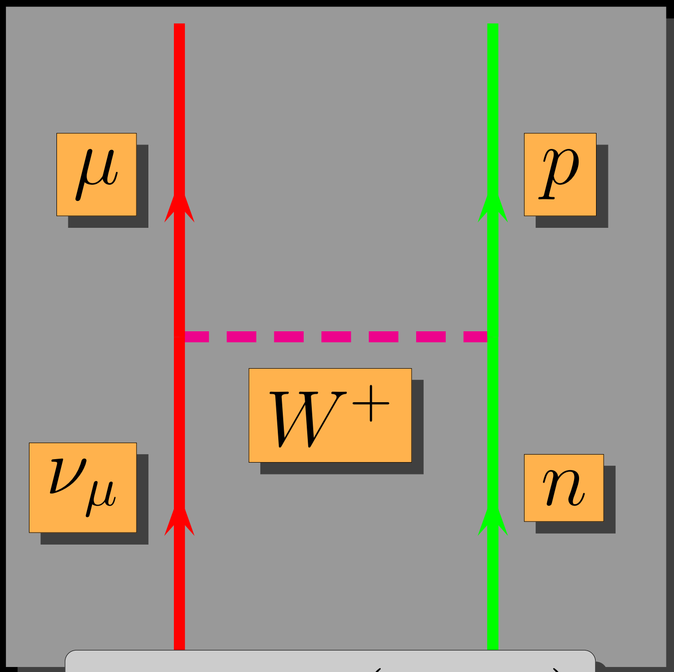

CC QE (ν_l, l^-)

1 General formalism

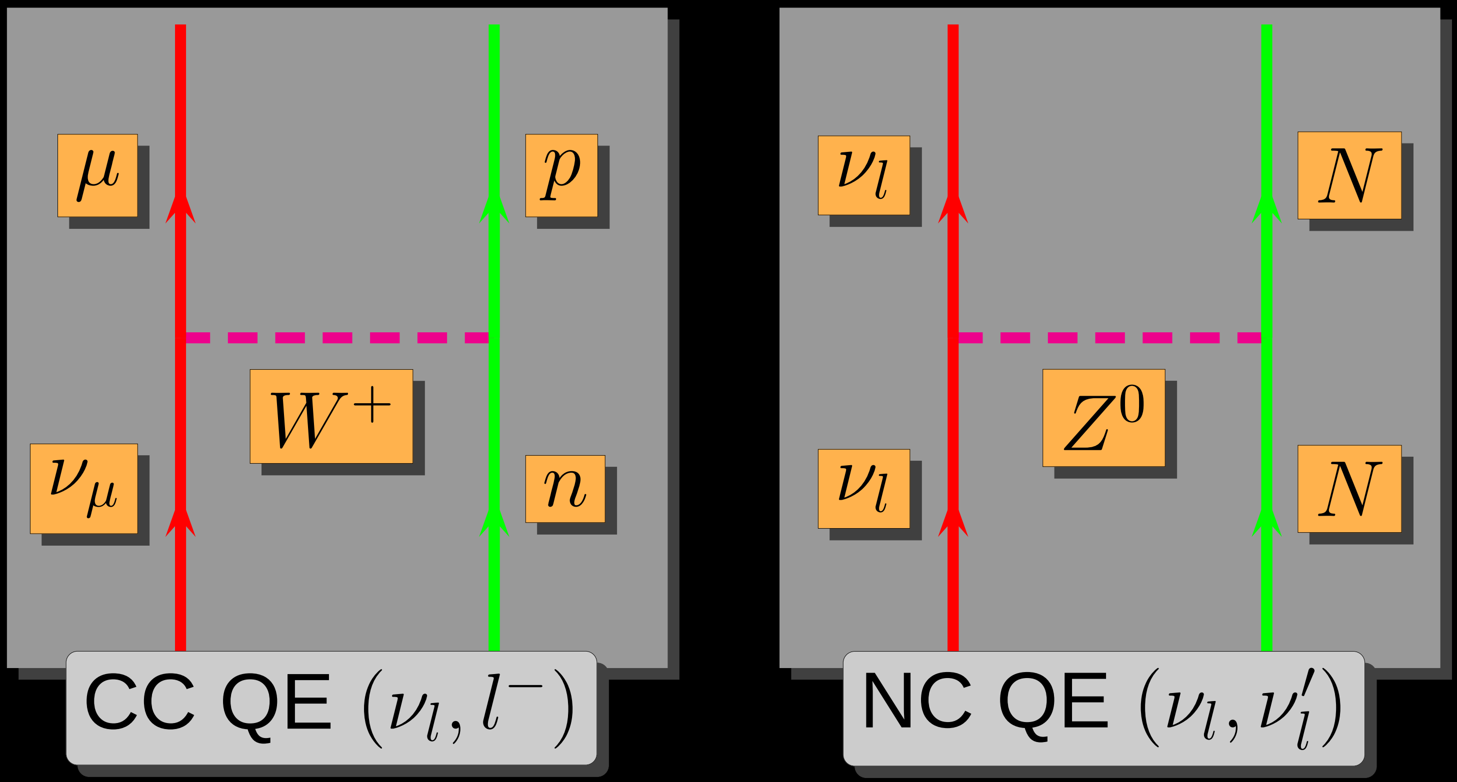

Kinematics

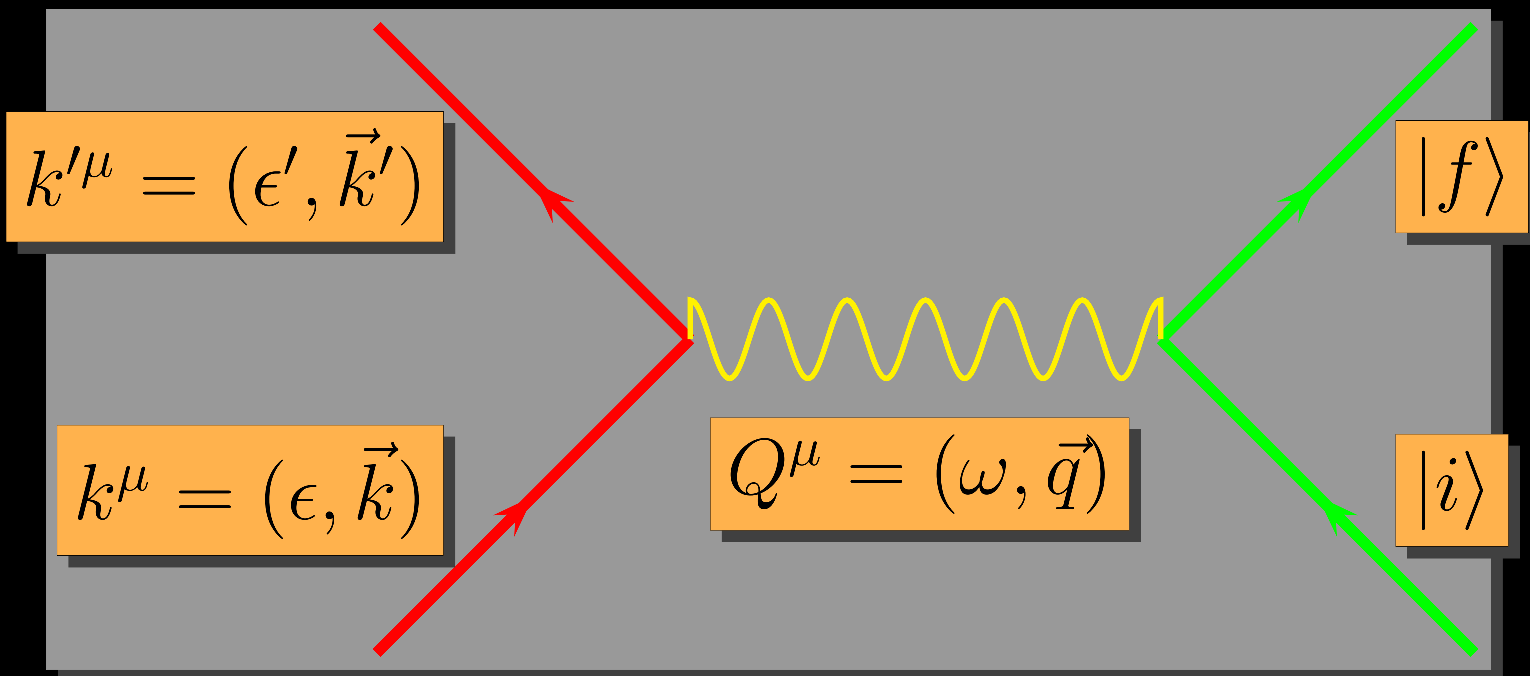

$$Q^2 = \omega^2 - q^2 < 0$$

Adimensional variables

$$\lambda = \frac{\omega}{2m_N} \qquad \kappa = \frac{q}{2m_N} \qquad \tau = \kappa^2 - \lambda^2$$

Example: CC neutrino reaction

$$\nu + A \rightarrow l^- + B$$

Effective Hamiltonian

$$\mathcal{H}_{eff} = \frac{G\cos\theta_c}{\sqrt{2}} j^\mu(x)\hat{J}_\mu(x)$$

Couplig constant: $G = 1.1664 \times 10^{-5}\mathrm{GeV}^{-2}$
Cabibbo angle: $\theta_c = 0.974$
Leptonic current ($\nu \rightarrow l$): $j^\mu = \overline{u}_l(\mathbf{k}')\gamma^\mu(1-\gamma_5)u_\nu(\mathbf{k})$
Hadronic current (single nucleon $n \rightarrow p$) is of the form $V - A$

$$\hat{J}_\mu = \overline{u}_p(\mathbf{p}')\left[F_1(Q^2)\gamma_\mu + F_2(Q^2)i\sigma_{\mu\nu}\frac{Q^\nu}{2m_N} - G_A(Q^2)\gamma_\mu\gamma_5 - G_P(Q^2)\frac{Q_\mu}{2m_N}\gamma_5\right]u_n(\mathbf{p})$$

Momentum transfer $Q^\mu = K^\mu - K'^\mu = P'^\mu - P^\mu$

Axial form factor $G_A = \dfrac{g_A}{1 - Q^2/M_A^2}$

$g_A = 1.26$, $M_A = 1032$ MeV

Example: S-matrix element

Neutrino scattering with initial and final hadronic states $|i\rangle \to |f\rangle$
Transition matrix element to first order in the interaction

$$S_{fi} = -i \int d^4 \, \langle l, f | \mathcal{H}_{eff}(x) | \nu_l, i \rangle = \boxed{-2\pi i \delta(E_f - E_i - \omega) \frac{G \cos\theta_c}{\sqrt{2}} l^\mu J_\mu}$$

Lepton current matrix element

$$l^\mu = \left[\frac{m'}{V\epsilon'} \frac{m}{V\epsilon} \right]^{1/2} \overline{u}_l(\mathbf{k}') \gamma^\mu (1 - \gamma_5) u_\nu(\mathbf{k})$$

Hadronic current matrix element

$$J_\mu = \langle f | \hat{J}_\mu(\mathbf{q}) | i \rangle$$

Example: cross Section

Inclusive: only the final lepton is detected

$$d\sigma = \frac{\overline{\sum}|S_{fi}|^2}{T}\frac{V}{v_{rel}}\frac{V d^3k'}{(2\pi)^3}$$

Performing the lepton traces

$$\frac{d\sigma}{d\Omega' d\epsilon'} = \frac{G^2\cos^2\theta_c}{4\pi^2}\frac{k'}{\epsilon}(s_{\mu\nu} + i a_{\mu\nu}) W^{\mu\nu}$$

Hadronic tensor

$$W^{\mu\nu} = \overline{\sum_{fi}}\delta(E_f - E_i - \omega)\langle f|J^\mu(\mathbf{q})|i\rangle^*\langle f|J^\nu(\mathbf{q})|i\rangle$$

Leptonic tensors

$$\begin{aligned} s^{\mu\nu} &= 2P^\mu P^\nu - \frac{1}{2}Q^\mu Q^\nu + \frac{Q^2 - m'^2}{2}g^{\mu\nu} \\ a^{\mu\nu} &= \epsilon^{\mu\nu\alpha\beta}Q_\alpha P_\beta \end{aligned}$$

$$P^\mu = \frac{K^\mu + K'^\mu}{2}$$
$$Q^\mu = K^\mu - K'^\mu$$

(ν_l, l^-) *formalism*

Cross section:

$$\frac{d\sigma}{d\Omega' d\epsilon'} = \sigma_0 \mathcal{F}_+^2$$

Similar to $\sigma_{\rm Mott}$:

$$\sigma_0 = \frac{G^2 \cos^2\theta_c}{2\pi^2} k'\epsilon' \cos^2\frac{\tilde{\theta}}{2}$$

Fermi constant:

$$G = 1.166 \times 10^{-11} \quad {\rm MeV}^{-2}$$

Cabibbo angle:

$$\cos\theta_c = 0.975$$

Generalized scattering angle:

$$\tan^2\frac{\tilde{\theta}}{2} = \frac{|Q^2|}{(\epsilon+\epsilon')^2 - q^2}$$

(ν_l, l^-) formalism (II)

Nuclear structure information:

$$\mathcal{F}_+^2 = \widehat{V}_{CC} R_{CC} + 2\widehat{V}_{CL} R_{CL} + \widehat{V}_{LL} R_{LL} + \widehat{V}_T R_T + 2\widehat{V}_{T'} R_{T'}$$

(ν_l, l^-) formalism (II)

Nuclear structure information:

$$\mathcal{F}_+^2 = \widehat{V}_{CC} R_{CC} + 2\widehat{V}_{CL} R_{CL} + \widehat{V}_{LL} R_{LL} + \widehat{V}_T R_T + 2\widehat{V}_{T'} R_{T'}$$

kinematical factors $\widehat{V}_K$ from the leptonic tensor

$$\begin{aligned}
\widehat{V}_{CC} &= 1 - \delta^2 \tan^2 \frac{\tilde{\theta}}{2} \\
\widehat{V}_{CL} &= \frac{\omega}{q} + \frac{\delta^2}{\rho'} \tan^2 \frac{\tilde{\theta}}{2} \\
\widehat{V}_{LL} &= \frac{\omega^2}{q^2} + \left(1 + \frac{2\omega}{q\rho'} + \rho\delta^2\right) \delta^2 \tan^2 \frac{\tilde{\theta}}{2} \\
\widehat{V}_{T} &= \tan^2 \frac{\tilde{\theta}}{2} + \frac{\rho}{2} - \frac{\delta^2}{\rho'} \left(\frac{\omega}{q} + \frac{1}{2}\rho\rho'\delta^2\right) \tan^2 \frac{\tilde{\theta}}{2} \\
\widehat{V}_{T'} &= \frac{1}{\rho'} \left(1 - \frac{\omega\rho'}{q}\delta^2\right) \tan^2 \frac{\tilde{\theta}}{2}
\end{aligned}$$

(ν_l, l^-) formalism (II)

Nuclear structure information:

$$\mathcal{F}_+^2 = \widehat{V}_{CC} R_{CC} + 2\widehat{V}_{CL} R_{CL} + \widehat{V}_{LL} R_{LL} + \widehat{V}_T R_T + 2\widehat{V}_{T'} R_{T'}$$

kinematical factors $\widehat{V}_K$ from the leptonic tensor

$$\begin{aligned}
\widehat{V}_{CC} &= 1 - \delta^2 \tan^2 \frac{\tilde{\theta}}{2} \\
\widehat{V}_{CL} &= \frac{\omega}{q} + \frac{\delta^2}{\rho'} \tan^2 \frac{\tilde{\theta}}{2} \\
\widehat{V}_{LL} &= \frac{\omega^2}{q^2} + \left(1 + \frac{2\omega}{q\rho'} + \rho\delta^2\right) \delta^2 \tan^2 \frac{\tilde{\theta}}{2} \\
\widehat{V}_T &= \tan^2 \frac{\tilde{\theta}}{2} + \frac{\rho}{2} - \frac{\delta^2}{\rho'} \left(\frac{\omega}{q} + \frac{1}{2}\rho\rho'\delta^2\right) \tan^2 \frac{\tilde{\theta}}{2} \\
\widehat{V}_{T'} &= \frac{1}{\rho'} \left(1 - \frac{\omega\rho'}{q}\delta^2\right) \tan^2 \frac{\tilde{\theta}}{2}
\end{aligned}$$

Adimensional variables:

$$\begin{aligned}
\delta &= \frac{m'}{\sqrt{|Q^2|}} \\
\rho &= \frac{|Q^2|}{q^2} \\
\rho' &= \frac{q}{\epsilon + \epsilon'} .
\end{aligned}$$

The only dependence on the muon mass m' is in δ

(ν_l, l^-) formalism (III)

Weak response functions

$$
\begin{aligned}
R_{CC} &= W^{00} \\
R_{CL} &= -\frac{1}{2}\left(W^{03} + W^{30}\right) \\
R_{LL} &= W^{33} \\
R_T &= W^{11} + W^{22} \\
R_{T'} &= -\frac{i}{2}\left(W^{12} - W^{21}\right)
\end{aligned}
$$

NuFact 10

(ν_l, l^-) formalism (III)

Weak response functions

$$
\begin{aligned}
R_{CC} &= W^{00} \\
R_{CL} &= -\frac{1}{2}\left(W^{03}+W^{30}\right) \\
R_{LL} &= W^{33} \\
R_{T} &= W^{11}+W^{22} \\
R_{T'} &= -\frac{i}{2}\left(W^{12}-W^{21}\right)
\end{aligned}
$$

Weak CC hadronic tensor:

$$W^{\mu\nu}(q,\omega) = \overline{\sum_{fi}}\delta(E_f - E_i - \omega)\langle f|J^\mu(Q)|i\rangle^*\langle f|J^\nu(Q)|i\rangle \ .$$

(ν_l, l^-) formalism (III)

Weak response functions

$$
\begin{aligned}
R_{CC} &= W^{00} \\
R_{CL} &= -\frac{1}{2}\left(W^{03} + W^{30}\right) \\
R_{LL} &= W^{33} \\
R_T &= W^{11} + W^{22} \\
R_{T'} &= -\frac{i}{2}\left(W^{12} - W^{21}\right)
\end{aligned}
$$

Weak CC hadronic tensor:

$$
W^{\mu\nu}(q,\omega) = \overline{\sum_{fi}} \delta(E_f - E_i - \omega)\langle f|J^\mu(Q)|i\rangle^* \langle f|J^\nu(Q)|i\rangle \ .
$$

$J^\mu(Q)$: the hadronic CC current operator

Nuclear Weak responses

Expand into vector and axial-vector contributions

$$R_{CC} = R_{CC}^{VV} + R_{CC}^{AA} \qquad R_{CL} = R_{CL}^{VV} + R_{CL}^{AA}$$
$$R_{LL} = R_{LL}^{VV} + R_{LL}^{AA}$$
$$R_{T} = R_{T}^{VV} + R_{T}^{AA} \qquad R_{T'} = R_{T'}^{VA}$$

$$R_{CL}^{VV} = -\frac{\omega}{q} R_{CC}^{VV} \qquad R_{LL}^{VV} = \frac{\omega^2}{q^2} R_{CC}^{VV}$$

Conserved vector current

$$\widehat{V}_{CC} R_{CC}^{VV} + 2\widehat{V}_{CL} R_{CL}^{VV} + \widehat{V}_{LL} R_{LL}^{VV} = \widehat{V}_L R_L^{VV} \equiv X_L^{VV}$$

traditional longitudinal contribution

$$\widehat{V}_{CC} R_{CC}^{AA} + 2\widehat{V}_{CL} R_{CL}^{AA} + \widehat{V}_{LL} R_{LL}^{AA} \equiv X_{C/L}^{AA}$$

Collapse does not occur for the AA terms.

$$\widehat{V}_T \left[R_T^{VV} + R_T^{AA} \right] \equiv X_T$$

Transverse components

$$2\widehat{V}_{T'} R_{T'}^{VA} \equiv X_{T'}$$

V/A interference term

Full response: $\mathcal{F}_{\pm}^2 = X_L^{VV} + X_{C/L}^{AA} + X_T \pm X_{T'}$

2 The relativistic Fermi gas (RFG)

Nuclear response functions for (ν_μ, μ^-) reactions

$$R_K = N\Lambda_0 U_K f_{RFG}(\psi), \quad K = CC, CL, LL, T, T',$$

- N is the neutron number,
- $\Lambda_0 = \frac{\xi_F}{m_N \eta_F^3 \kappa}, \quad \eta_F = k_F/m_N, \quad \xi_F = \sqrt{1+\eta_F^2} - 1.$
- Scaling function $f_{RFG}(\psi) = \frac{3}{4}(1-\psi^2)\theta(1-\psi^2)$
- Scaling variable

$$\psi = \frac{1}{\sqrt{\xi_F}} \frac{\lambda - \tau}{\sqrt{(1+\lambda)\tau + \kappa\sqrt{\tau(1+\tau)}}}$$

- single-nucleon responses U_K

Single-nucleon responses, $K = CC$

$$U_{CC} = U^V_{CC} + \left(U^A_{CC}\right)_{\text{c.}} + \left(U^A_{CC}\right)_{\text{n.c.}}$$

$$U^V_{CC} = \frac{\kappa^2}{\tau}\left[(2G^V_E)^2 + \frac{(2G^V_E)^2 + \tau(2G^V_M)^2}{1+\tau}\Delta\right] ,$$

$$\Delta = \frac{\tau}{\kappa^2}\xi_F(1-\psi^2)\left[\kappa\sqrt{1+\frac{1}{\tau}} + \frac{\xi_F}{3}(1-\psi^2)\right]$$

The axial-vector response is the sum of conserved (c.) plus non conserved (n.c.) parts,

$$\left(U^A_{CC}\right)_{\text{c.}} = \frac{\kappa^2}{\tau}G_A^2\Delta \;\;,\;\; \left(U^A_{CC}\right)_{\text{n.c.}} = \frac{\lambda^2}{\tau}{G'_A}^2.$$

NuFact 10

Single-nucleon responses, $K = CL, LL$

$$U_{CL} = U^V_{CL} + \left(U^A_{CL}\right)_{\rm c.} + \left(U^A_{CL}\right)_{\rm n.c.}$$
$$U_{LL} = U^V_{LL} + \left(U^A_{LL}\right)_{\rm c.} + \left(U^A_{LL}\right)_{\rm n.c.} \ ,$$

The vector and conserved axial-vector parts are determined by current conservation

$$U^V_{CL} = -\frac{\lambda}{\kappa} U^V_{CC} \qquad \left(U^A_{CL}\right)_{\rm c.} = -\frac{\lambda}{\kappa}\left(U^A_{CC}\right)_{\rm c.}$$
$$U^V_{LL} = \frac{\lambda^2}{\kappa^2} U^V_{CC} \qquad \left(U^A_{LL}\right)_{\rm c.} = \frac{\lambda^2}{\kappa^2}\left(U^A_{CC}\right)_{\rm c.} \ ,$$

Non-conserved n.c. parts:

$$\left(U^A_{CL}\right)_{\rm n.c.} = -\frac{\lambda\kappa}{\tau} {G'_A}^2 \ , \quad \left(U^A_{LL}\right)_{\rm n.c.} = \frac{\kappa^2}{\tau} {G'_A}^2 \ .$$

Single-nucleon responses, $K = T, T'$

$$
\begin{aligned}
U_T &= U_T^V + U_T^A \\
U_T^V &= 2\tau(2G_M^V)^2 + \frac{(2G_E^V)^2 + \tau(2G_M^V)^2}{1+\tau}\Delta \\
U_T^A &= 2(1+\tau)G_A^2 + G_A^2\Delta \\
U_{T'} &= 2G_A(2G_M^V)\sqrt{\tau(1+\tau)}[1+\tilde{\Delta}]
\end{aligned}
$$

with

$$
\tilde{\Delta} = \sqrt{\frac{\tau}{1+\tau}}\frac{\xi_F(1-\psi^2)}{2\kappa} .
$$

3 Super-Scaling Analysis (SuSA)

Scaling in the RFG (Relativistic Fermi gas)

$$R_K = G_K f_{RFG}(\psi)$$

Functions G_K from the RFG for electrons ($K = L, T$) and neutrinos $K = CC, CL, LL, T, T'$.

Scaling function in the RFG

$$f_{RFG}(\psi) = \frac{3}{4}(1-\psi^2)\theta(1-\psi^2)$$

Scaling variable:

$$\psi = \frac{1}{\sqrt{\xi_F}} \frac{\lambda - \tau}{\sqrt{(1+\lambda)\tau + \kappa\sqrt{\tau(1+\tau)}}}$$

Experimental scaling function from (e, e')

$$f(\psi') = \frac{\left(\frac{d\sigma}{d\Omega' d\epsilon'}\right)_{exp}}{\sigma_{Mott}(v_L G_L + v_T G_T)}$$

shifted $\longrightarrow \psi' = \frac{1}{\sqrt{\xi_F}} \frac{\lambda' - \tau'}{\sqrt{(1+\lambda')\tau' + \kappa\sqrt{\tau'(1+\tau')}}}$

$$\lambda' = (\omega - E_s)/2m_N, \quad \tau' = \kappa^2 - \lambda'^2$$

k_F y E_s are fitted to the data

$f_L = \frac{R_L}{G_L}$ Longitudinal $\qquad f_T = \frac{R_T}{G_T}$ Transverse

NuFact 10

Superscaling

- Plot the experimental $f(\psi')$ versus ψ' for different kinematics and nuclei
- Fit E_s and k_F to get scaling (one universal scaling function)

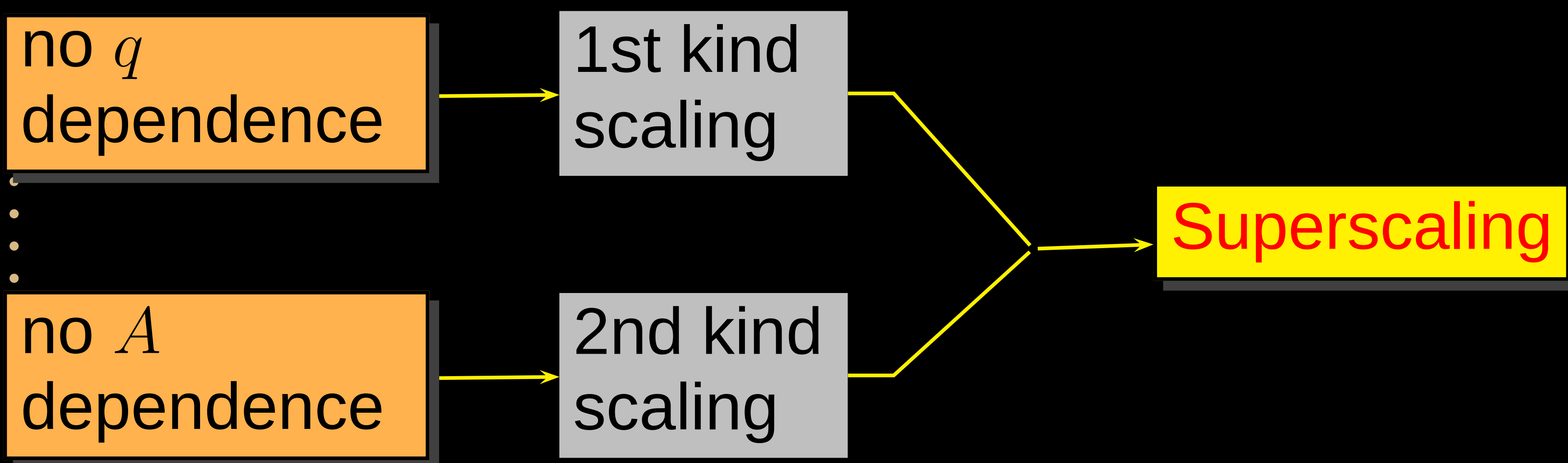

Scaling in the QE peak

Summary of past work by Donnelly & Sick PRC 60 (1999)

T. W. DONNELLY AND INGO SICK — PHYSICAL REVIEW C **60** 065502

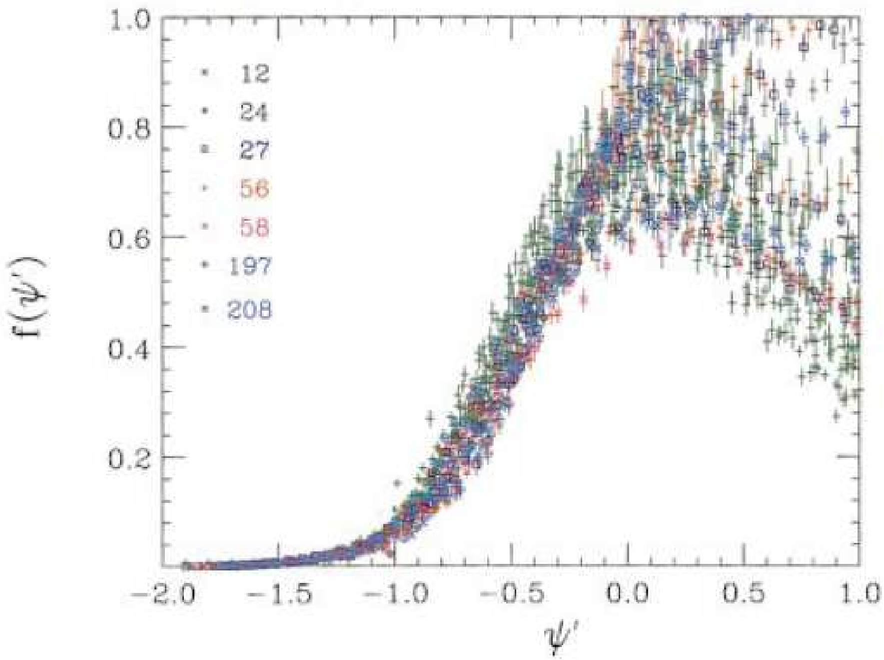

FIG. 2. (Color) Scaling function $f(\psi')$ as function of ψ' for all nuclei $A \geq 12$ and all kinematics. The values of A corresponding to different symbols are shown in the inset.

Scaling in the QE peak

Summary of past work by Donnelly & Sick PRC 60 (1999)

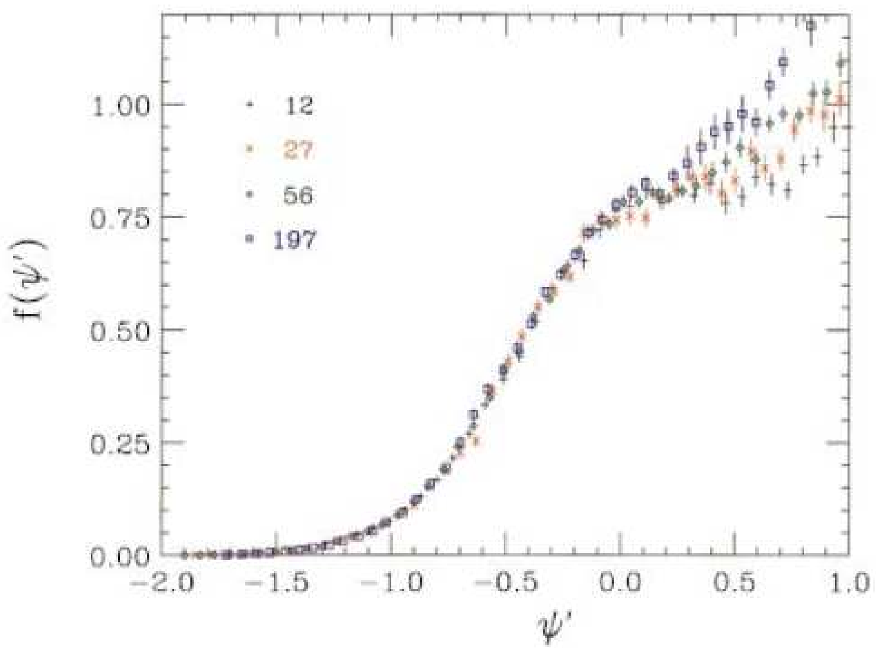

FIG. 3. (Color) Scaling function for C, Al, Fe, and Au and fixed kinematics ($q \approx 1000$ MeV/c).

065502-6

Scaling in the QE peak

Summary of past work by Donnelly & Sick PRC 60 (1999)

SUPERSCALING OF INCLUSIVE ELECTRON . . .

PHYSICAL REVIEW C **60** 065502

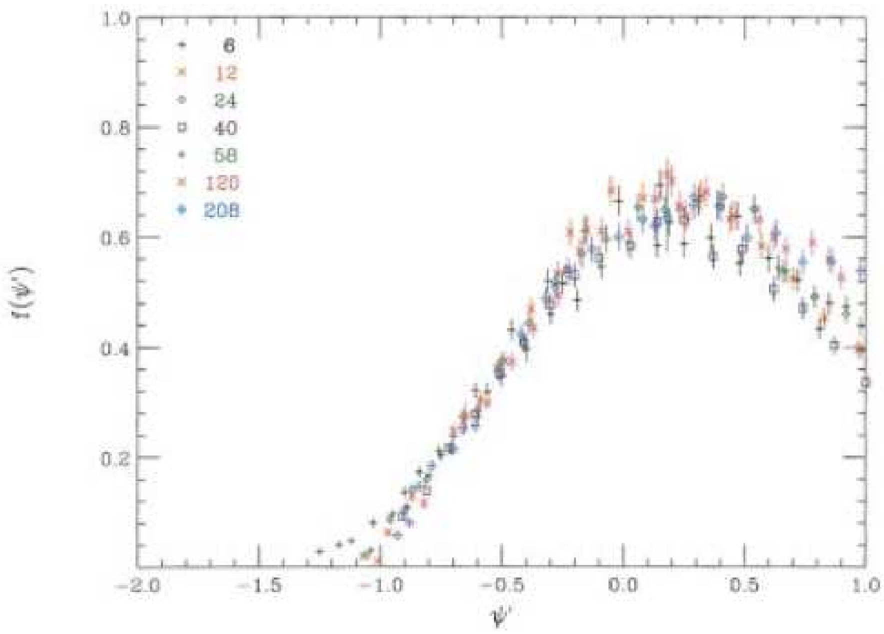

FIG. 4. (Color) Scaling function for Li, C, Mg, Ca, Ni, Sn, and Pb and fixed kinematics ($q \approx 460$ MeV/c).

Scaling in the QE peak

Summary of past work by Donnelly & Sick PRC 60 (1999)

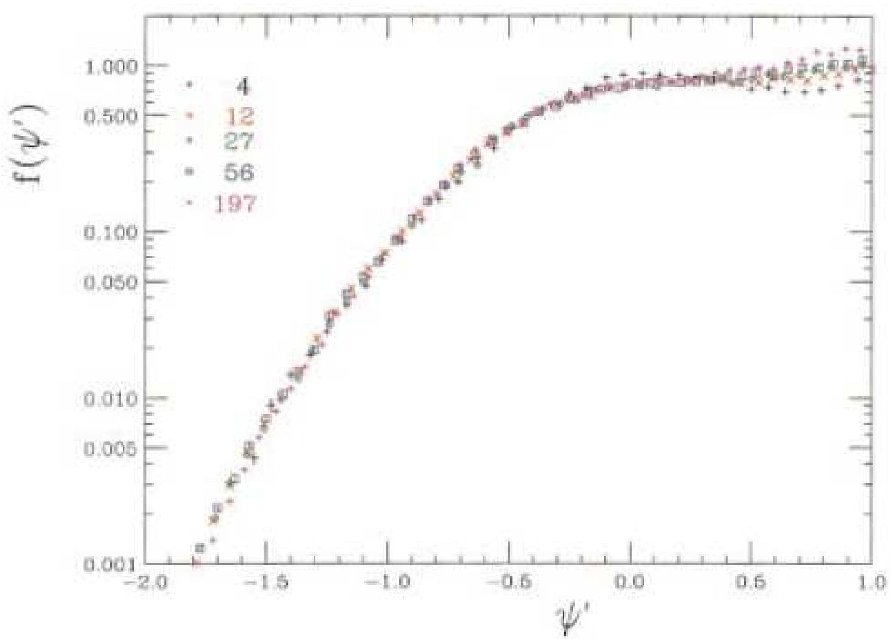

FIG. 5. (Color) Scaling function for nuclei $A = 4-197$ and fixed kinematics ($q \sim 1000$ MeV/c) on a logarithmic scale.

065502-7

Scaling in the QE peak

Summary of past work by Donnelly & Sick PRC 60 (1999)

T. W. DONNELLY AND INGO SICK — PHYSICAL REVIEW C **60** 065502

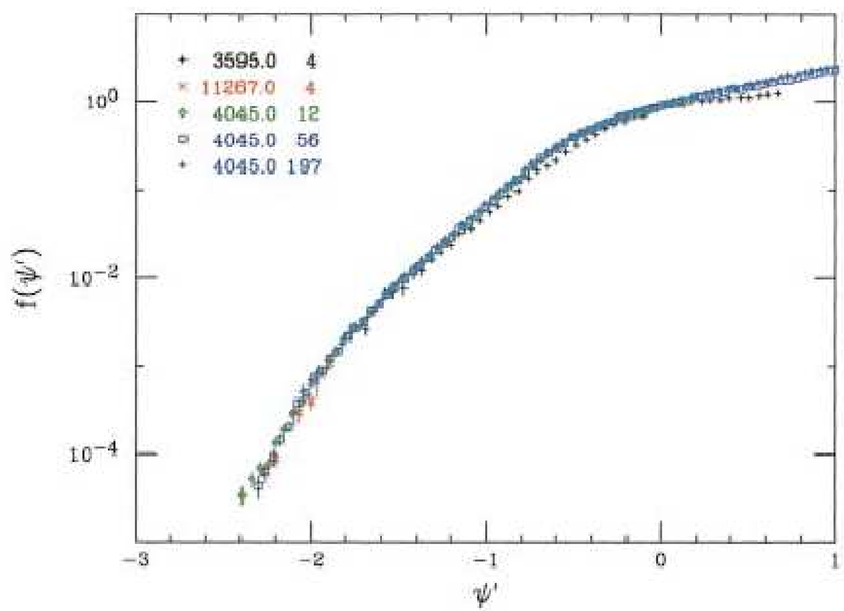

FIG. 6. (Color) Scaling function for nuclei $A = 4-197$ at $q \approx 1650$ MeV/c. The 4.405 GeV data have been taken at 23° scattering angle, the ^{4}He data at 25° and 8°.

Scaling in the QE peak

Summary of past work by Donnelly & Sick PRC 60 (1999)

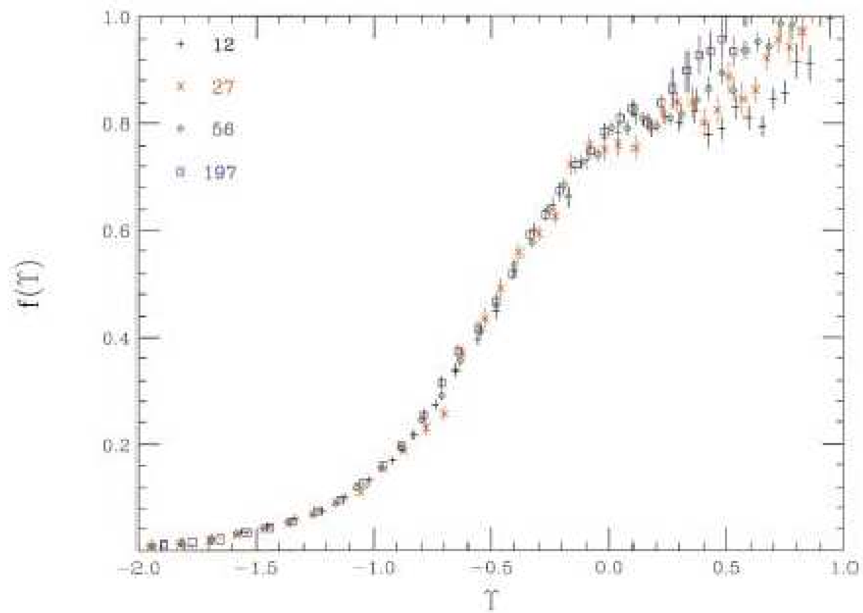

FIG. 7. (Color) Scaling function $f(\Upsilon)$ for nuclei $A=12$–197 at 3.6 GeV energy and 16° scattering angle as a function of the scaling variable Υ.

065502-8

Scaling in the QE peak

Summary of past work by Donnelly & Sick PRC 60 (1999)

SUPERSCALING OF INCLUSIVE ELECTRON . . . PHYSICAL REVIEW C **60** 065502

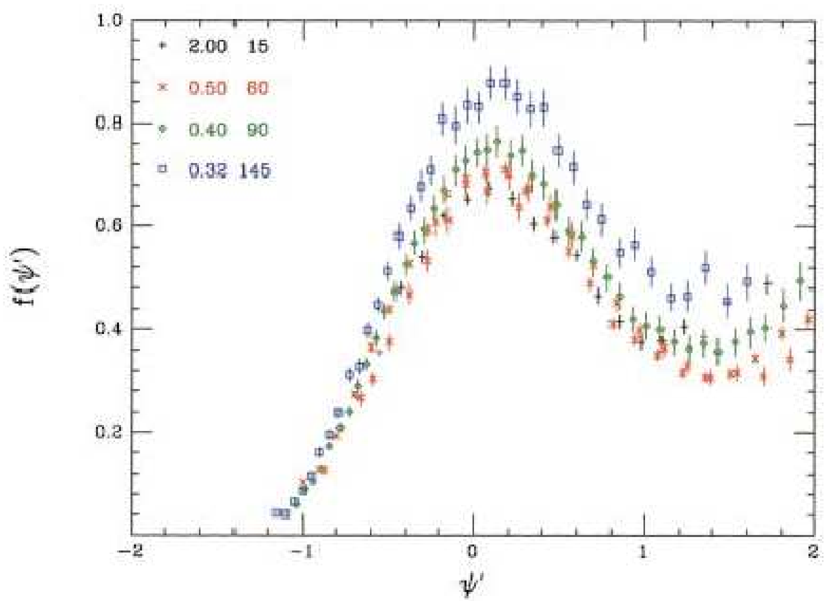

FIG. 8. (Color) Scaling function for ^{12}C at approximately constant $q \approx 500$ MeV/c, but varying angle. The energies (in GeV) and angles (in degrees) of the different data sets are identified in the plot.

Scaling in the QE peak

Summary of past work by Donnelly & Sick PRC 60 (1999)

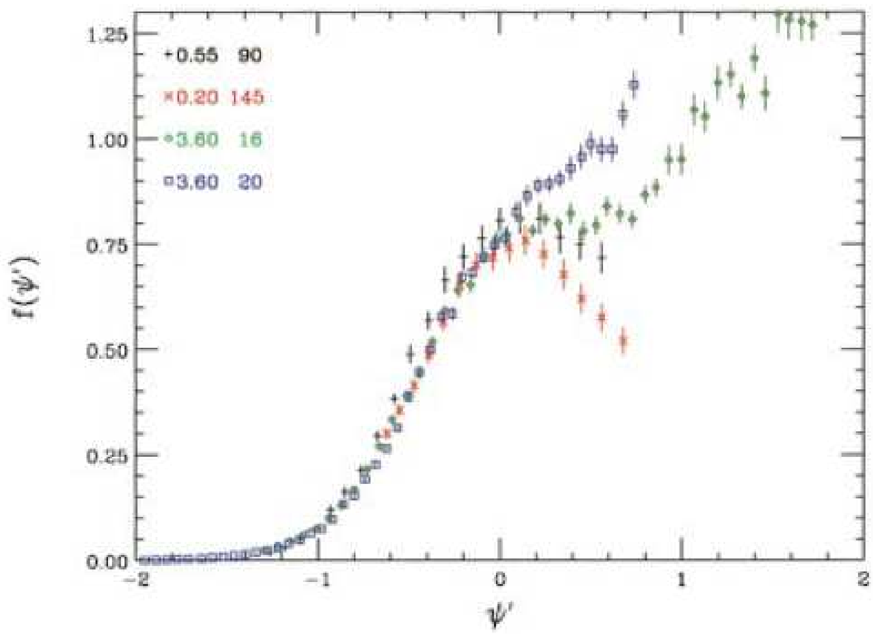

FIG. 9. (Color) Scaling function for ^{12}C and roughly constant ratio of the longitudinal and transverse *e-p* elastic cross section, as a function of the momentum transfer *q*.

Scaling in the QE peak

Summary of past work by Donnelly & Sick PRC 60 (1999)

SUPERSCALING OF INCLUSIVE ELECTRON . . .

PHYSICAL REVIEW C **60** 065502

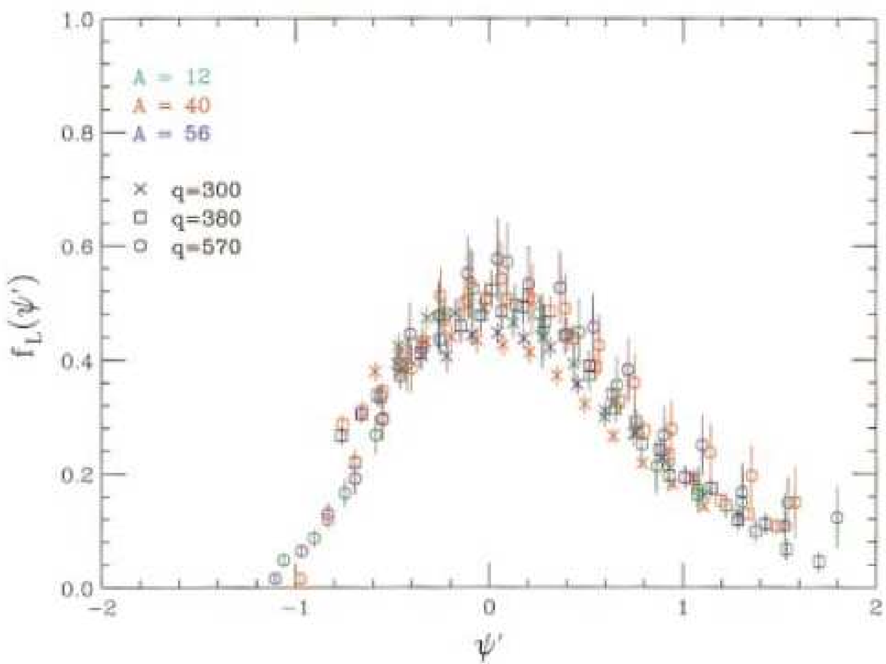

FIG. 10. (Color) Scaling function $f_L(\psi')$ from the longitudinal response.

Scaling in the QE peak

Summary of past work by Donnelly & Sick PRC 60 (1999)

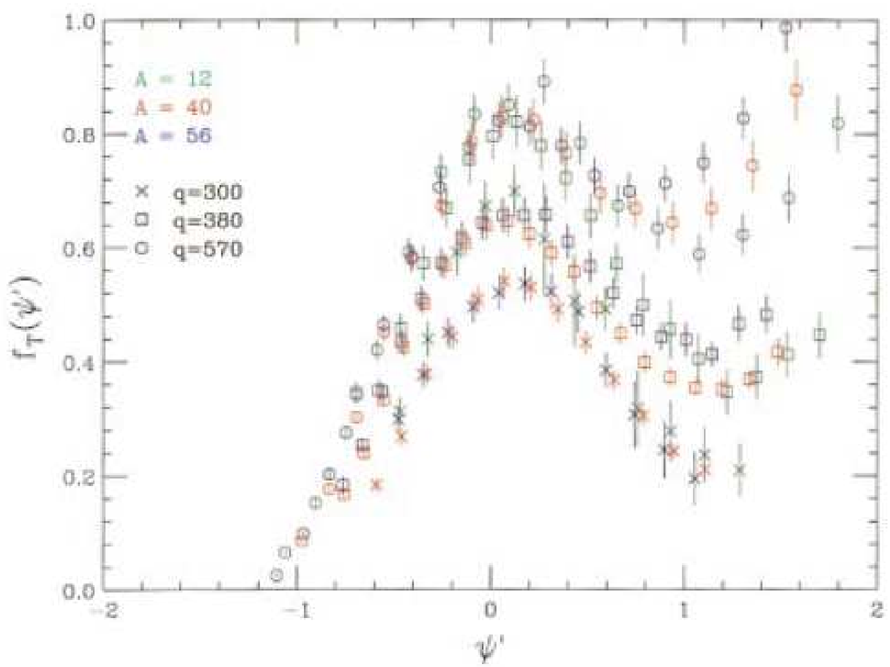

FIG. 11. (Color) Scaling function $f_T(\psi')$ from the transverse response.

Scaling properties of data

- Good 1st-kind scaling below the QE peak (scaling region)

Scaling properties of data

- Good 1st-kind scaling below the QE peak (scaling region)
- Above the peak the scaling is broken (Δ region)

Scaling properties of data

- Good 1st-kind scaling below the QE peak (scaling region)
- Above the peak the scaling is broken (Δ region)
- Scaling of the 2nd-kind works well in the scaling region

Scaling properties of data

- Good 1st-kind scaling below the QE peak (scaling region)
- Above the peak the scaling is broken (Δ region)
- Scaling of the 2nd-kind works well in the scaling region
- The longitudinal response appears to superscale

Scaling properties of data

- Good 1st-kind scaling below the QE peak (scaling region)
- Above the peak the scaling is broken (Δ region)
- Scaling of the 2nd-kind works well in the scaling region
- The longitudinal response appears to superscale
- Scaling violations reside in the transverse response,

NuFact 10

Fit in the Quasi-elastic peak

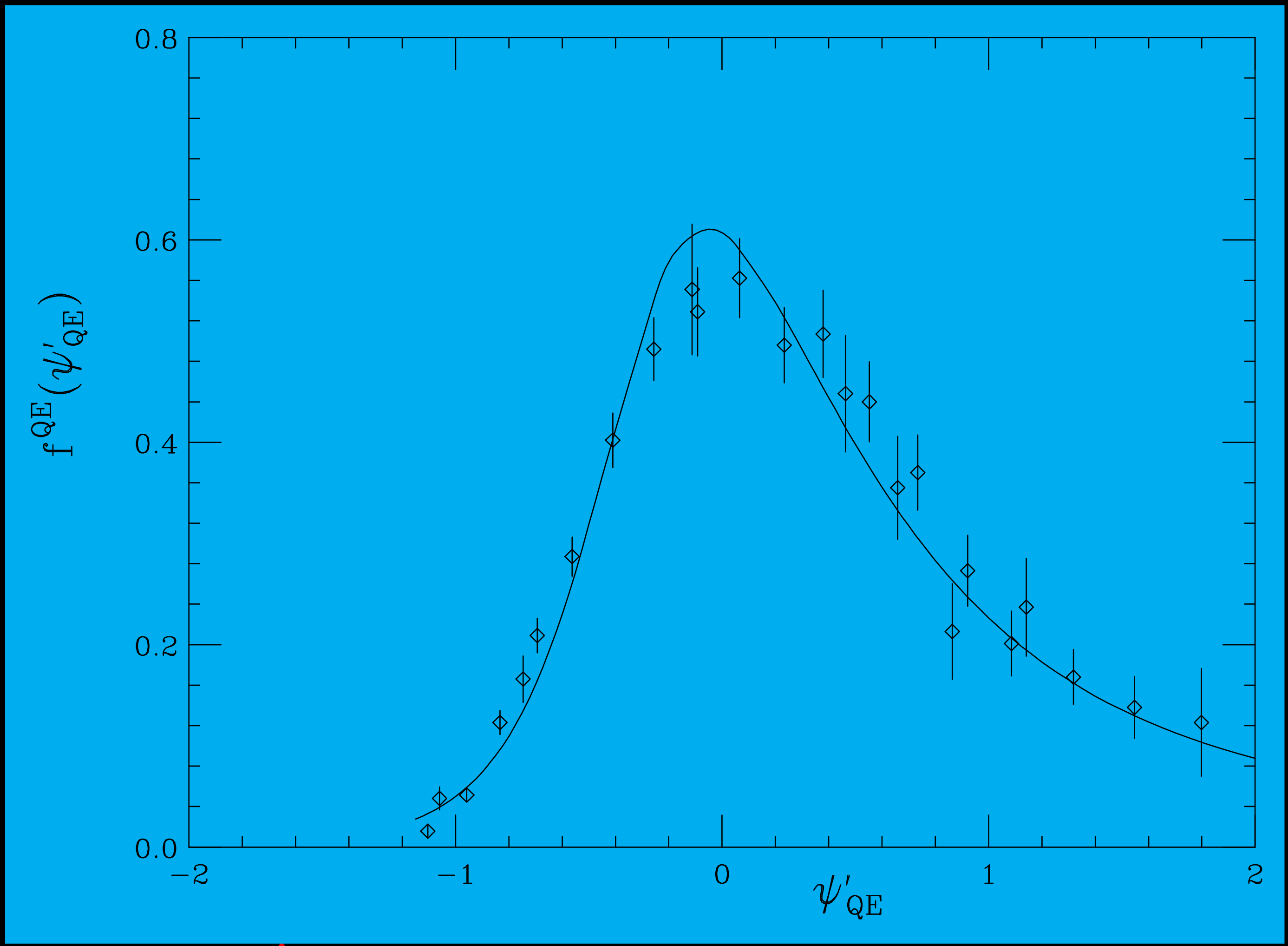

Fit in the Quasi-elastic peak

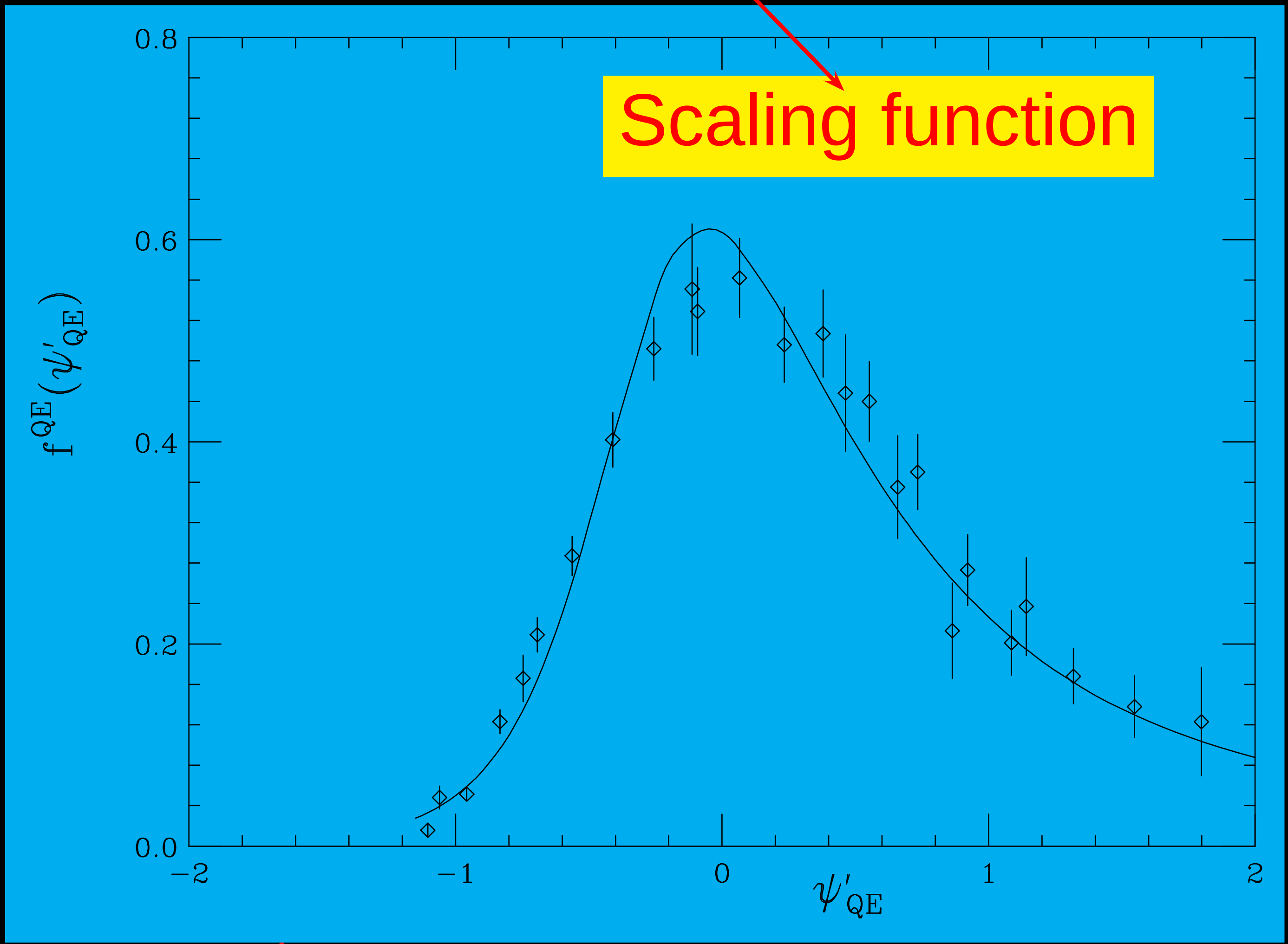

Fit in the Quasi-elastic peak

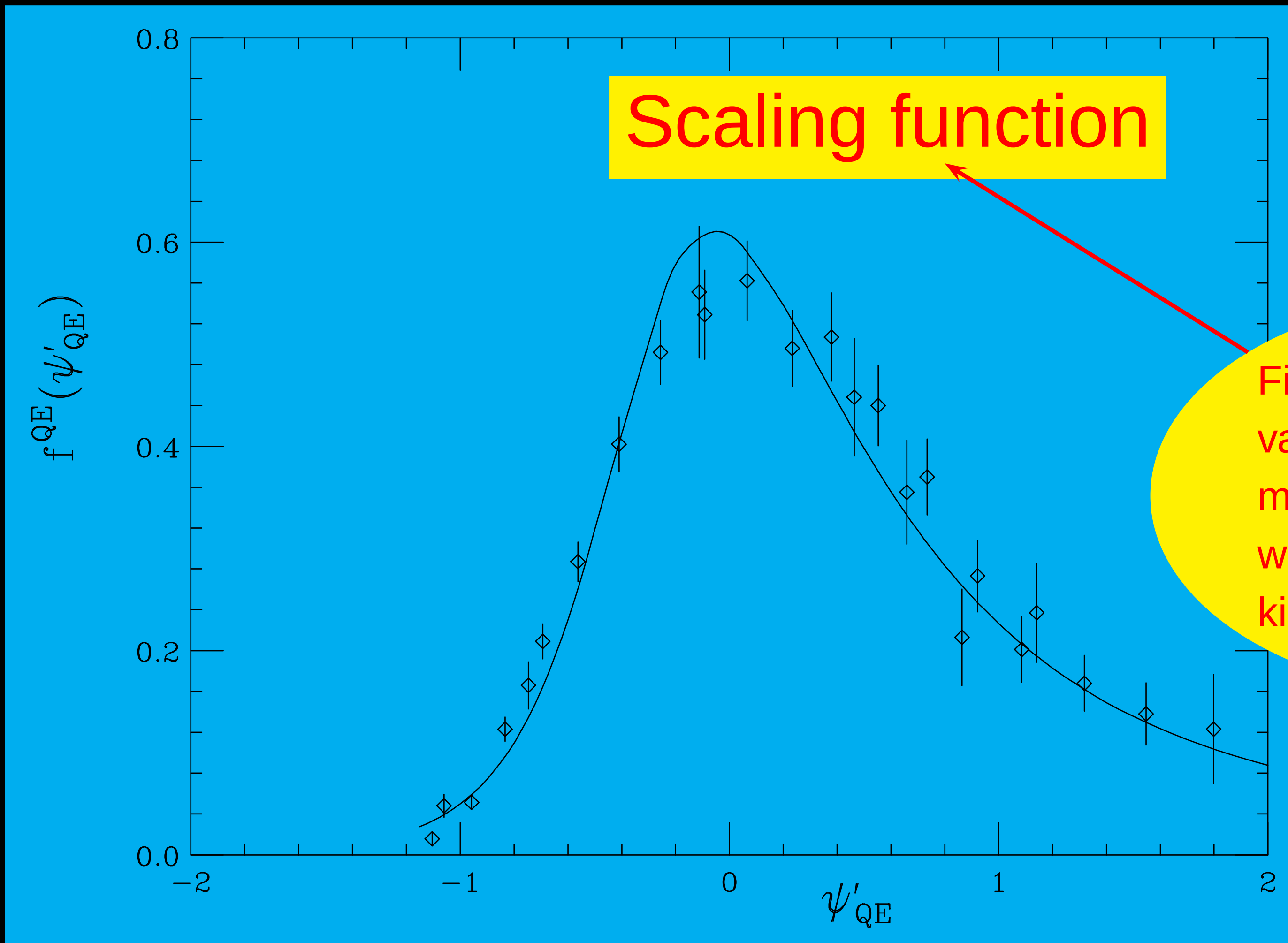

Fitted to the set of f_L values for the higher momentum transfer where scaling of the first kind is seen to occur

SuSA (Super Scaling Analysis)

- Using the experimental (e, e') scaling function to predict neutrino cross sections

SuSA (Super Scaling Analysis)

- Using the experimental (e, e') scaling function to predict neutrino cross sections
- Use the RFG equations to compute the (ν_l, l^-) response functions with the substitution $f_{RFG}(\psi) \longrightarrow f_{exp}(\psi)$

SuSA (Super Scaling Analysis)

- Using the experimental (e, e') scaling function to predict neutrino cross sections
- Use the RFG equations to compute the (ν_l, l^-) response functions with the substitution $f_{RFG}(\psi) \longrightarrow f_{exp}(\psi)$
- Needed to justify theoretically the validity of SuSA

4 The semirelativistic shell model

- Study the scaling properties in realistic models

4 The semirelativistic shell model

- Study the scaling properties in realistic models
- Estimate the validity range of SuSA

4 *The semirelativistic shell model*

- Study the scaling properties in realistic models
- Estimate the validity range of SuSA
- Include relativistic effects in the model

4 The semirelativistic shell model

- Study the scaling properties in realistic models
- Estimate the validity range of SuSA
- Include relativistic effects in the model
- Compare with the experimental scaling function

The continuum shell-model (CSM)

- Closed-shell nuclei ^{12}C, ^{16}O and ^{40}Ca,
- Initial state $|i\rangle$: Slater determinant with all shells occupied.
- Impulse approximation: final states are particle-hole excitations coupled to total angular momentum

$$|f\rangle = |(ph^{-1})J\rangle$$

- Single hole wave function $|h\rangle = |\epsilon_h l_h j_h\rangle$
- Single particle wave function $|p\rangle = |\epsilon_p l_p j_p\rangle$
- Obtained by solving the Schrödinger equation

Woods-Saxon potential

$$V(r) = -V_0 f(r, R_0, a_0) + \frac{V_{ls}}{m_\pi^2 r} \frac{df(r, R_0, a_0)}{dr} \mathbf{l} \cdot \boldsymbol{\sigma} + V_C(r)$$

$$f(r, R, a) = \frac{1}{1 + e^{(r-R)/a}}$$

$V_C(r)$: Coulomb potential.

	V_0^p	V_{LS}^p	V_0^n	V_{LS}^n	r_0	a_0
^{12}C	62.0	3.20	60.00	3.15	1.25	0.57
^{16}O	52.5	7.00	52.50	6.54	1.27	0.53
^{40}Ca	57.5	11.11	55.00	8.50	1.20	0.53

The SR approach

A — Expand the relativistic single-nucleon current

$$j^\mu(\vec{p'},\vec{p}) = \overline{u}(\vec{p'})\Gamma^\mu(Q)u(\vec{p})$$

in powers of $\vec{\eta} = \vec{p}/m_N$. to first order $O(\eta)$

Not expand in $\vec{p'}/m_N$.

$\Longrightarrow q, \omega$ can be large

Relativistic kinematics

B

USE RELATIVISTIC KINEMATICS.

- The energy transfer is the difference between the (non-relativistic) single-particle energies of particle and hole $\omega = \epsilon_p - \epsilon_h$.
- The relativistic kinematics are taken into account by the substitution

$$\epsilon_p \longrightarrow \epsilon_p(1 + \epsilon_p/2m_N)$$

as the eigenvalue of the Schrödinger equation for the particle

The SR vector current

$$J_V^0 = \xi_0 + i\xi_0'(\boldsymbol{\kappa} \times \boldsymbol{\eta}) \cdot \boldsymbol{\sigma}$$
$$\mathbf{J}_V^\perp = \xi_1 \boldsymbol{\eta}^\perp + i\xi_1' \boldsymbol{\sigma} \times \boldsymbol{\kappa} \,,$$

(q, ω)-dependent factors:

$$\xi_0 = \frac{\kappa}{\sqrt{\tau}} 2G_E^V \quad , \quad \xi_0' = \frac{2G_M^V - G_E^V}{\sqrt{1+\tau}}$$

$$\xi_1' = 2G_M^V \frac{\sqrt{\tau}}{\kappa} \quad , \quad \xi_1 = 2G_E^V \frac{\sqrt{\tau}}{\kappa}$$

provide the required relativistic behavior.

The longitudinal component is given from vector current conservation, $J_V^3 = \frac{\lambda}{\kappa} J_V^0$.

The SR axial-vector current

$$\mathbf{J}_A^\perp = \zeta_1' \boldsymbol{\sigma}^\perp, \quad \zeta_1' = \sqrt{1+\tau} G_A \, .$$

Transverse

Neglect the terms of order $O(\eta)$

$$\begin{aligned} J_A^0 &= \zeta_0' \boldsymbol{\kappa} \cdot \boldsymbol{\sigma} + \zeta_0'' \boldsymbol{\eta}^\perp \cdot \boldsymbol{\sigma} \\ J_A^z &= \zeta_3' \boldsymbol{\kappa} \cdot \boldsymbol{\sigma} + \zeta_3'' \boldsymbol{\eta}^\perp \cdot \boldsymbol{\sigma} \, , \end{aligned}$$

Time component

Longitudinal component

NuFact 10

The SR axial-vector current

$$\mathbf{J}_A^{\perp} = \zeta_1' \boldsymbol{\sigma}^{\perp}, \quad \zeta_1' = \sqrt{1+\tau} G_A \,.$$

Transverse

Neglect the terms of order $O(\eta)$

$$J_A^0 = \zeta_0' \boldsymbol{\kappa} \cdot \boldsymbol{\sigma} + \zeta_0'' \boldsymbol{\eta}^{\perp} \cdot \boldsymbol{\sigma}$$

$$J_A^z = \zeta_3' \boldsymbol{\kappa} \cdot \boldsymbol{\sigma} + \zeta_3'' \boldsymbol{\eta}^{\perp} \cdot \boldsymbol{\sigma} \,,$$

Time component

Longitudinal component

$$\zeta_0' = \frac{1}{\sqrt{\tau}} \frac{\lambda}{\kappa} G_A' \quad , \quad \zeta_0'' = \frac{\kappa}{\sqrt{\tau}} \left[G_A - \frac{\lambda^2}{\kappa^2 + \kappa\sqrt{\tau(\tau+1)}} G_A' \right]$$

$$\zeta_3' = \frac{1}{\sqrt{\tau}} G_A' \quad , \quad \zeta_3'' = \frac{\lambda}{\sqrt{\tau}} \left[G_A - \frac{\kappa}{\kappa + \sqrt{\tau(\tau+1)}} G_A' \right]$$

$G_A' = G_A - \tau G_P$ small due to cancellations

The $O(\eta)$ term, proportional to $\vec{\eta}^{\perp} \cdot \vec{\sigma}$ is dominant

^{2}C

Test of the SR approach: *V responses*

$k_F = 220$ MeV/c

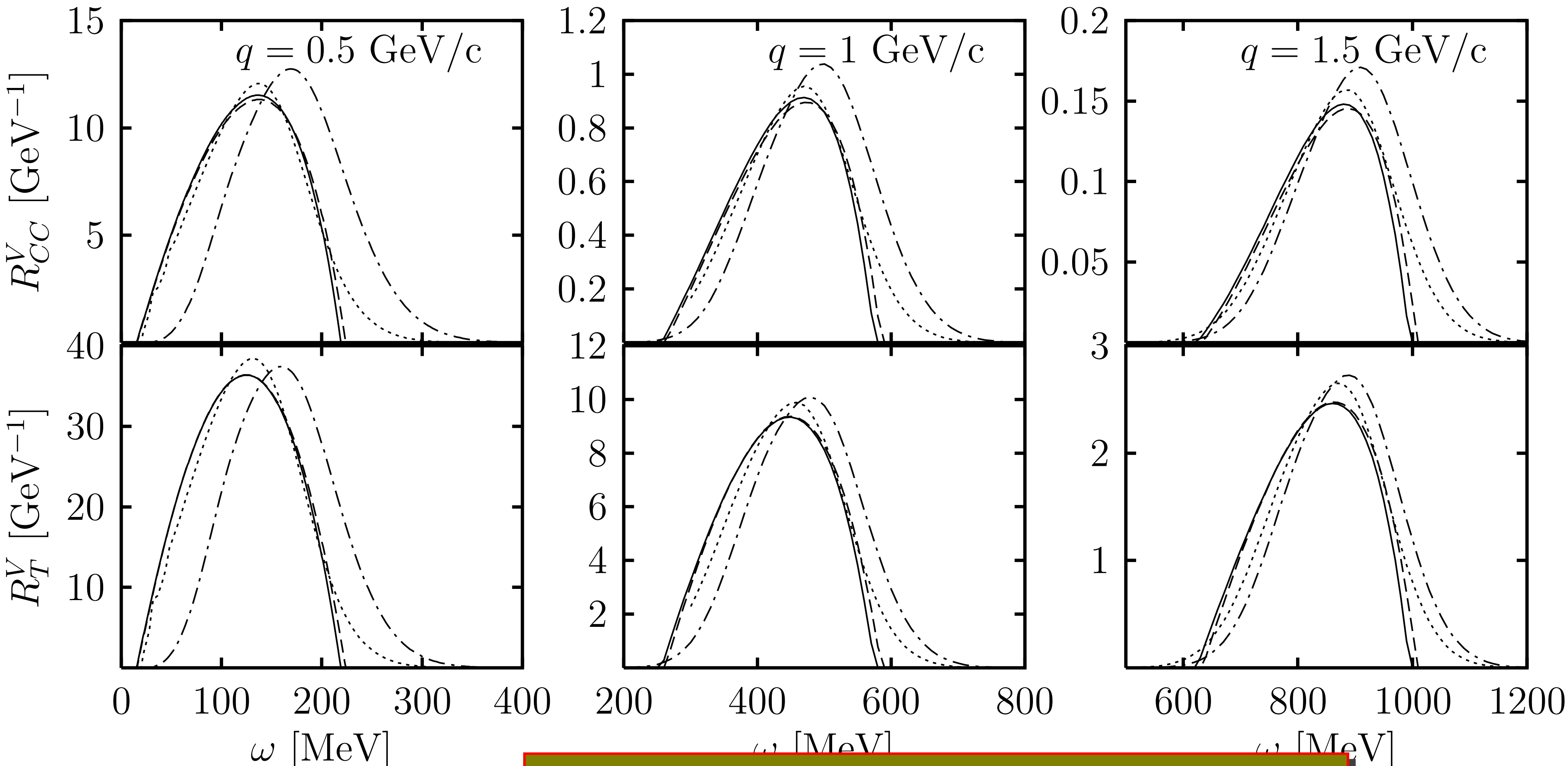

Solid lines: RFG   Dashed lines: SRFG

Dotted: CSM   Dot-dashed: PWIA.

A responses

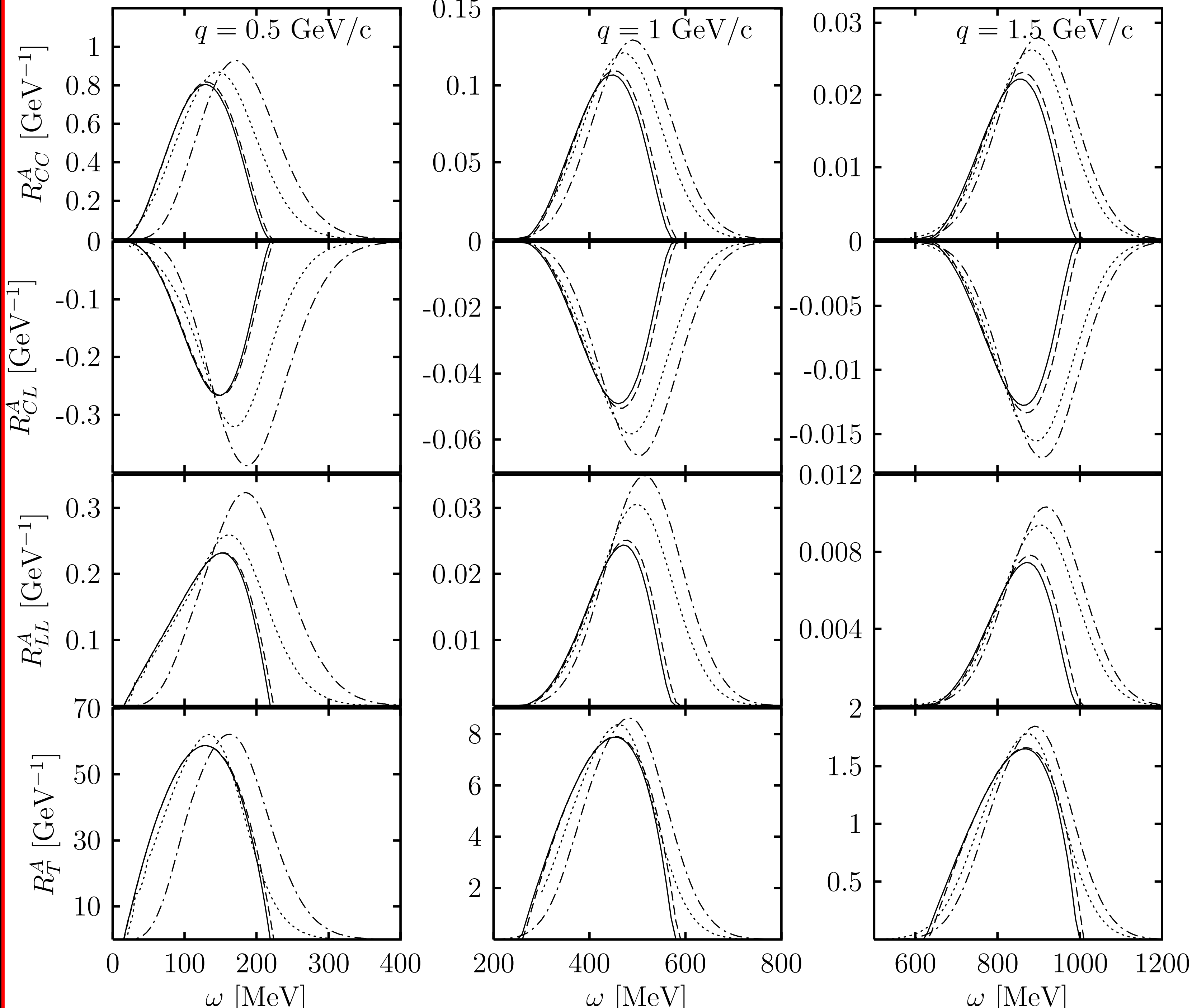

q = 0.5 GeV/c
q = 1 GeV/c
q = 1.5 GeV/c
R^A_{CC} [GeV^{-1}]
R^A_{CL} [GeV^{-1}]
R^A_{LL} [GeV^{-1}]
R^A_T [GeV^{-1}]
ω [MeV]
ω [MeV]
ω [MeV]

Total responses

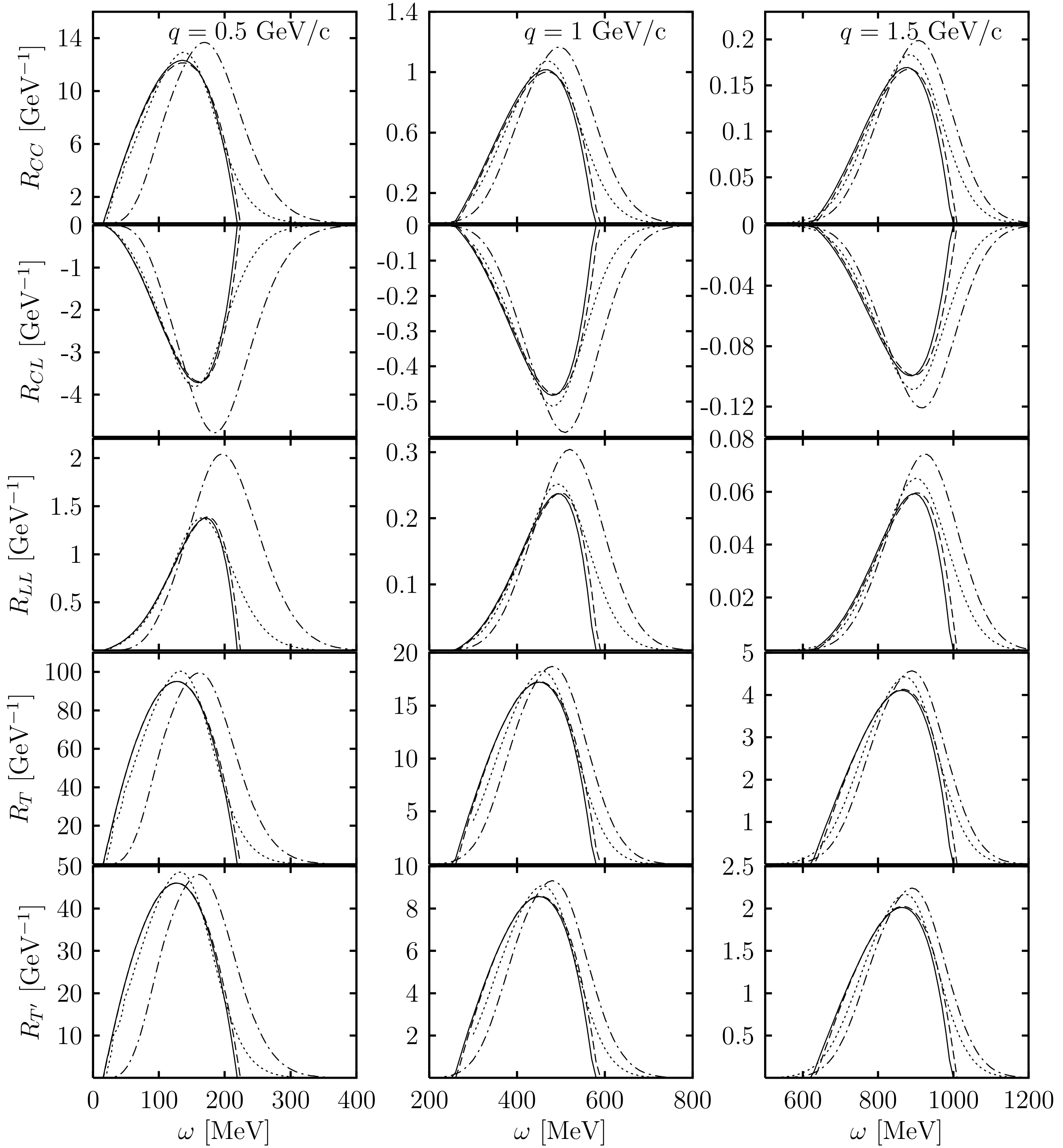

Test of the SR approach: Cross section

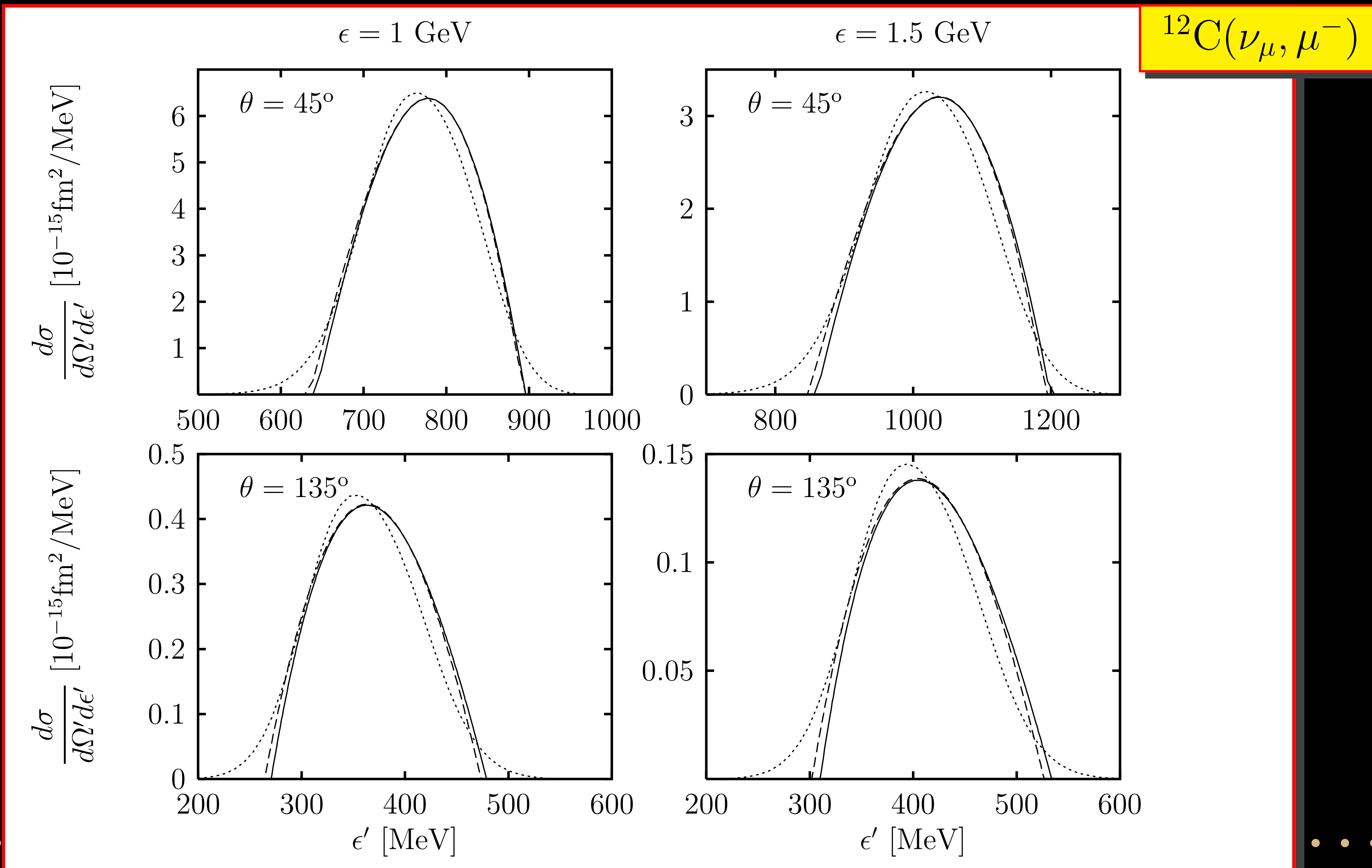

Scaling of the first kind

SR Shell model

Curves for
$q = 0.5, 0.7, 1, 1.3, 1.5$ GeV
collapse into one

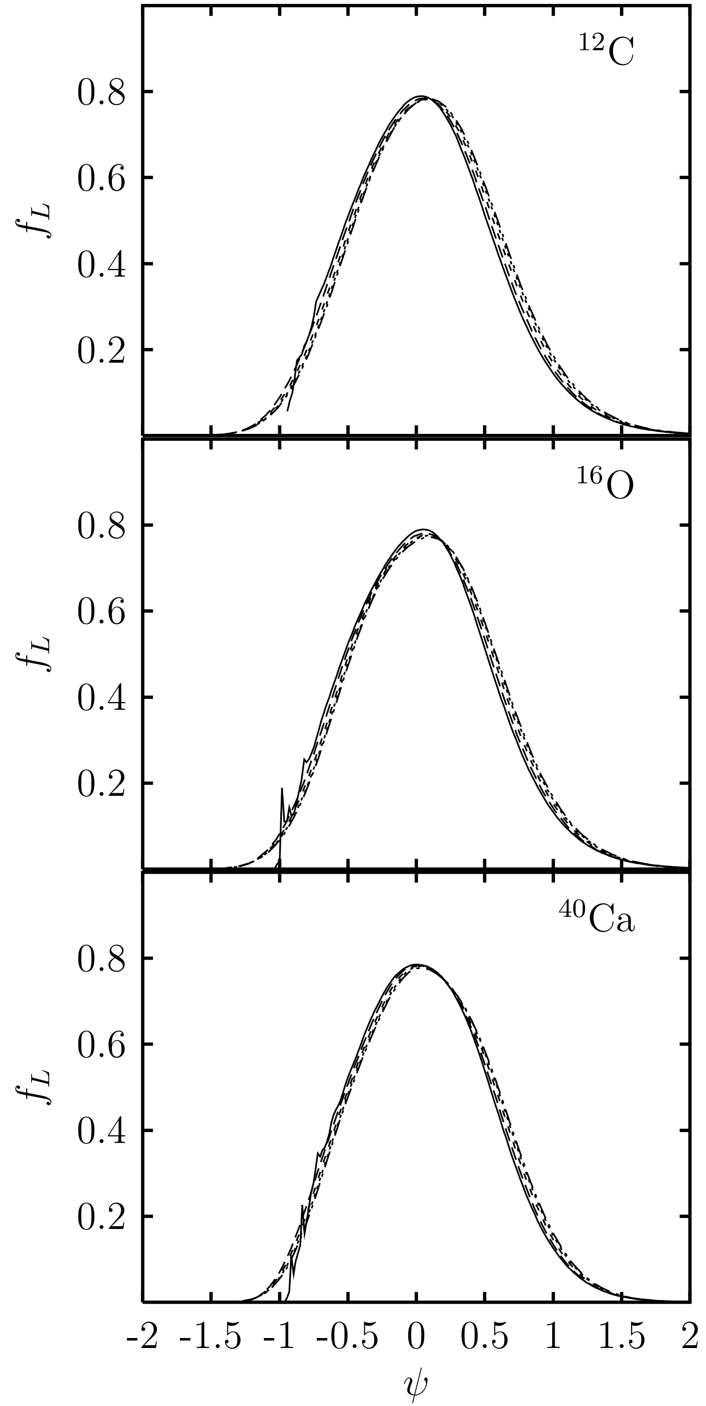

Scaling of the second kind

Curves for ^{12}C, ^{16}O and ^{40}Ca collapse into one

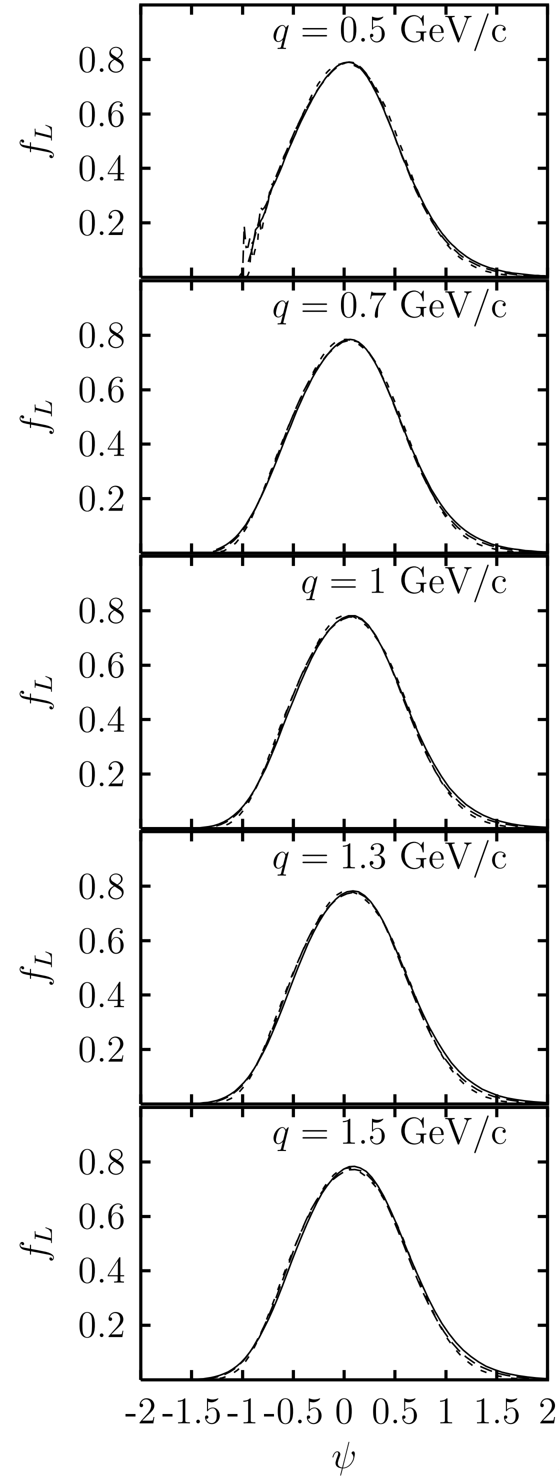

Superscaling

Scaling of the first kind

+ Scaling of the second kind

= Superscaling
in the CSM

Improvement of the FSI

C

DEB+D potential (Dirac-equation-based plus Darwin term) in the final state:

- Rewrite Dirac eqution as a second-order equation for the up component $\psi_{up}(\vec{r})$
- Darwin term: $\psi_{up}(\vec{r}) = K(r,E)\phi(\vec{r})$
- The function $\phi(\vec{r})$ verifies the Schrödinger equation

$$\left[-\frac{1}{2m_N}\nabla^2 + U_{DEB}(r,E)\right]\phi(\vec{r}) = \frac{E^2 - m_N^2}{2m_N}\phi(\vec{r})$$

- Both the DEB potential $U_{DEB}(r,E)$ and Darwin term $K(r,E)$ are energy-dependent

DEB+D FSI effect

Dotted: SR Woods-Saxon
Solid: SR DEB+D
Dashed: RMF

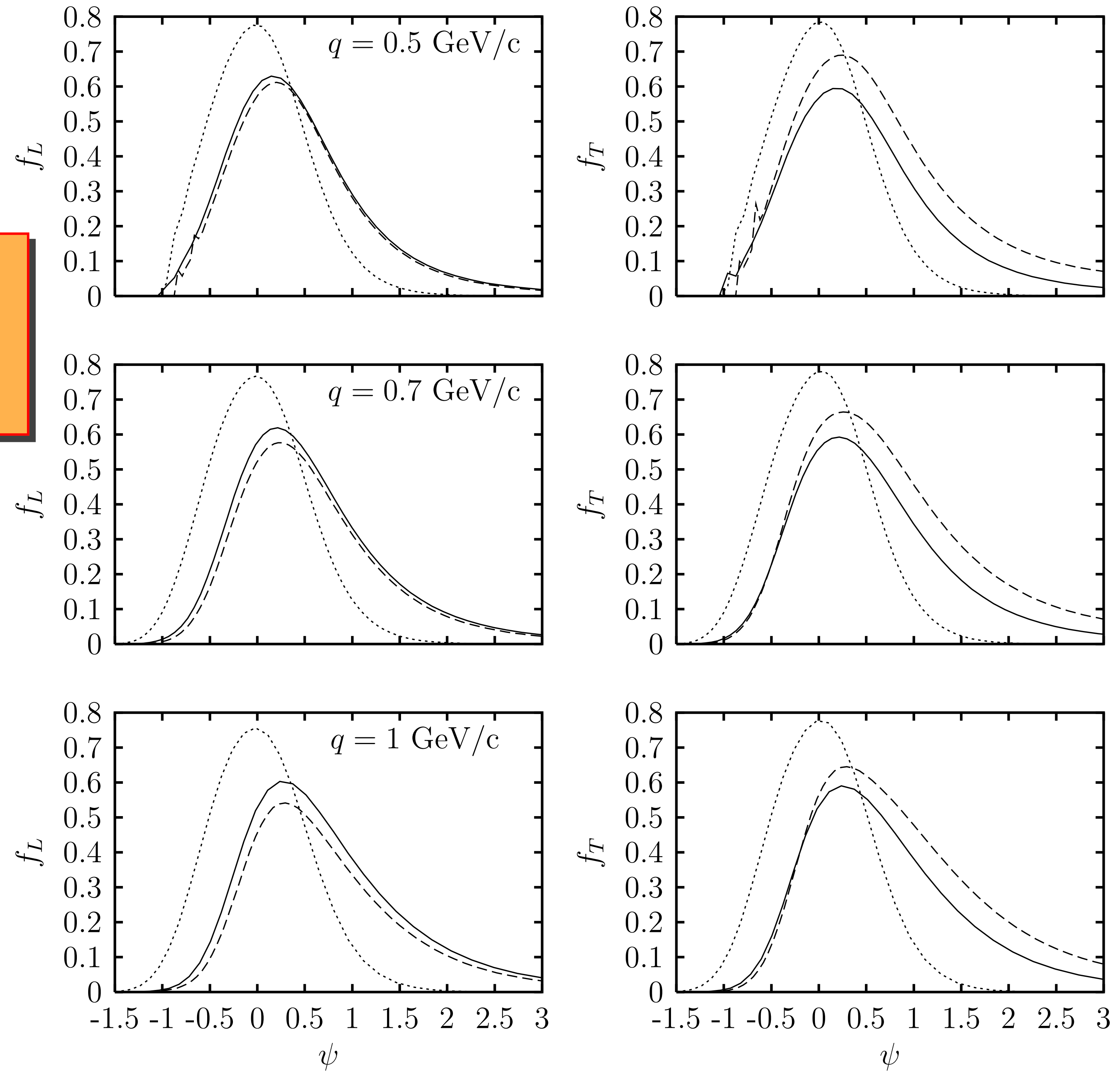

Scaling of 1st kind DEB+D

$q = 0.5$, 0.7
1.0, 1.3
and 1.5 GEV/c

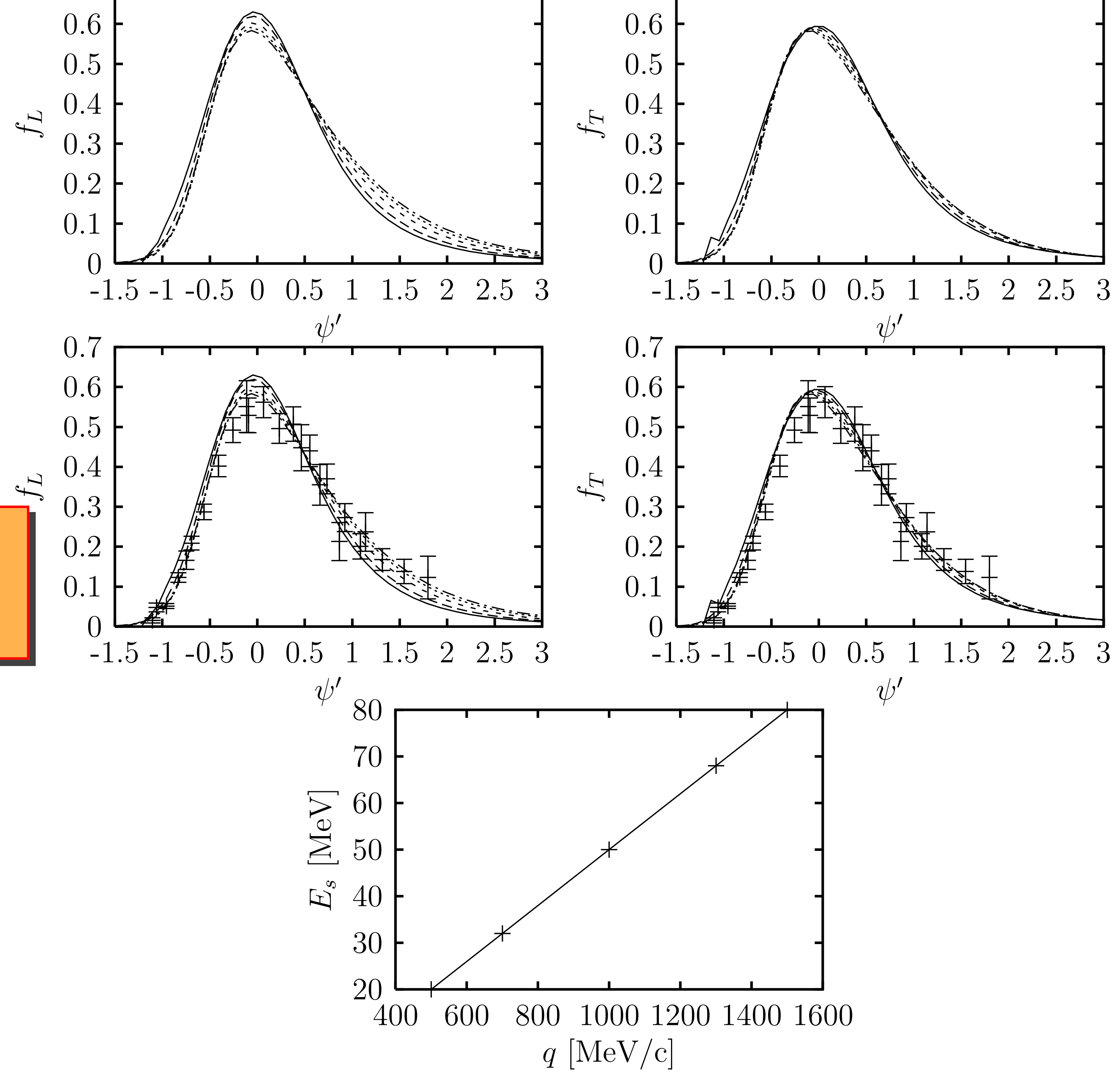

CC neutrino reactions

- SuSA reconstruction of the (ν_μ, μ^-) cross section from the (e, e') one
- Test of the SuSA in the CSM
- The CSM electromagnetic scaling function is used to compute neutrino cross sections.
- Compare with the exact CSM result

NuFact 10

^{12}C(ν_μ, μ^-)

$\epsilon = 1$ GeV

Dotted: Woods-Saxon
Solid: DEB+D
Dashed: SuSA

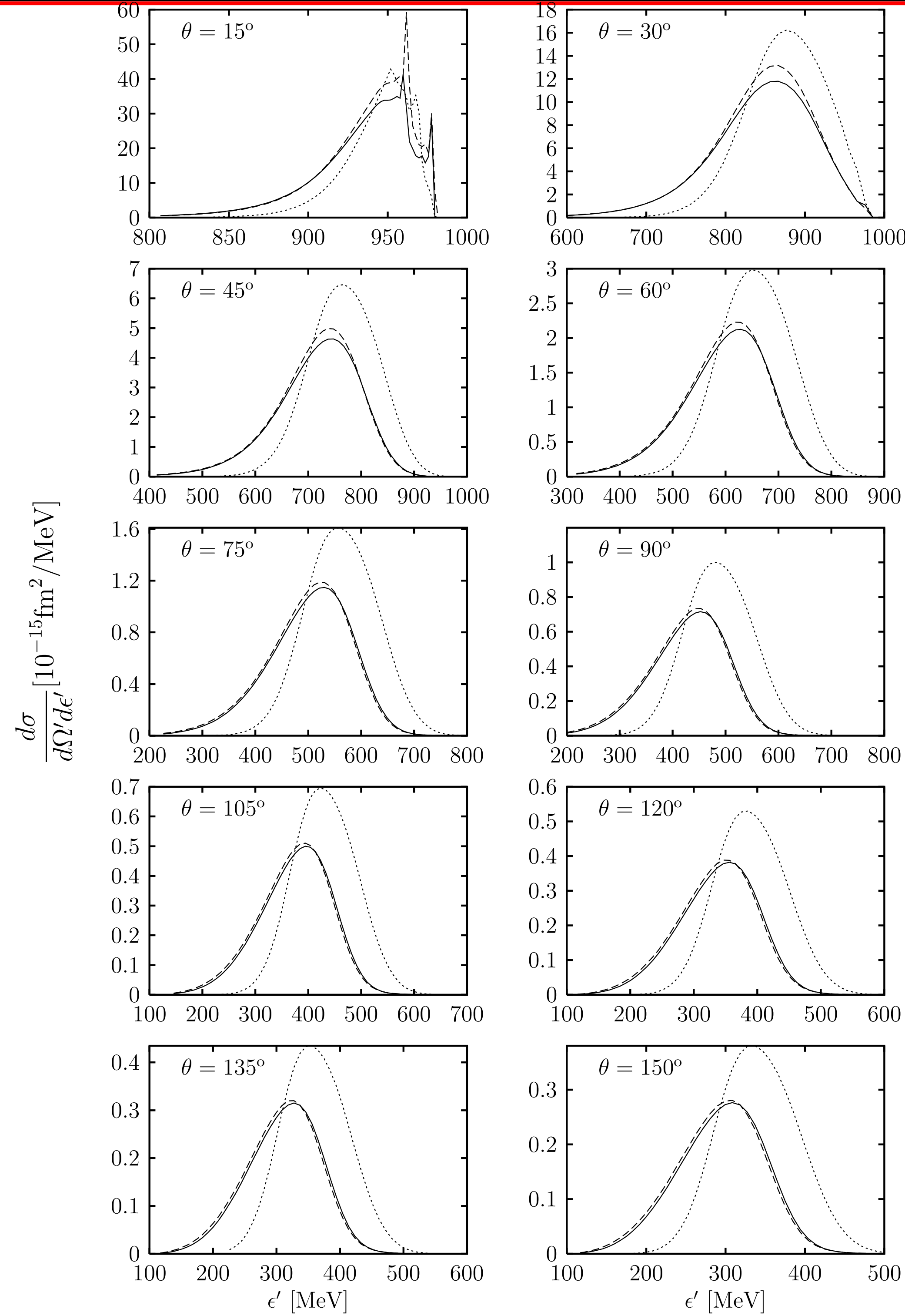

Scaling violation for low q

Scaling violation for low q

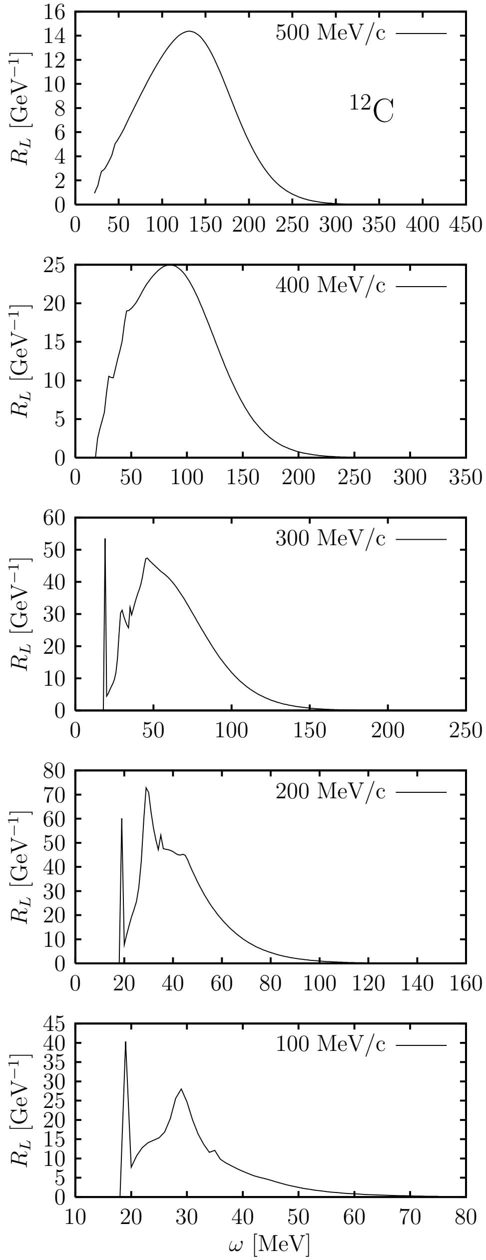

Scaling violation for low q

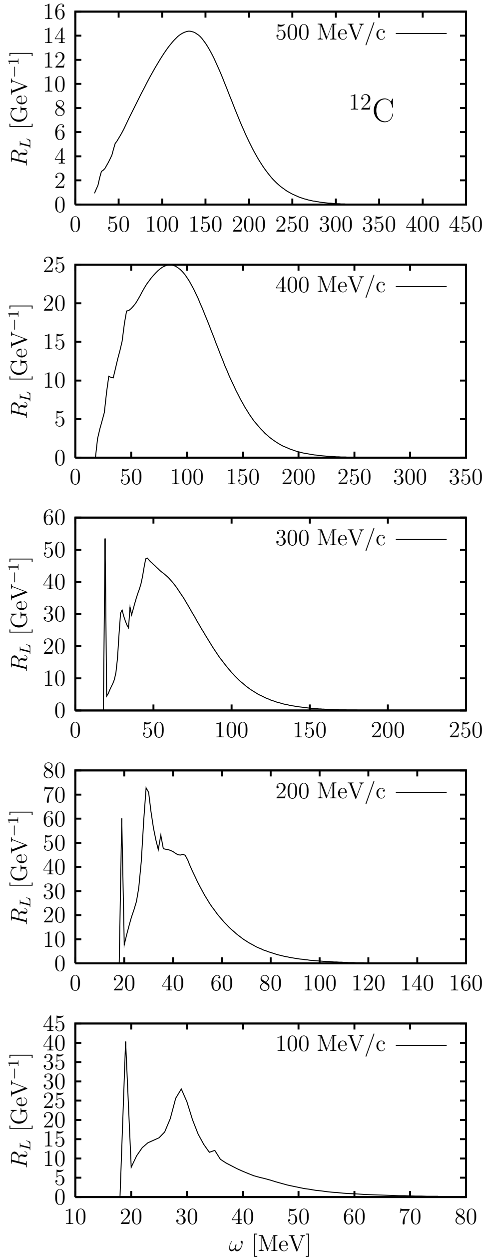

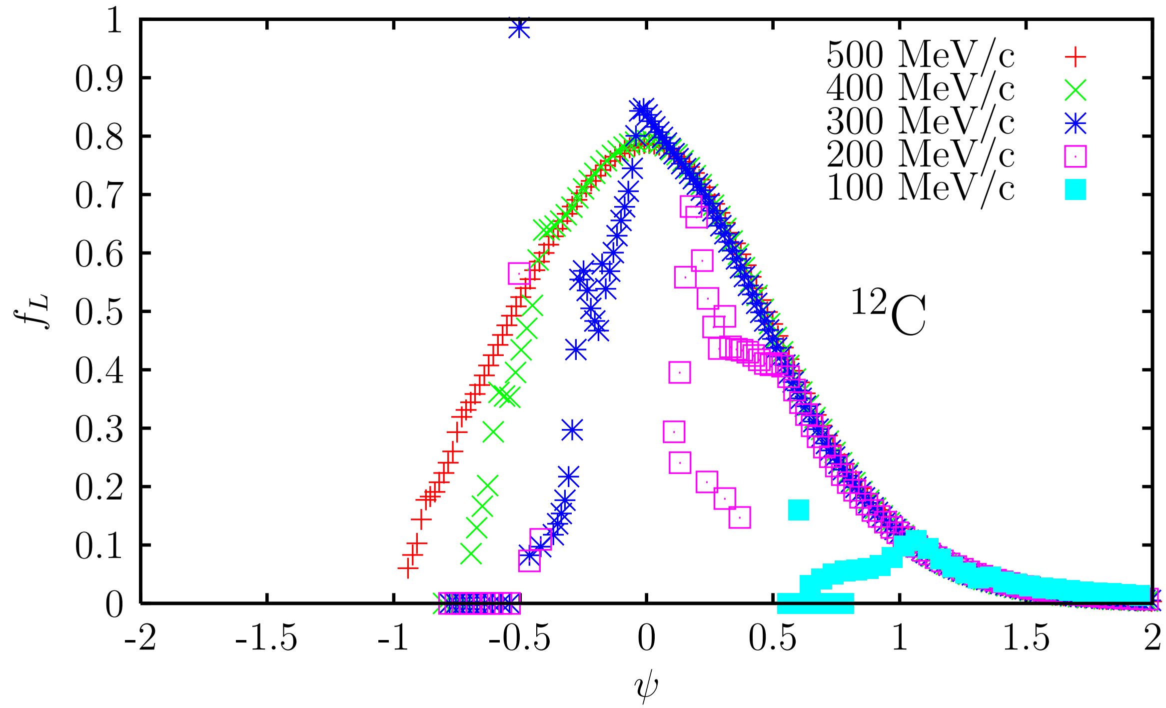

5 *The Relativistic Mean Field (RMF)*

- Solve the exact relativistic Dirac equation for the initial and final nucleons
- Use the exact relativistic V and A current operators
- Describe the bound nucleon states as self-consistent Dirac-Hartree solutions using a lagrangian containing σ, ω and ρ mesons
- Use the same relativistic Diract-Hartree potential for the final states (FSI)

(ν_μ, μ^-) results with the RMF

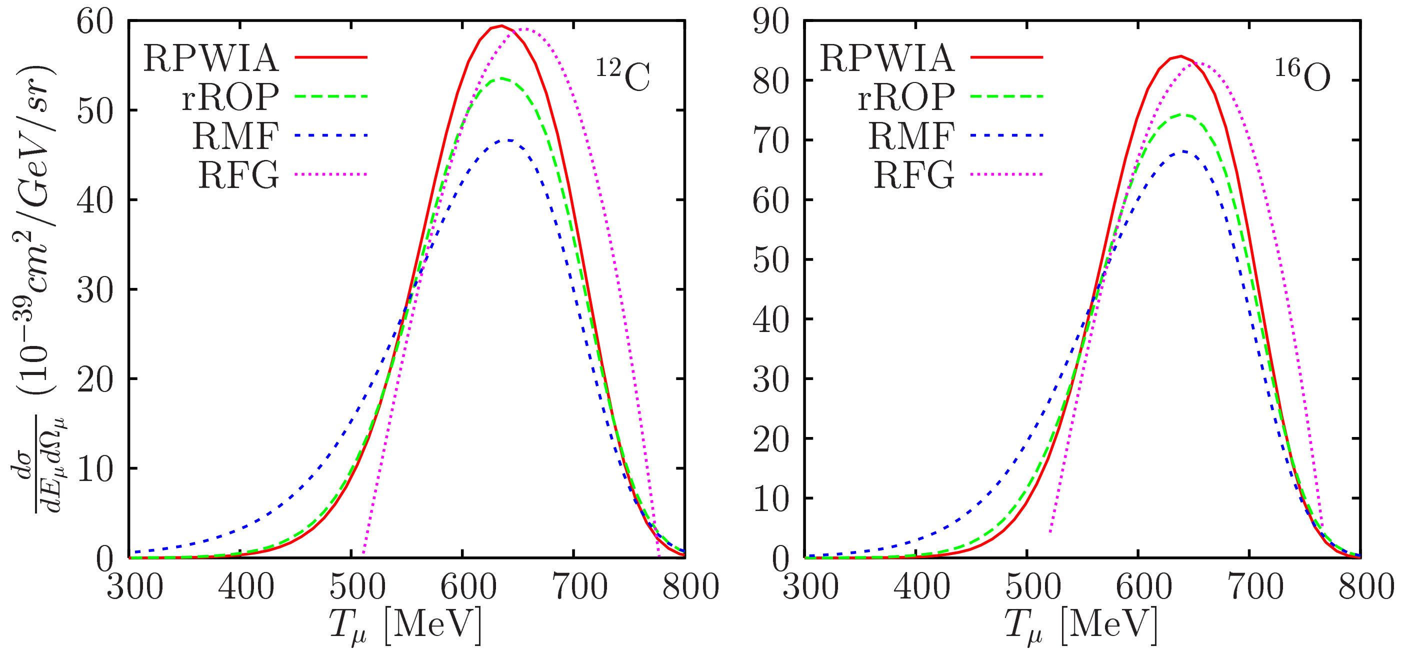

Quasi-elastic differential cross section $d\sigma/dE_\mu/d\Omega_\mu$ for (ν_μ, μ^-)

- Incident neutrino energy $\varepsilon_\nu = 1$ GeV.
- Muon scattering angle $\theta_\mu = 45^o$.
- RPWIA (solid), rROP (dashed) and RMF (dot-dashed), RFG (dotted).

From Caballero, Amaro, Barbaro, Donnelly, Maieron, and Udias, PRL 95 (2005)

(ν_μ, μ^-) results with the RMF

Neutrino scaling function Compared to the experimental scaling function

- RPWIA (solid),
- rROP (dashed)
- RMF (dot-dashed)
- Parameterization of data (dotted)

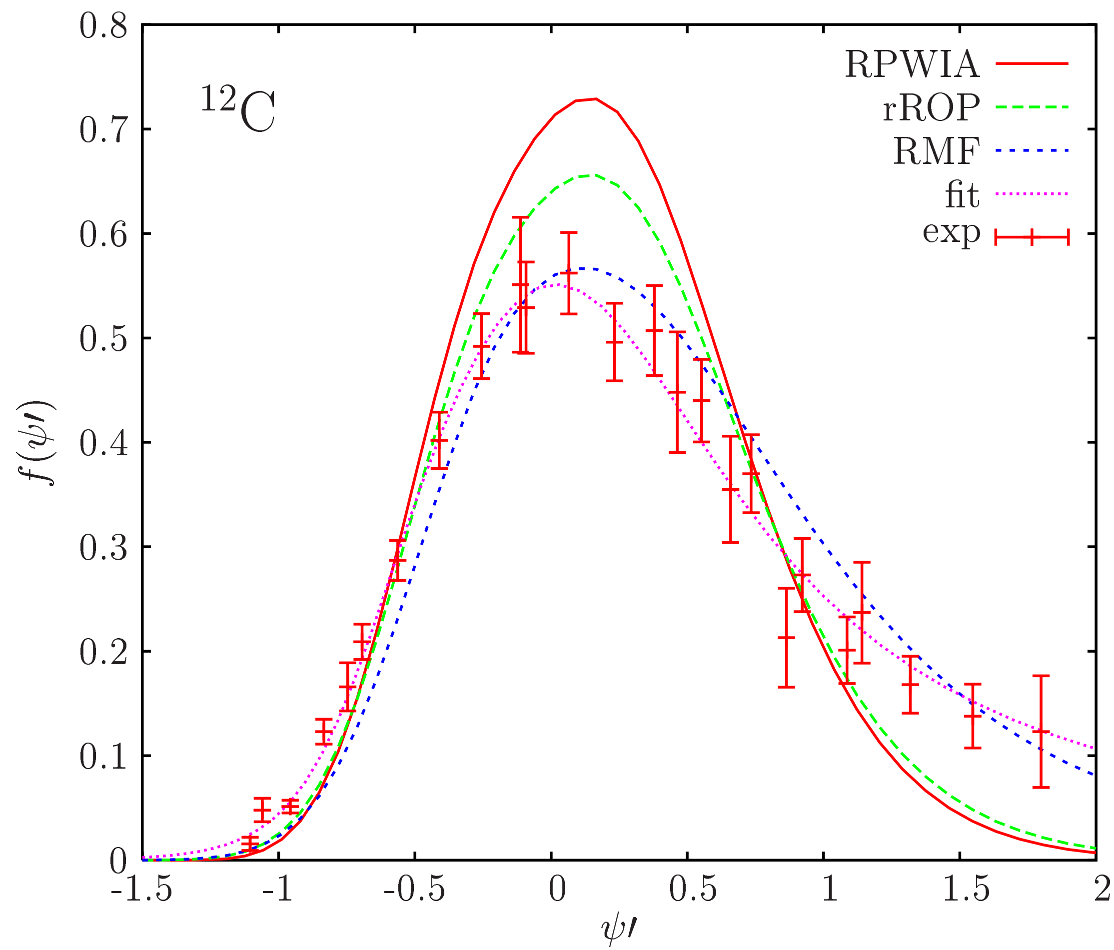

From Caballero, Amaro, Barbaro, Donnelly, Maieron, and Udias, PRL 95 (2005)

(ν_μ, μ^-) results with the RMF

Total integrated (ν_μ, μ) QE cross section for ^{12}C
as a function of the incident neutrino energy.

- RMF (squares),
- RFG (solid line)
- SuSA (dashed line),
- RPWIA (dot-dashed line)
- SRWS (circles)
- SRWS-tot (crosses).

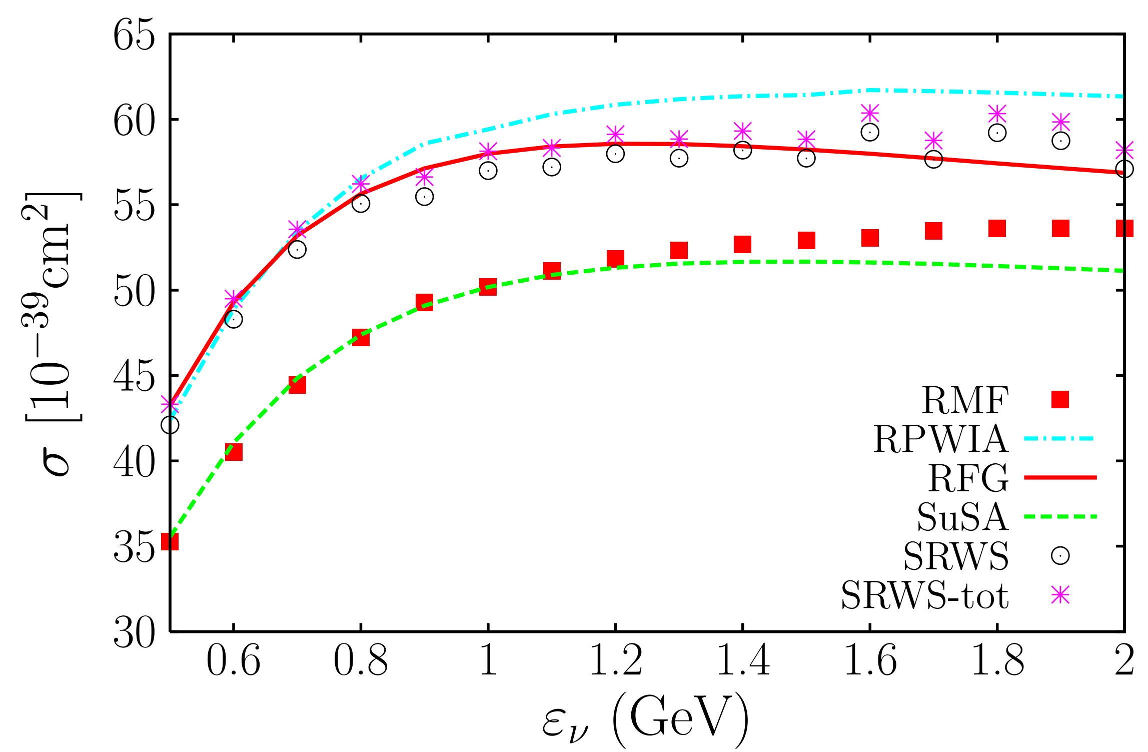

From Amaro, Barbaro, Caballero, Donnelly Phys. Rev. Lett. 98 (2007)

6 Neutrino excitation of the Δ peak

J.E. Amaro, M.B. Barbaro, J.A. Caballero, T.W. Donnelly, A. Molinari, Nucl. Phys. A **657** (1999) 161.

New scaling variable for the Δ peak :

$$\psi_\Delta \equiv \left[\frac{1}{\xi_F}\left(\kappa\sqrt{\rho_\Delta^2+1/\tau}-\lambda\rho_\Delta-1\right)\right]^{1/2} \times \begin{cases} +1 & \lambda \geq \lambda_\Delta^0 \\ -1 & \lambda \leq \lambda_\Delta^0 \end{cases}$$

$$\lambda_\Delta^0 = \frac{1}{2}\left[\sqrt{\mu_\Delta^2+4\kappa^2}-1\right], \qquad \mu_\Delta \equiv m_\Delta/m_N$$

$$\rho_\Delta \equiv 1+\beta_\Delta/\tau \qquad \beta_\Delta \equiv \frac{1}{4}\left(\mu_\Delta^2-1\right)$$

ψ_Δ Vanishes at the Δ peak $\Longrightarrow \omega = \omega_\Delta^0 = \sqrt{m_\Delta^2+q^2}-m_N$

Include a small energy shift $\omega \rightarrow \omega' \equiv \omega - E_{shift}$. yielding a shifted scaling variable ψ'_Δ.

RFG responses in the Δ peak

ignoring terms of order η_F^2:

$$
\begin{aligned}
R_L^{\Delta}(\kappa,\lambda)_0 &= \frac{1}{2}\Lambda_0\frac{\kappa^2}{\tau}\left[\left(1+\tau\rho_\Delta^2\right)w_2^{\Delta}(\tau)-w_1^{\Delta}(\tau)\right]\times f_{RFG}(\psi_\Delta)\\
R_T^{\Delta}(\kappa,\lambda)_0 &= \frac{1}{2}\Lambda_0\left[2w_1^{\Delta}(\tau)\right]\times f_{RFG}(\psi_\Delta),
\end{aligned}
$$

$$\Lambda_0=\frac{\mathcal{N}}{2\kappa k_F}$$

One should add the contributions:

$\mathcal{N}=Z$ and the $p\to\Delta^+$ structure functions

$\mathcal{N}=N$ and the $n\to\Delta^0$ responses.

Experimental Δ *scaling function*

- Substract from the total (e,e') experimental cross section the QE cross section recalculated using $f^{QE}(\psi'_{QE})$
- Divide by $S^{\Delta} \equiv \sigma_M \left[v_L G_L^{\Delta} + v_T G_T^{\Delta} \right]$

$$G_L^{\Delta} = \frac{\kappa}{2\tau k_F} \left[\mathcal{N} \left\{ \left(1 + \tau \rho_{\Delta}^2 \right) w_2^{\Delta}(\tau) - w_1^{\Delta}(\tau) \right\} \right] + \mathcal{O}(\eta_F^2)$$

$$G_T^{\Delta} = \frac{1}{\kappa k_F} \left[\mathcal{N} \left\{ w_1^{\Delta}(\tau) \right\} \right] + \mathcal{O}(\eta_F^2).$$

Scaling function in the Δ peak

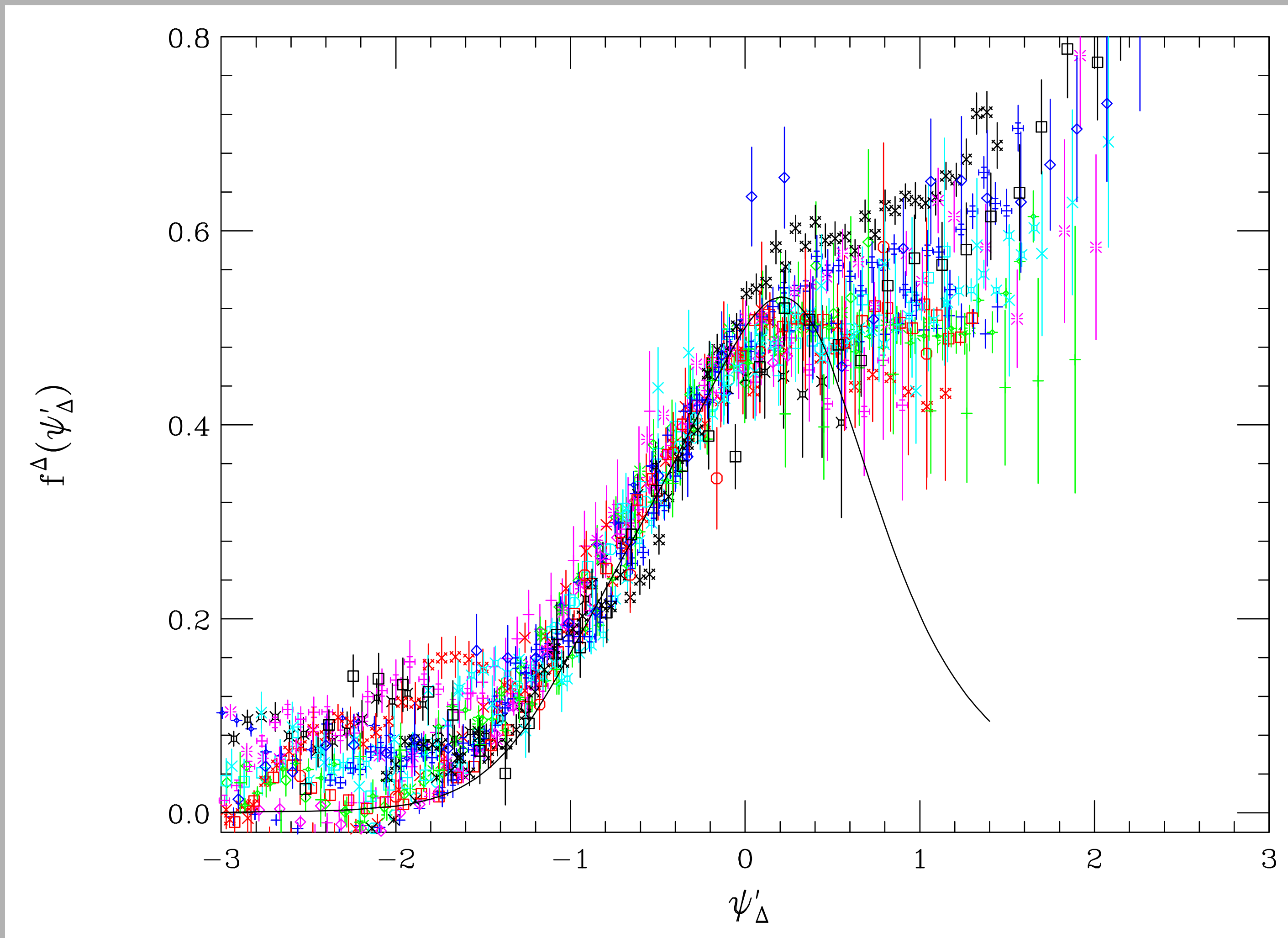

Scaling function in the Δ peak

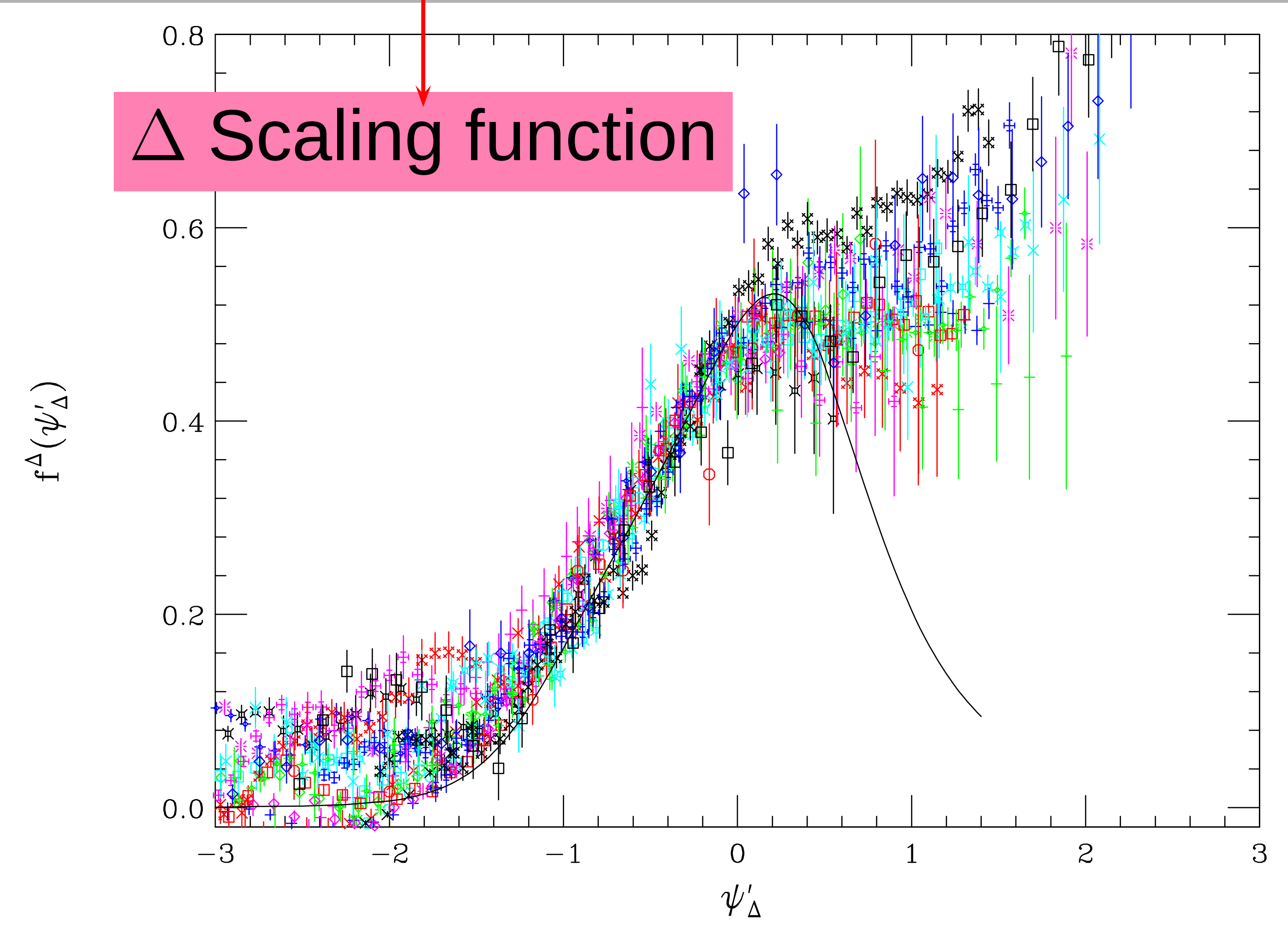

Scaling function in the Δ peak

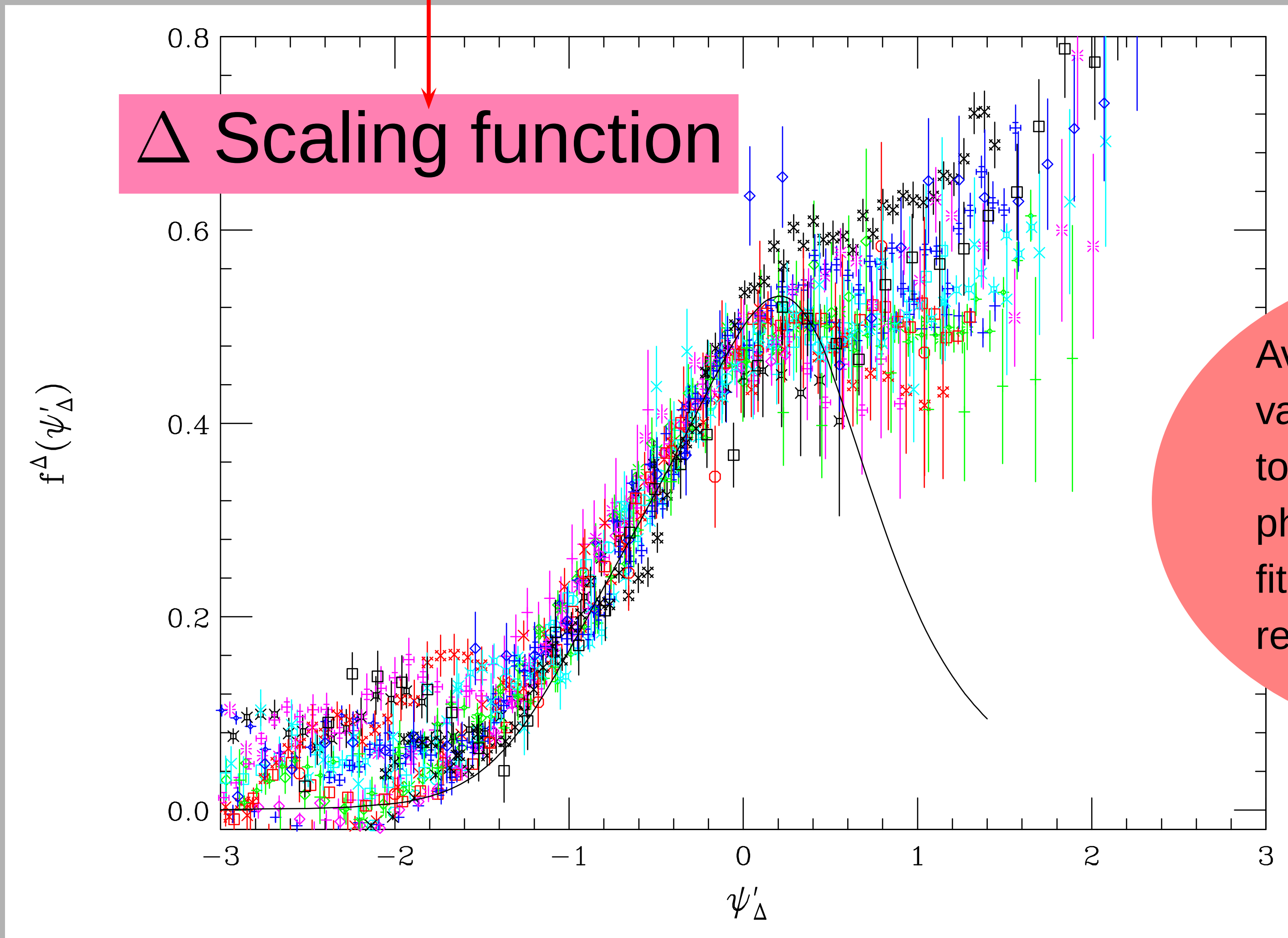

Averaged experimental values of $f^{\Delta}(\psi'_{\Delta})$ together with a phenomenological fit (whose validity is restricted to $\psi'_{\Delta} < 0$).

(e, e') *SuSA results (I)*

Cross section computed with scaling functions

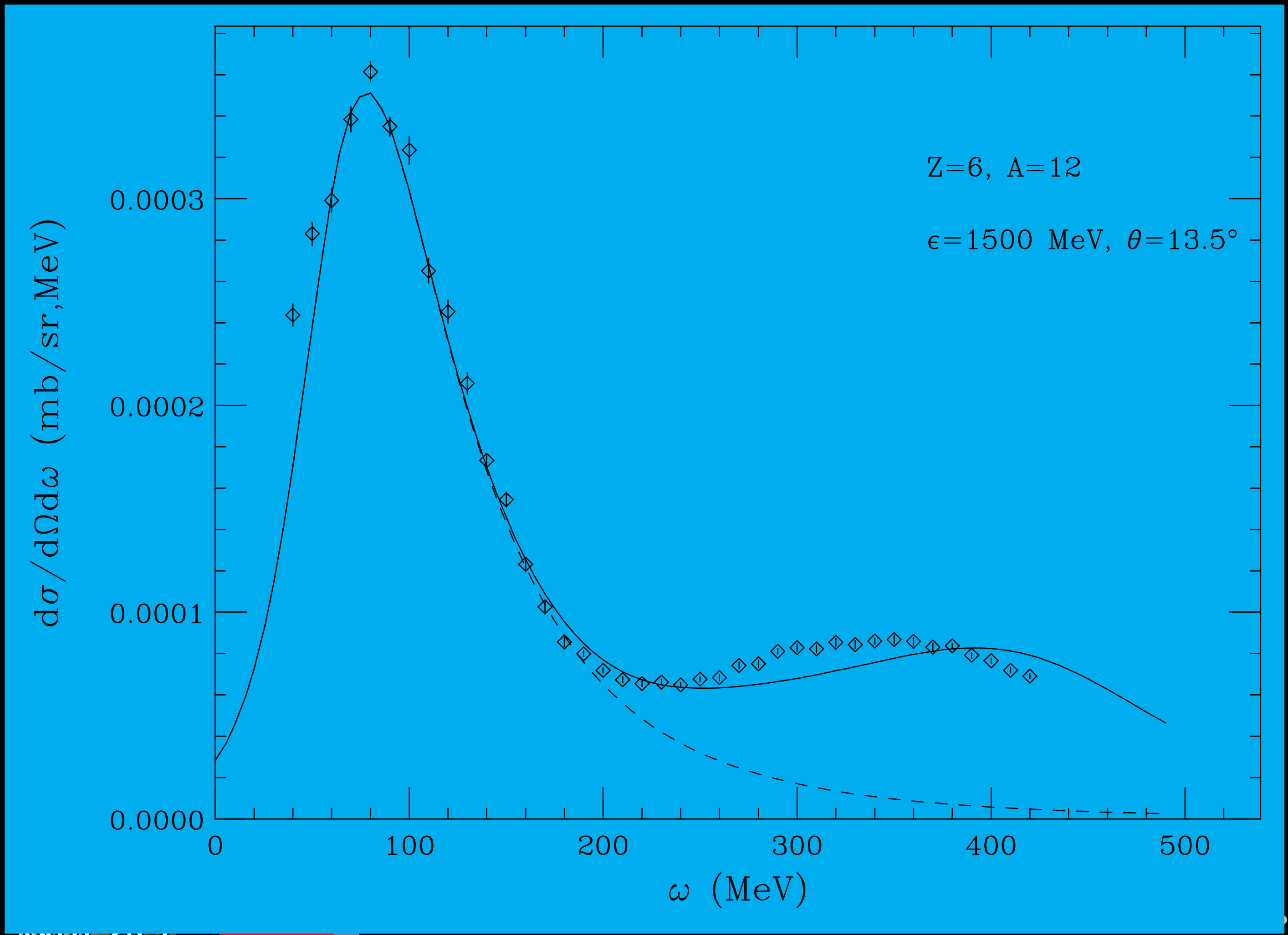

(e,e') *SuSA results (I)*

Cross section computed with scaling functions

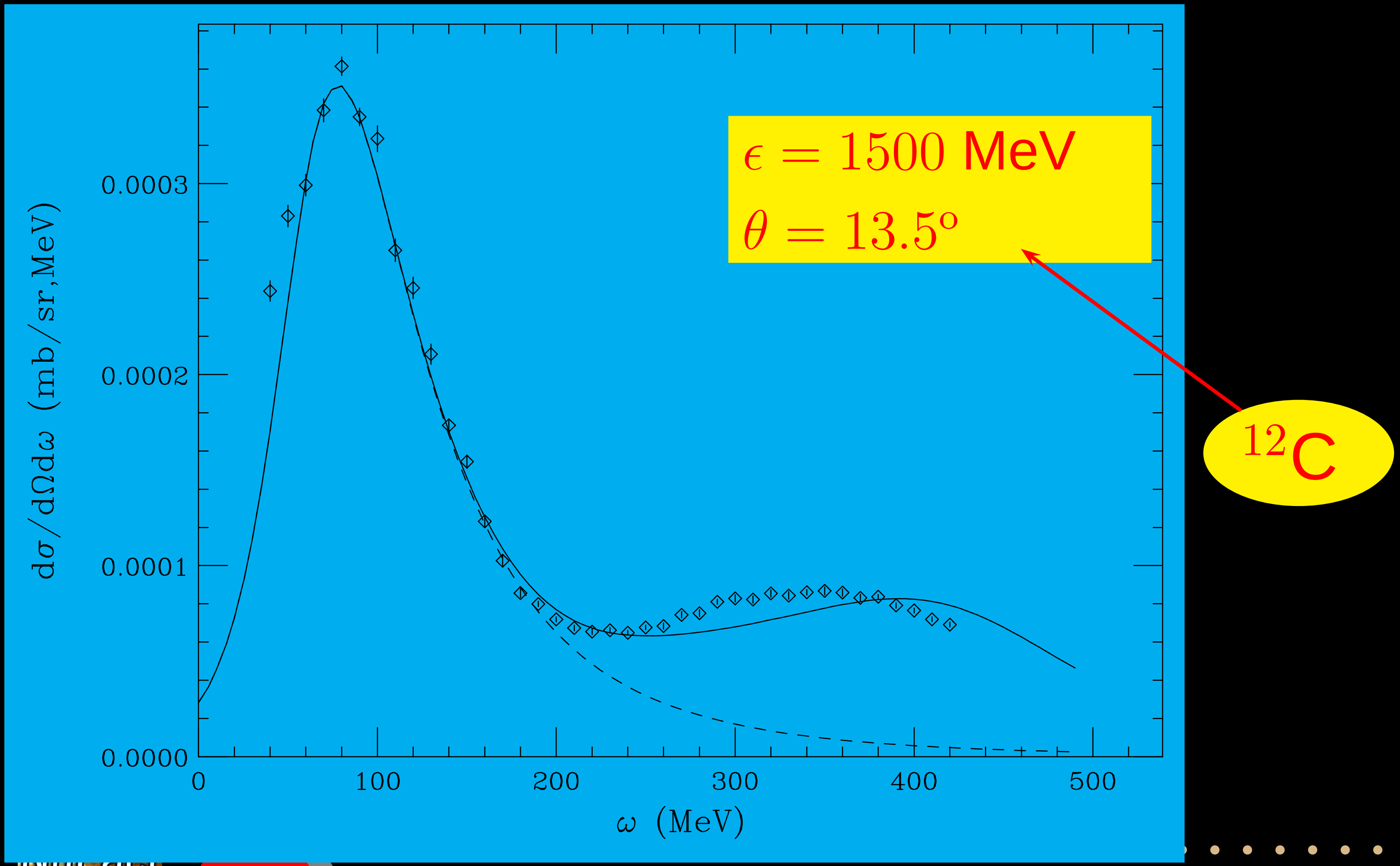

(e,e') *SuSA results (II)*

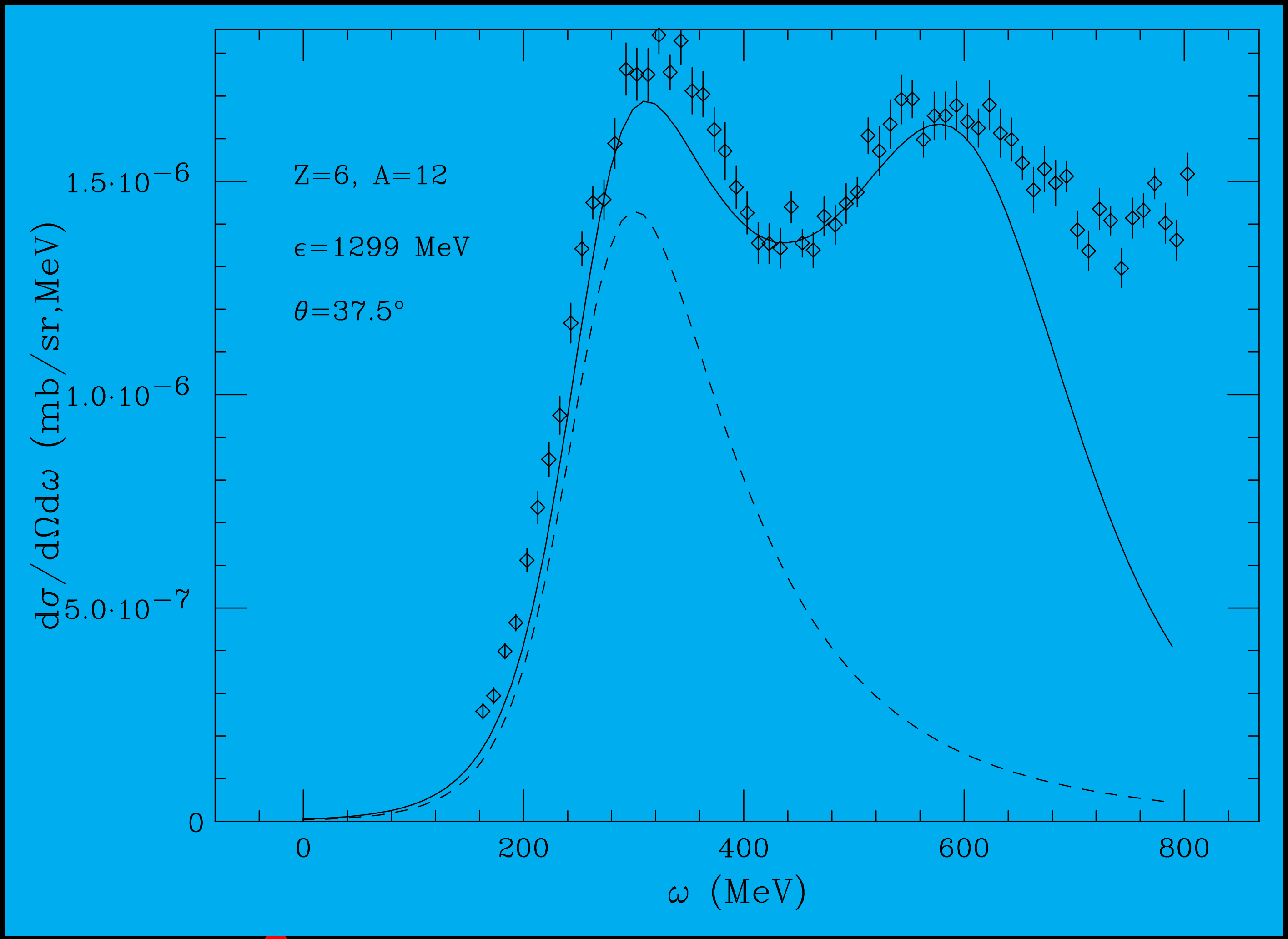

(e, e') *SuSA results (II)*

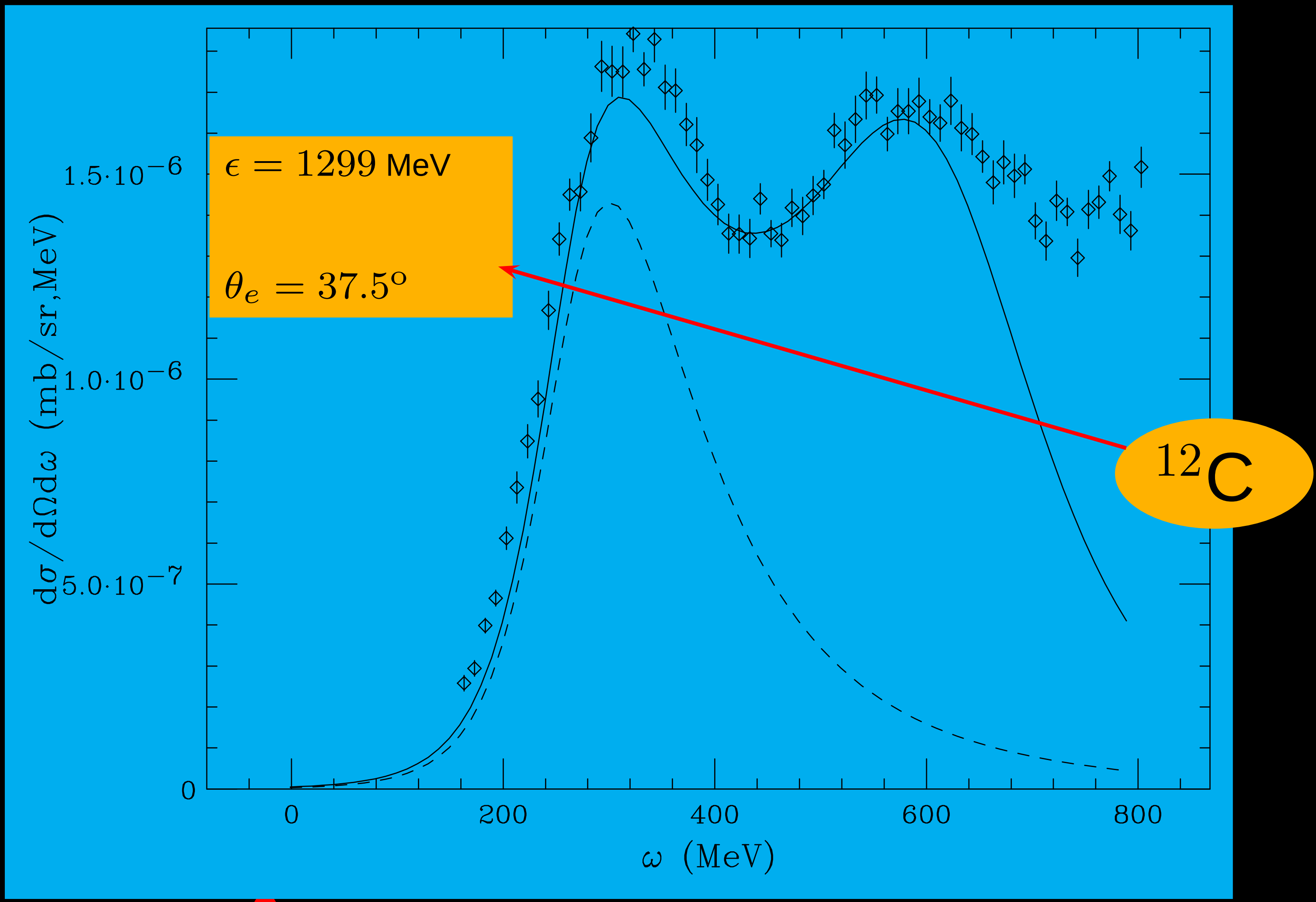

(e, e') *results (III)*

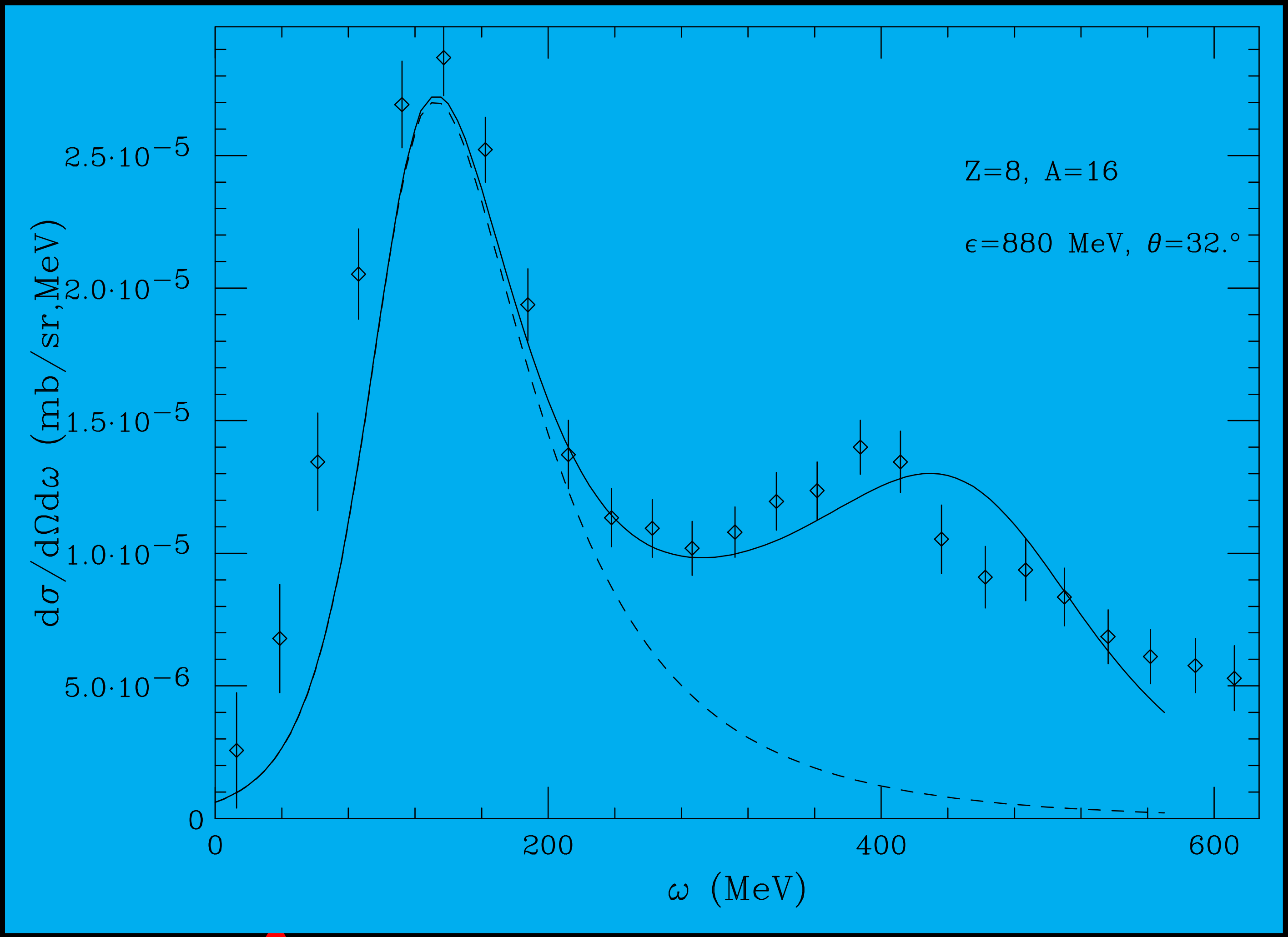

(e,e') *results (III)*

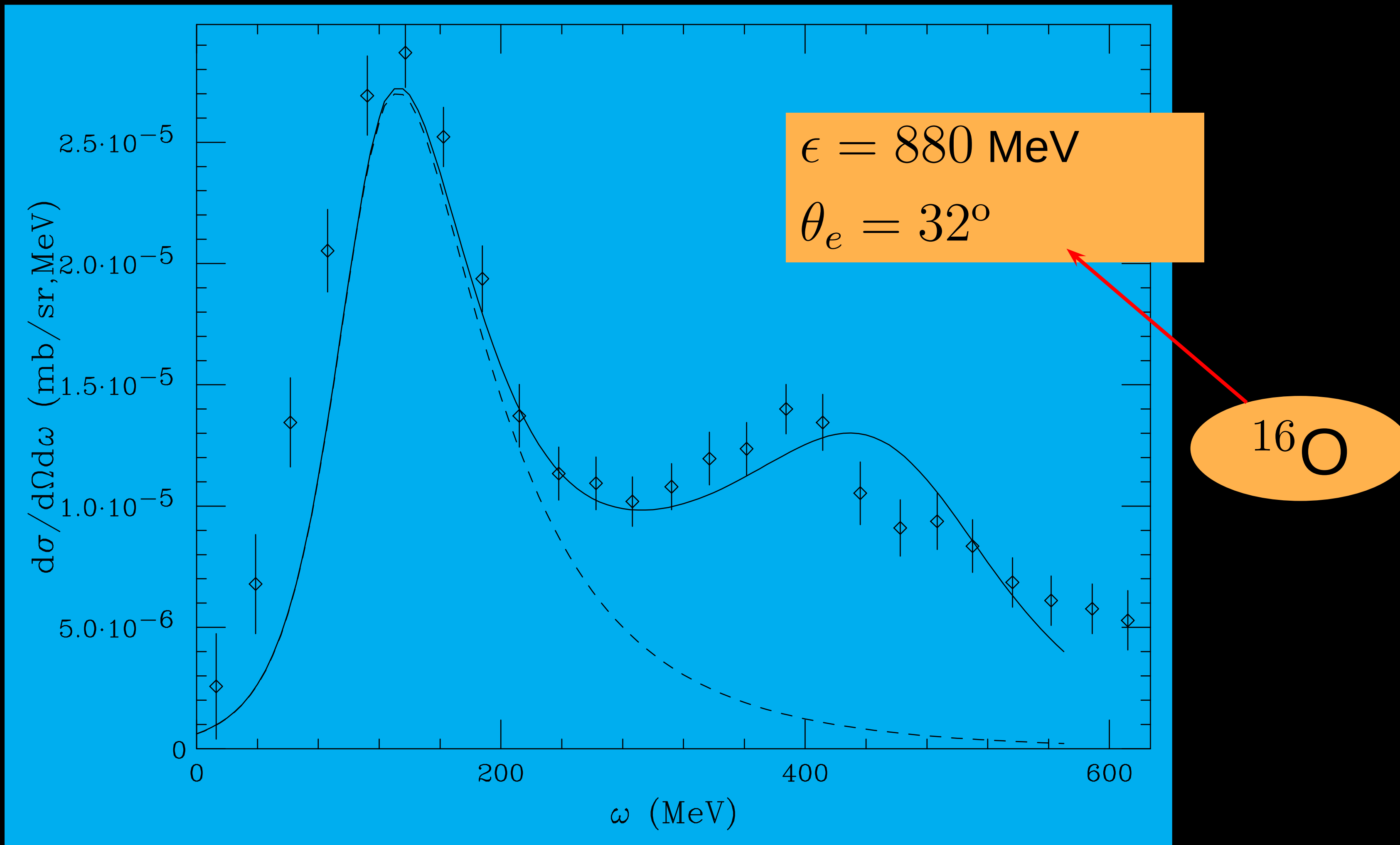

$N(\nu_\mu,\mu^-)\Delta$ *model*

Elementary reactions

$$\nu_\mu p \longrightarrow \mu^-\Delta^{++} \quad (1)$$

$$\nu_\mu n \longrightarrow \mu^-\Delta^{+} \quad (2)$$

$$\bar{\nu}_\mu p \longrightarrow \mu^+\Delta^{0} \quad (3)$$

$$\bar{\nu}_\mu n \longrightarrow \mu^+\Delta^{-}\ . \quad (4)$$

Associated currents [Alvarez-Ruso et al. (1998)]:

$$J^\mu(q) = \mathcal{T}\bar{u}_\alpha^{(\Delta)}(p',s')\Gamma^{\alpha\mu}u(p,s), \quad (5)$$

isospin factor: $\mathcal{T}=\sqrt{3}$ for Δ^{++} and Δ^- production and $=1$ for Δ^+ and Δ^0 production,

$u_\alpha^{(\Delta)}(p',s')$: Rarita-Schwinger spinor

$N(\nu_\mu, \mu^-)\Delta$ *model*

Vertex tensor [Alvarez-Ruso (1998)]

$$\Gamma^{\alpha\mu} =$$

$$= \left[\frac{C_3^V}{m_N}\left(g^{\alpha\mu}\not{q} - q^\alpha\gamma^\mu\right) + \frac{C_4^V}{m_N^2}\left(g^{\alpha\mu}q\cdot p' - q^\alpha p'^\mu\right) + \frac{C_5^V}{m_N^2}\left(g^{\alpha\mu}q\cdot p - q^\alpha p^\mu\right)\right]\gamma_5$$

$$+ \left[\frac{C_3^A}{m_N}\left(g^{\alpha\mu}\not{q} - q^\alpha\gamma^\mu\right) + \frac{C_4^A}{m_N^2}\left(g^{\alpha\mu}q\cdot p' - q^\alpha p'^\mu\right) + C_5^A g^{\alpha\mu} + \frac{C_6^A}{m_N^2}q^\alpha q^\mu\right]$$

CVC implies $C_6^V = 0$ and PCAC yields
$C_6^A = C_5^A(\mu_\pi^2 + 4\tau)^{-1}$, with $\mu_\pi = m_\pi/m_N$

SuSA (ν_μ, μ) predictions Δ peak

Neutrino energy: $\epsilon = 1$ GeV

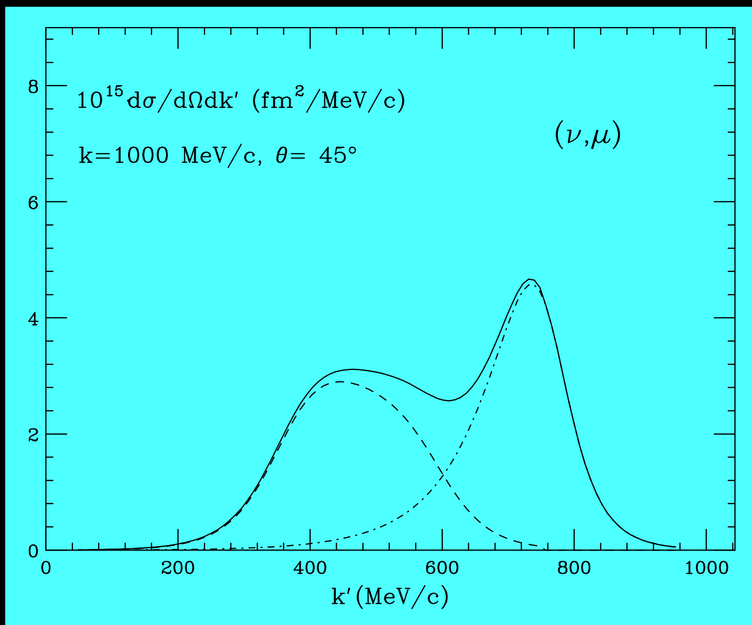

$\theta = 45^o$

SuSA (ν_μ, μ) predictions Δ peak

Neutrino energy: $\epsilon = 1$ GeV

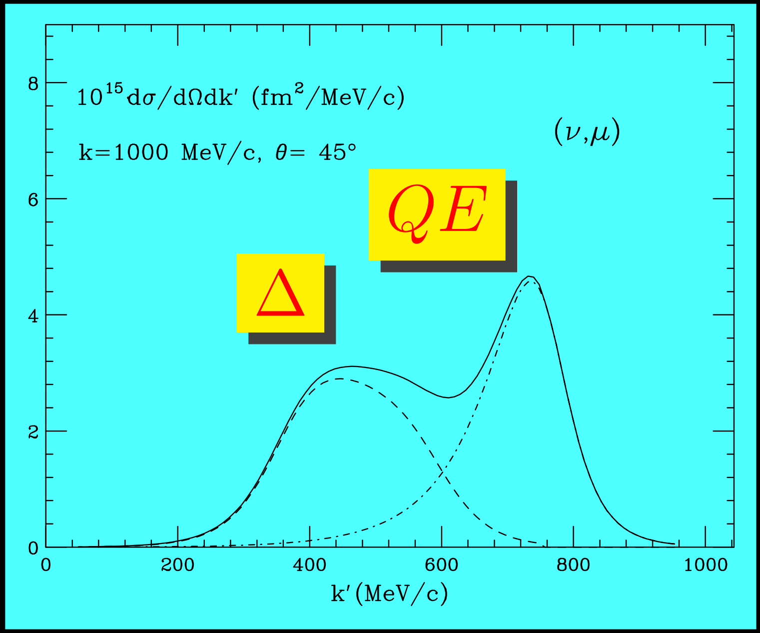

$\theta = 45^{\rm o}$

SuSA (ν_μ, μ) *predictions* Δ *peak*

Neutrino energy: $\epsilon = 1$ GeV

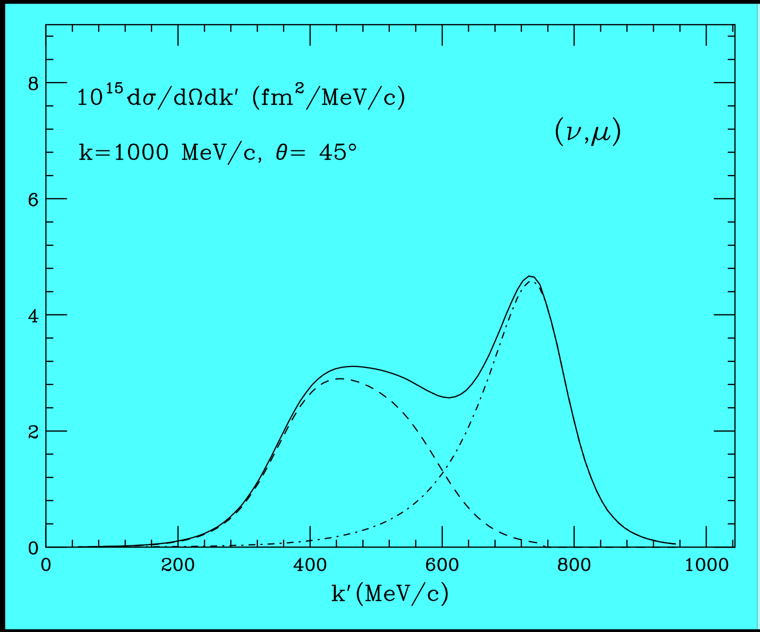

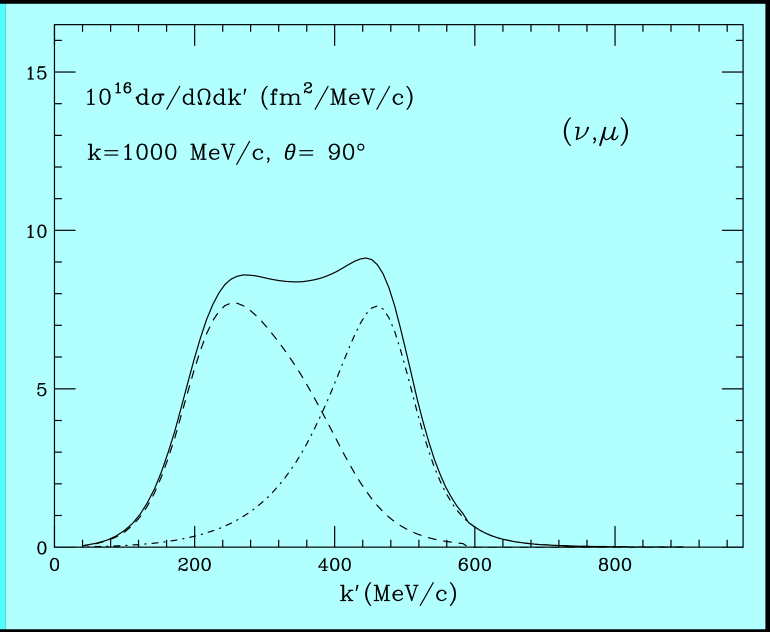

$\theta = 45^o$

$\theta = 90^o$

SuSA (ν_μ, μ) *predictions* Δ *peak*

Neutrino energy: $\epsilon = 1$ GeV

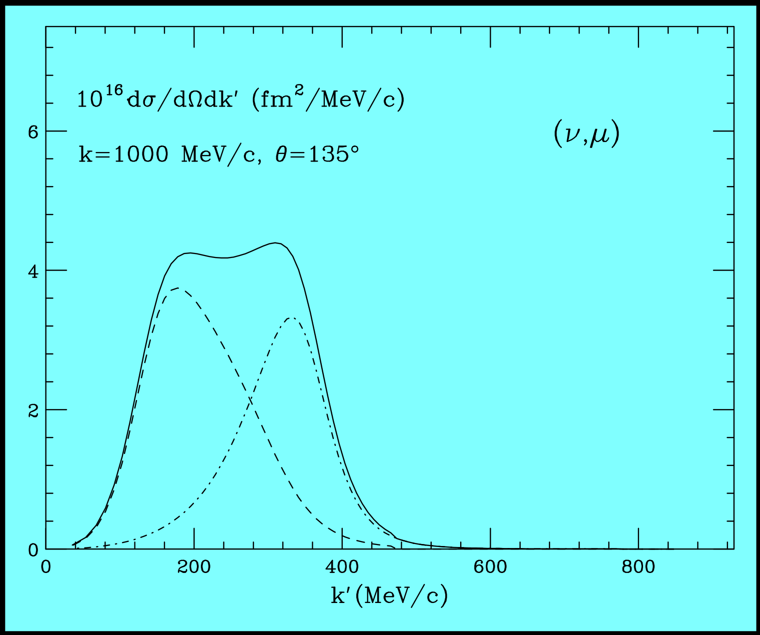

$\theta = 135^o$

SuSA (ν_μ, μ) predictions Δ peak

Neutrino energy: $\epsilon = 1$ GeV

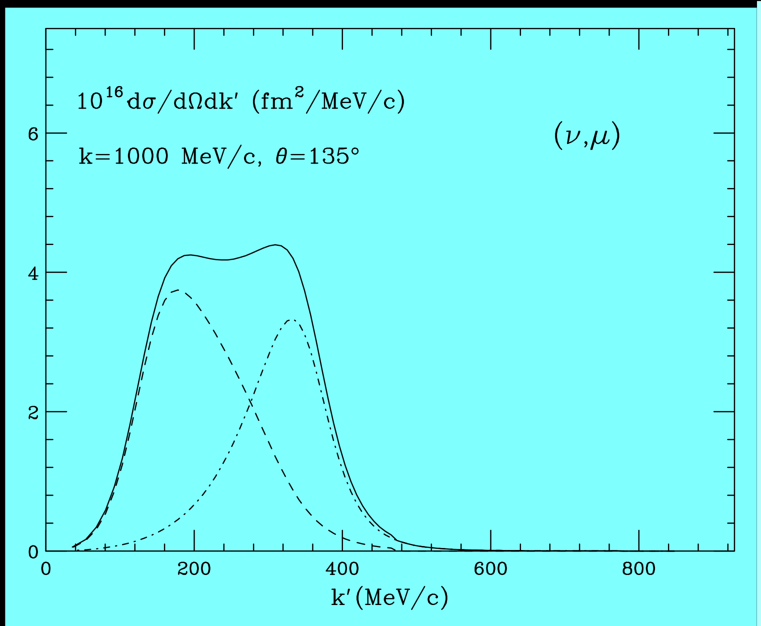

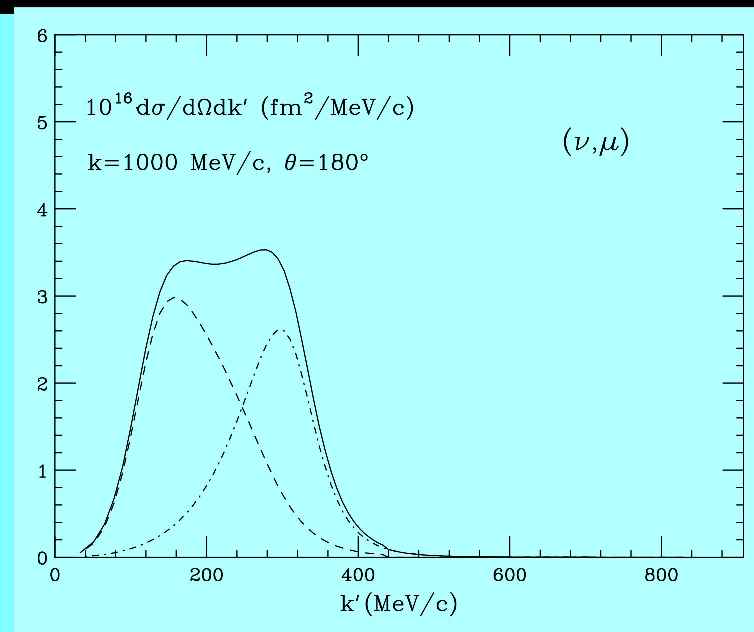

$\theta = 135^o$ $\theta = 180^o$

SuSA $(\overline{\nu}_\mu, \mu^+)$ *predictions* Δ *peak*

Neutrino energy: $\epsilon = 1$ GeV

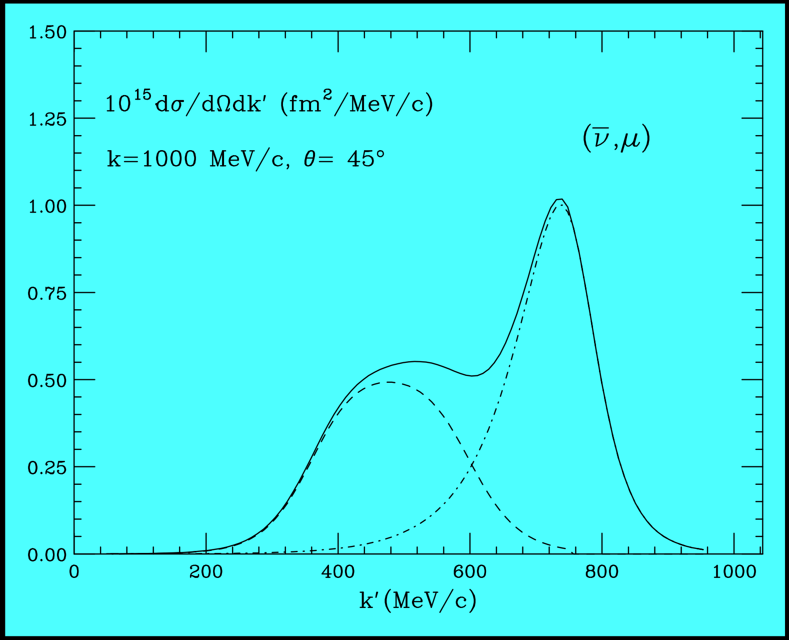

$\theta = 45^\circ$

SuSA $(\overline{\nu}_\mu, \mu^+)$ predictions Δ peak

Neutrino energy: $\epsilon = 1$ GeV

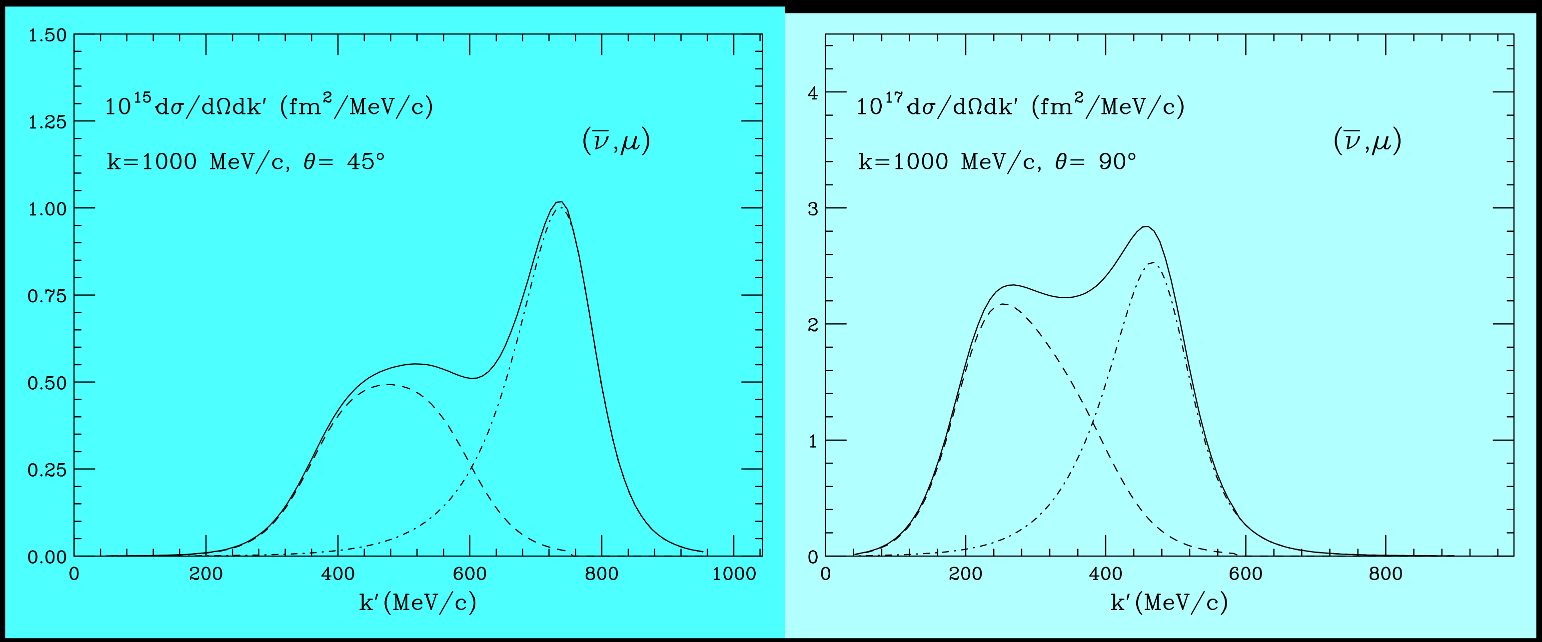

$\theta = 45^o$ $\theta = 90^o$

$(\overline{\nu}_\mu, \mu^+)$ predictions (II)

Neutrino energy: $\epsilon = 1$ GeV

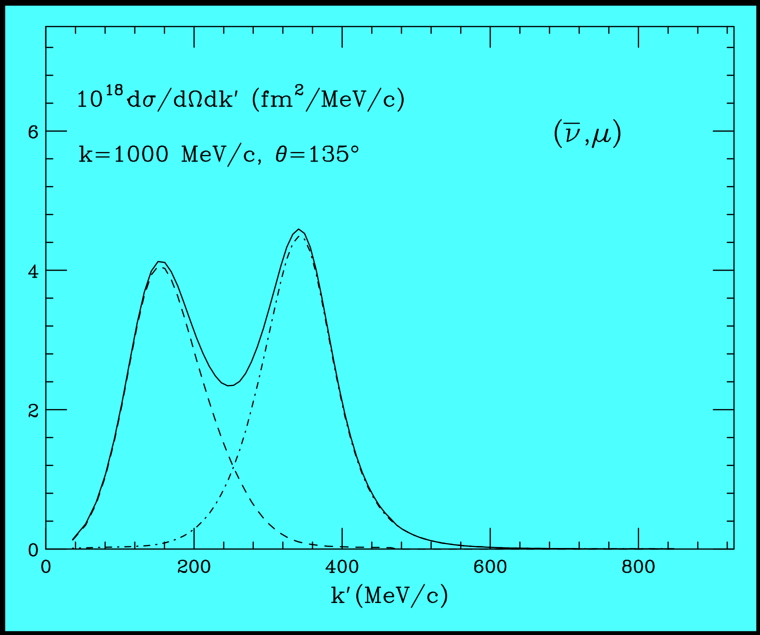

$\theta = 135^o$

$(\overline{\nu}_\mu, \mu^+)$ predictions (II)

Neutrino energy: $\epsilon = 1$ GeV

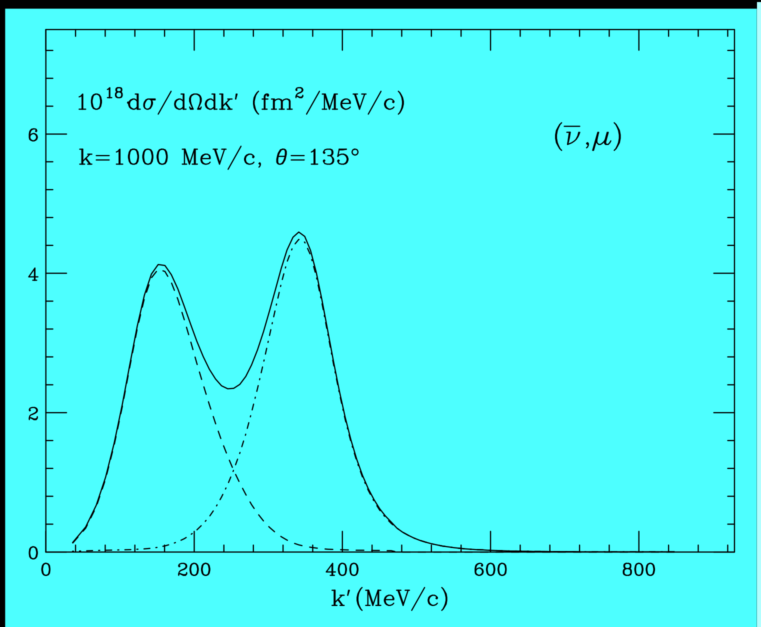

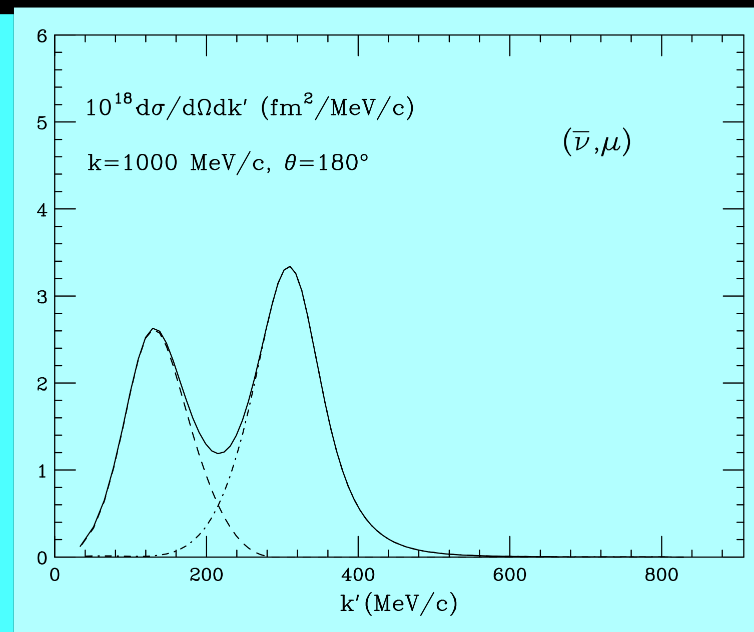

$\theta = 135^o$

$\theta = 180^o$

Angular distribution

At the tops of the QE and Δ peaks - $\epsilon = 1$ GeV

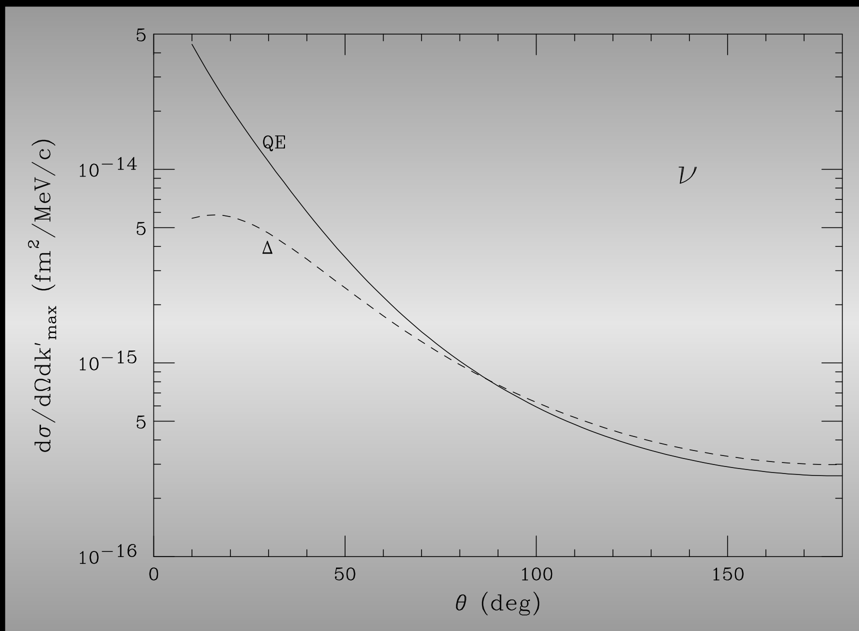

(ν_μ, μ)

Angular distribution

At the tops of the QE and Δ peaks - $\epsilon = 1$ GeV

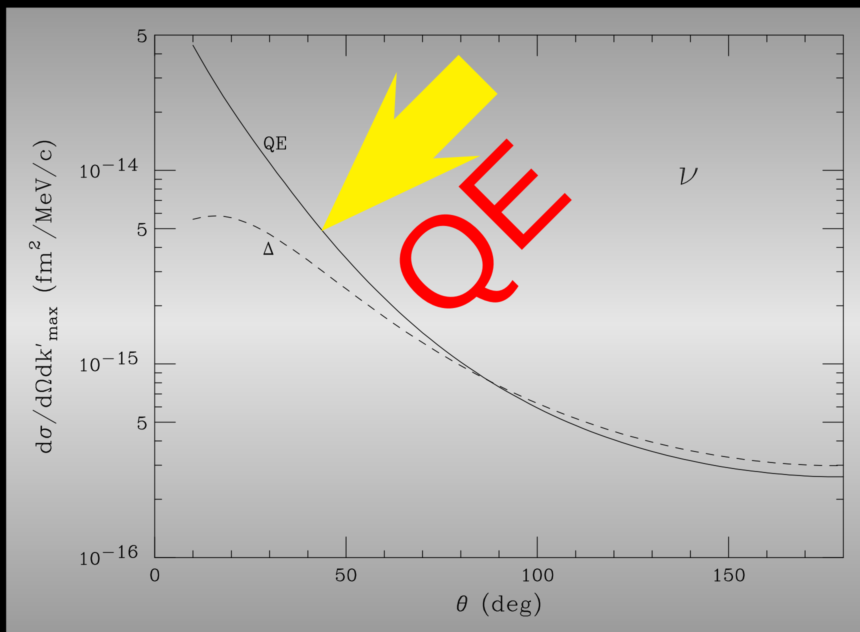

(ν_μ, μ)

Angular distribution

At the tops of the QE and Δ peaks - $\epsilon = 1$ GeV

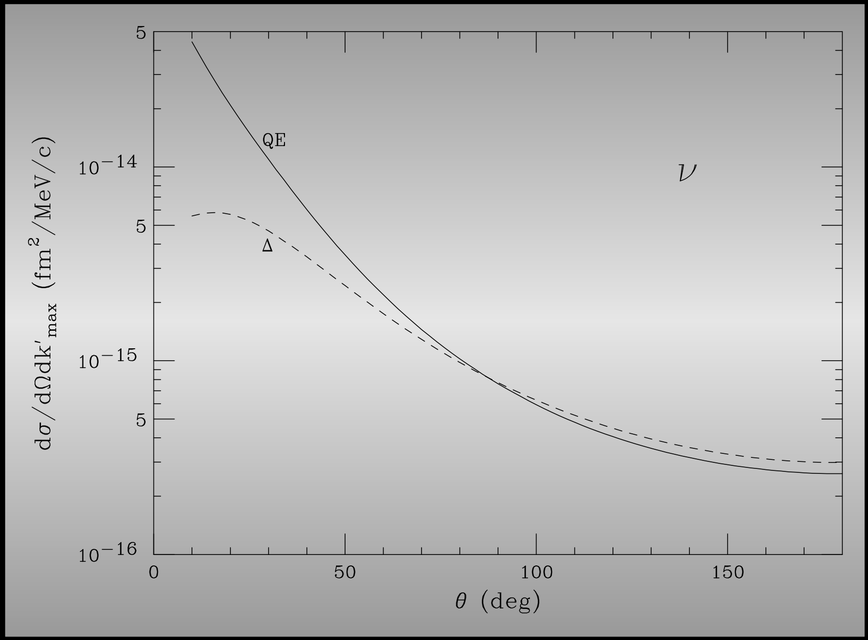

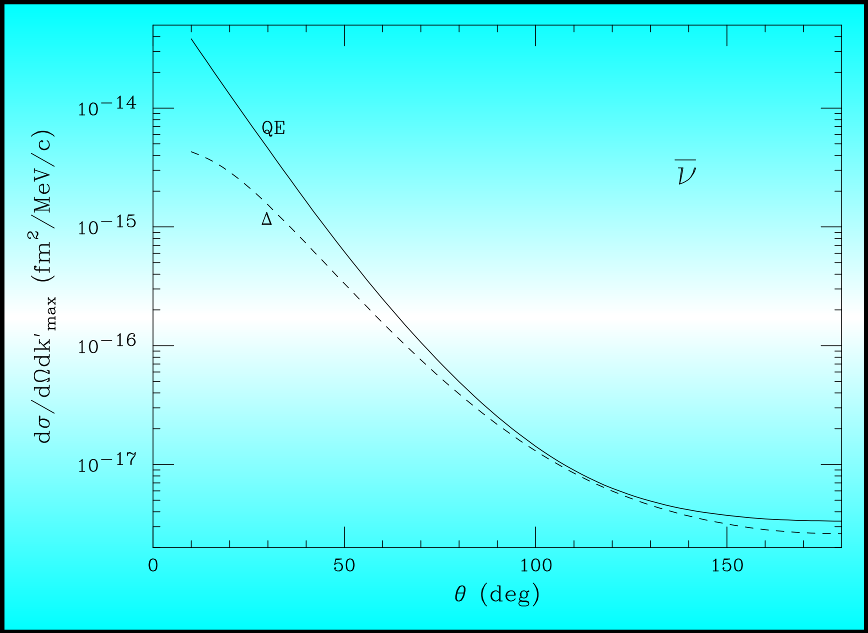

(ν_μ, μ)

$(\overline{\nu}_\mu, \mu^+)$

Comparison with the RFG

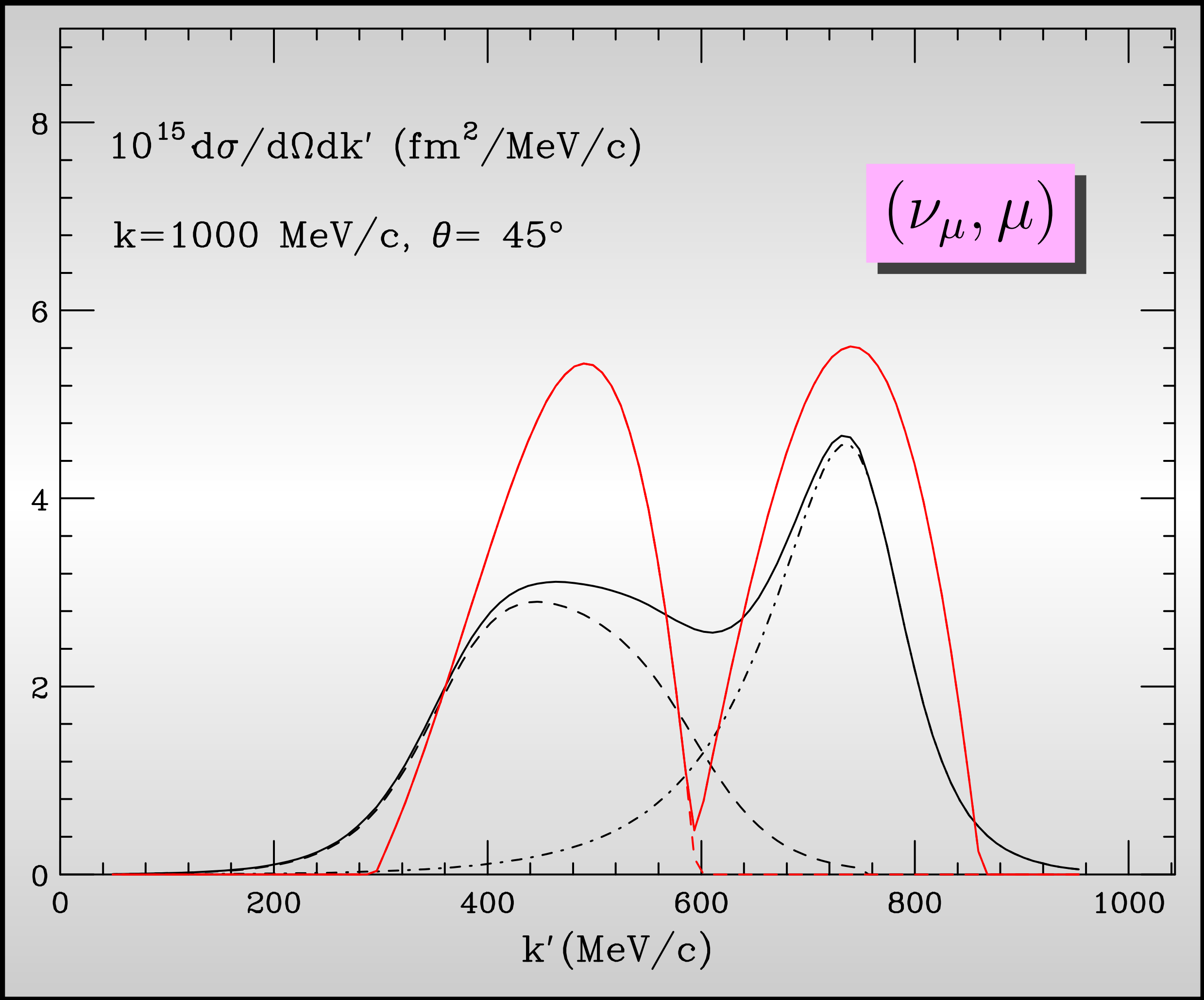

Comparison with the RFG

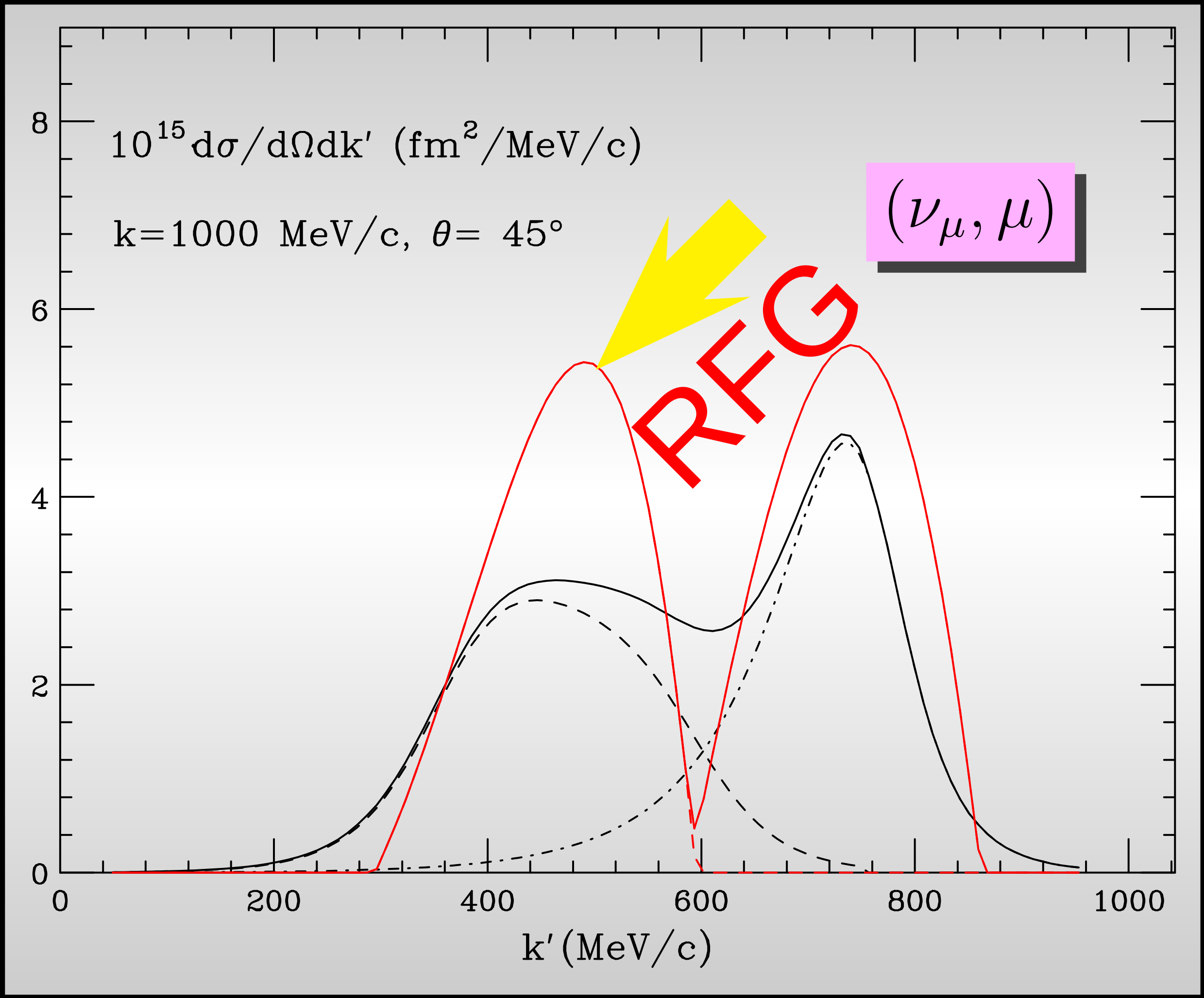

7 Neutral current neutrino reactions

t - Channel inclusive scattering

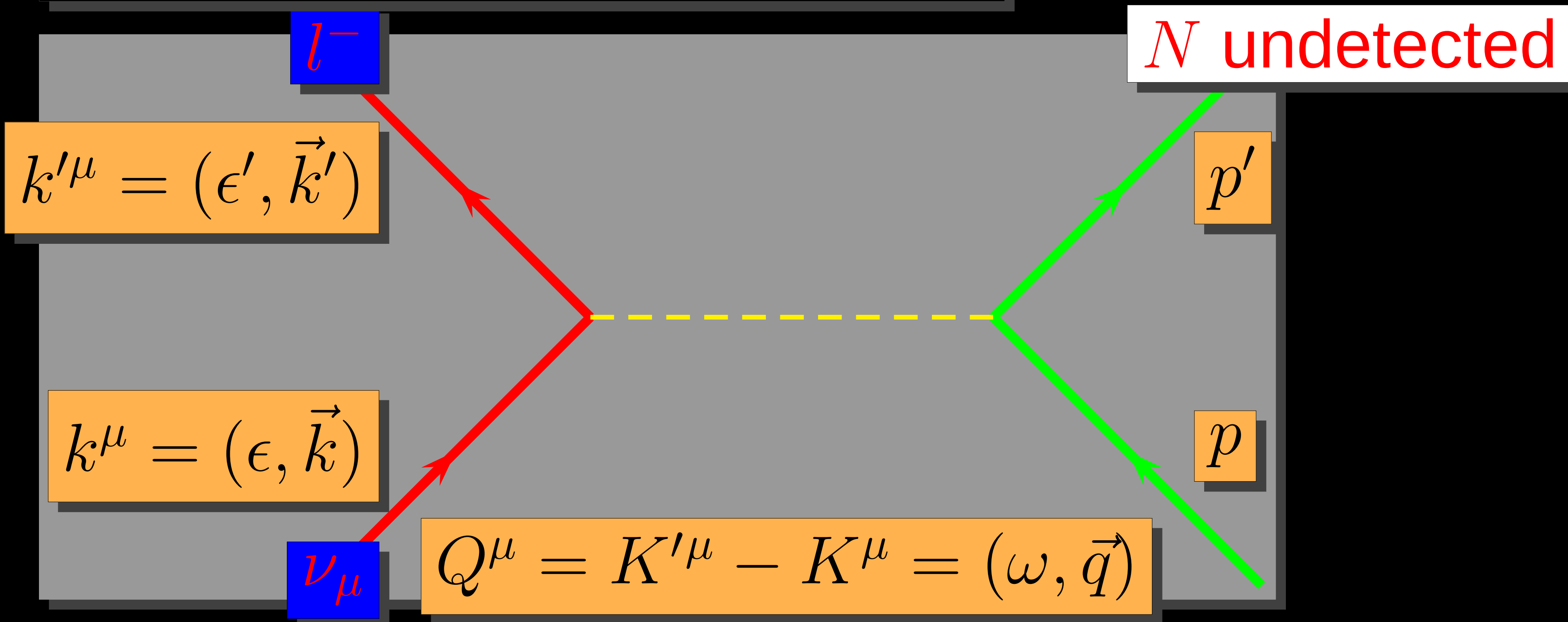

$$\lambda = \frac{\omega}{2m_N} \qquad \kappa = \frac{q}{2m_N} \qquad \tau = \kappa^2 - \lambda^2$$

7 Neutral current neutrino reactions

u - Channel inclusive scattering

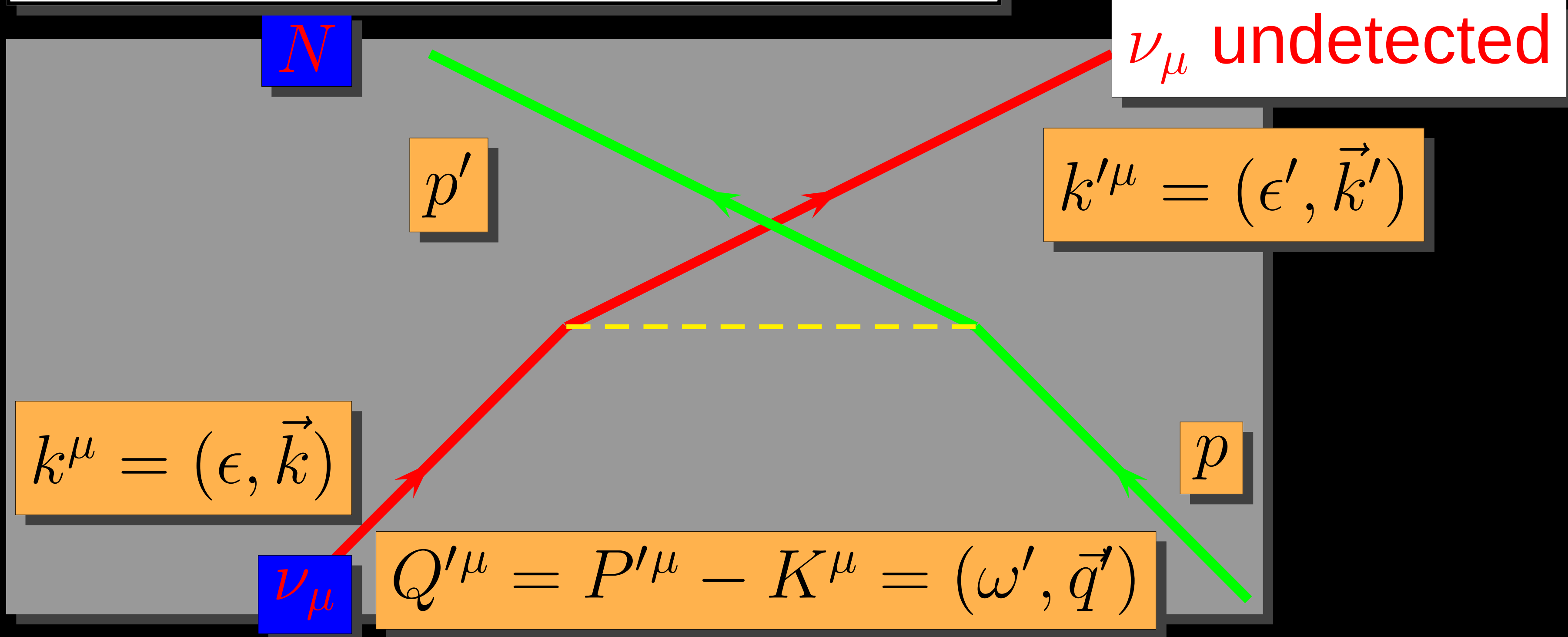

$$\lambda' = \frac{\omega'}{2m_N} \qquad \kappa' = \frac{q'}{2m_N} \qquad \tau' = \kappa'^2 - \lambda'^2$$

SuSA approach to NC neutrino scattering

t-channel (ν_l, l^-)

$$\frac{d\sigma}{d\Omega_{k'}dk'} = \int d\Omega_N dp_N \frac{d\sigma}{d\Omega_{k'}dk'd\Omega_N dp_N} \simeq \overline{\sigma}_{sn}^{(t)} F^{(t)}(\psi^{(t)})$$

Valid exactly for the RFG

u-channel (ν_l, N)

$$\frac{d\sigma}{d\Omega_N dp_N} = \int d\Omega_{k'}dk' \frac{d\sigma}{d\Omega_{k'}dk'd\Omega_N dp_N} \simeq \overline{\sigma}_{sn}^{(u)} F^{(u)}(\psi^{(u)})$$

Good approximation in the RFG

- Extend the SuSA model to the neutral current u-channel
- Assume that $F^{(u)}(\psi) = F^{(t)}(\psi)$
- Use the phenomenological scaling function extracted from (e, e') data to predict NC ν-nucleus cross sections.

Proton knock-out from ^{12}C

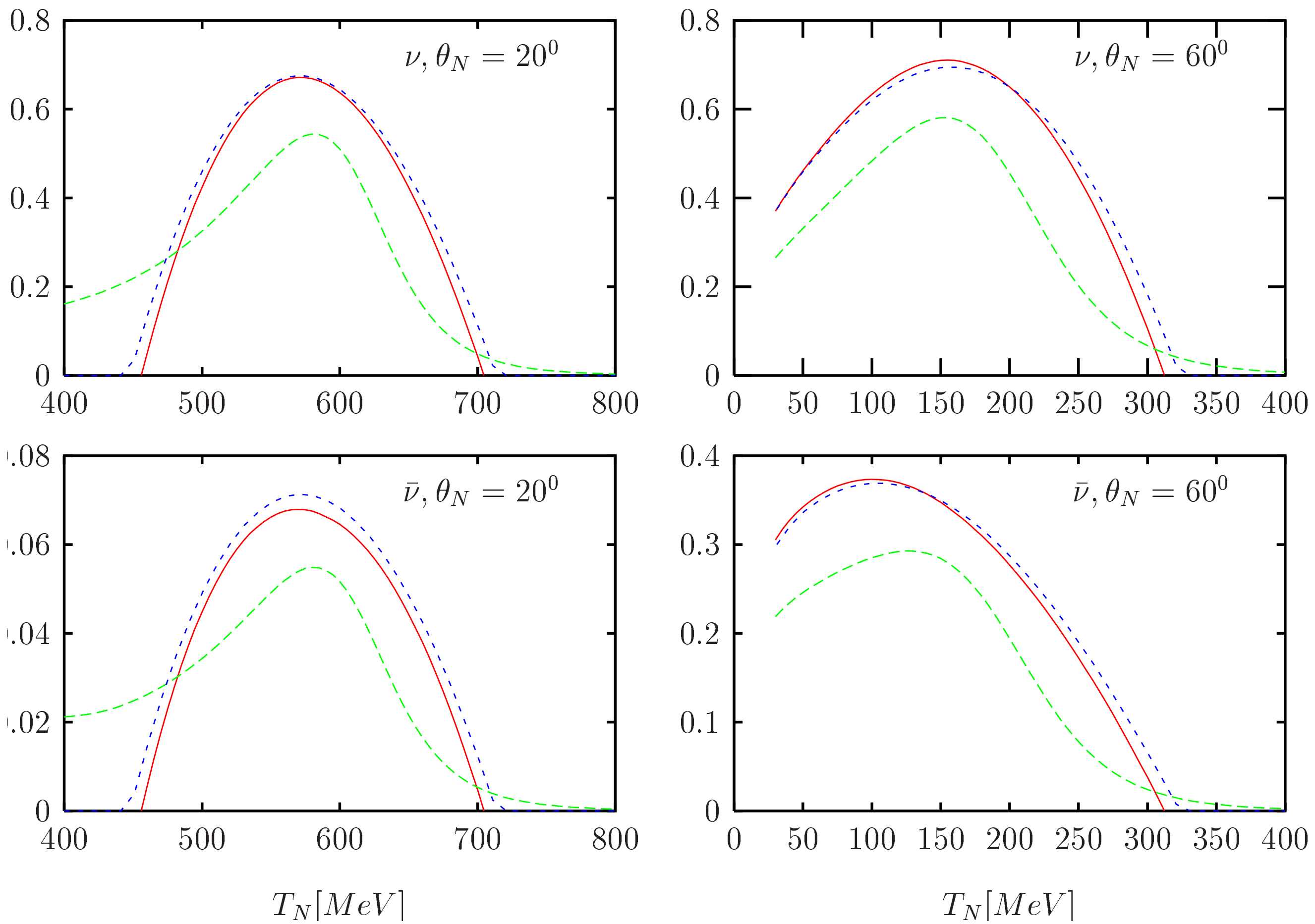

- Blue: RFG
- Red: factorized RFG
- Green: Phenomenological SuSA model

Nucleon strangeness effects

$^{12}\mathrm{C}(\nu_\mu, p)$

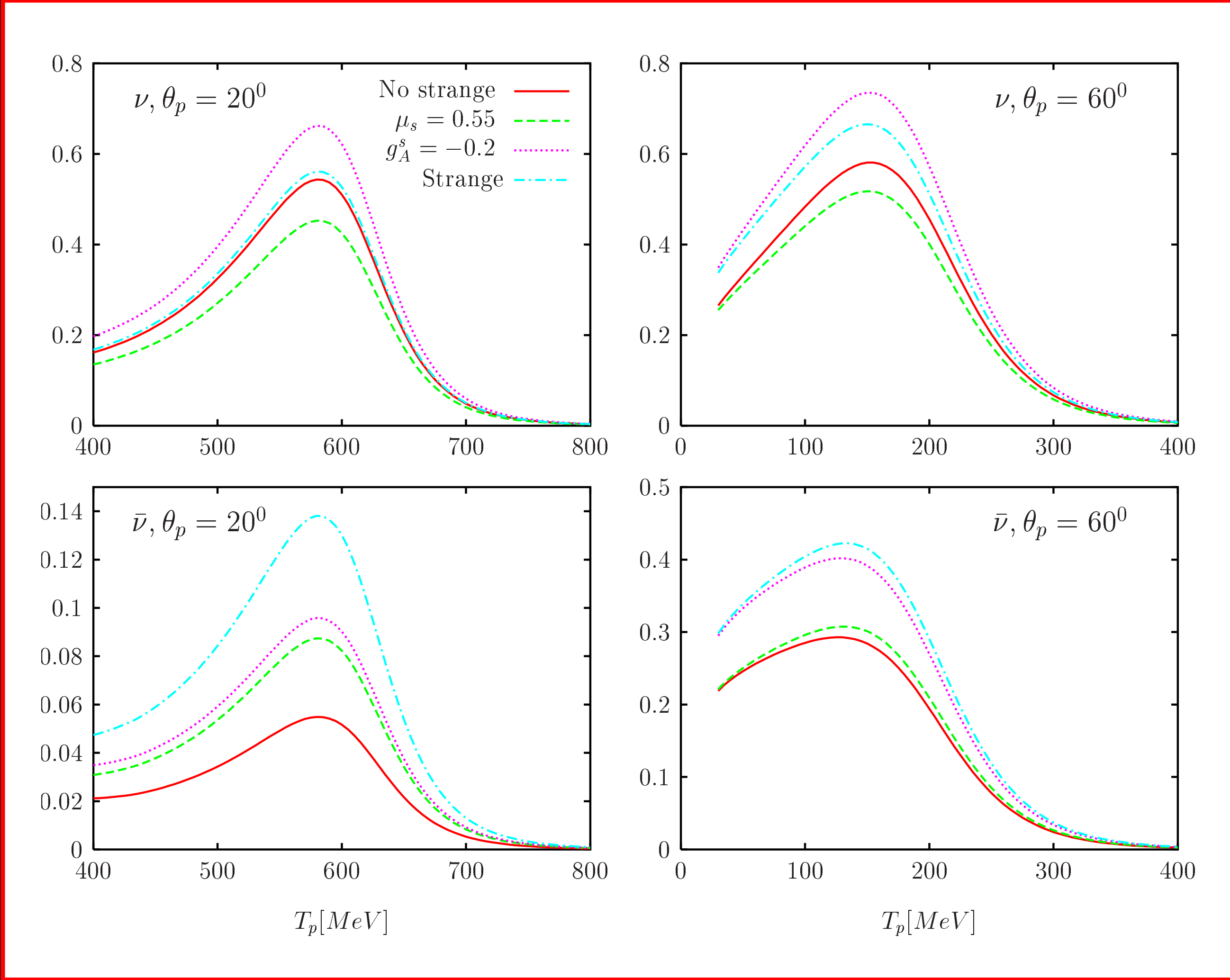

- Blue: strangeness
- Red: no strangeness

Nucleon strangeness effects

$^{12}\mathrm{C}(\nu_\mu, n)$

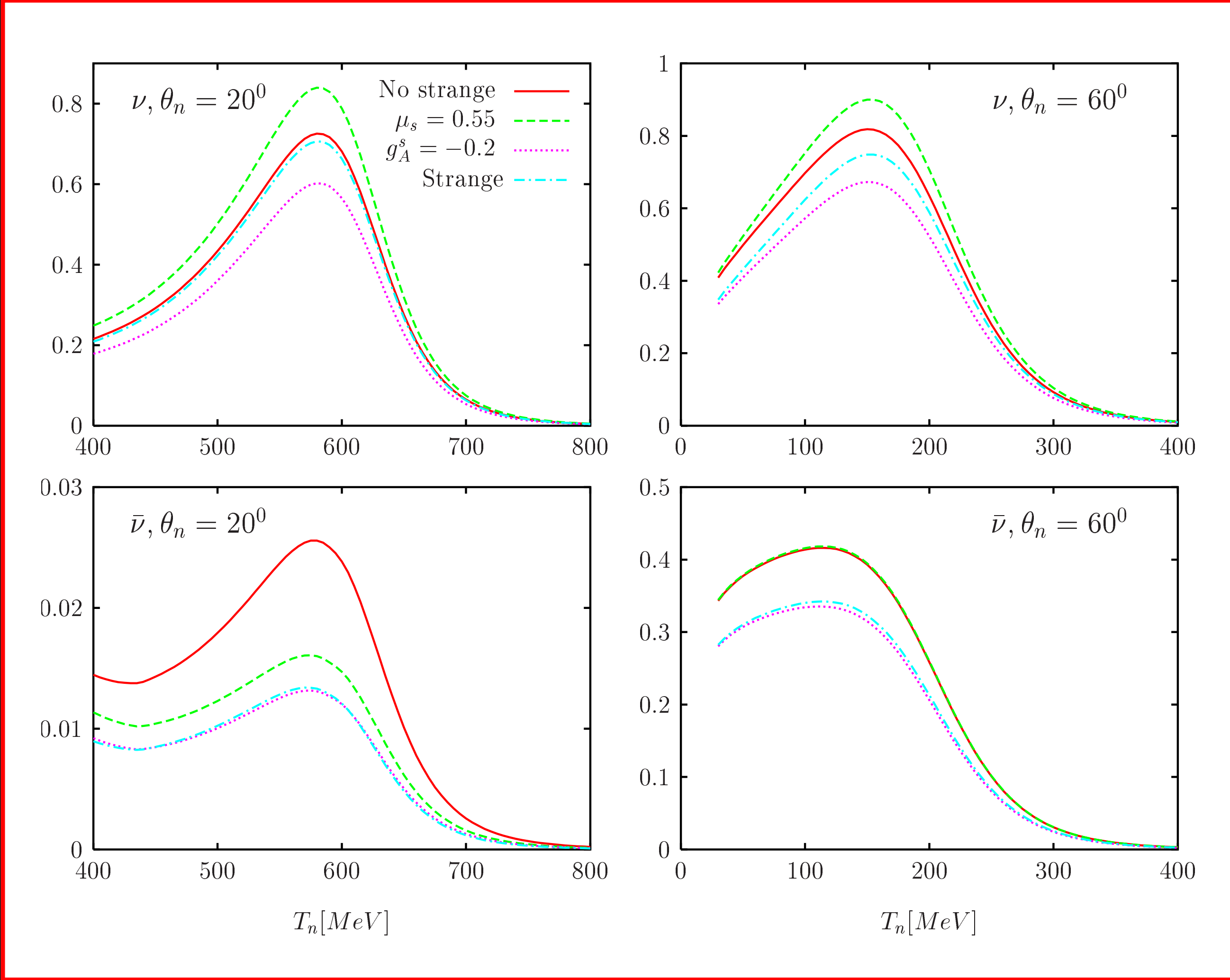

- Blue: strangeness
- Red: no strangeness

8 SuSA predictions for the MiniBooNE QE cross section

J.E. Amaro, M.B. Barbaro, J.A. Caballero, T.W. Donnelly, C.F. Williamson, arXiv:1010.1708, 8 Oct 2010

- Double differential neutrino cross sections from ^{12}C
- Integrated over the neutrino flux
- Data from A.A. Aguilar-Arevalo *et al.*, (MiniBooNE Collaboration), PRD 81, 092005 (2010)
- Contribution of vector meson-exchange currents in the 2p-2h sector

SuSA without MEC

Flux-integrated ν_μ CCQE cross section per target nucleon versus the muon kinetic energy T_μ for various bins of $\cos\theta$. SuSA results fall below the data

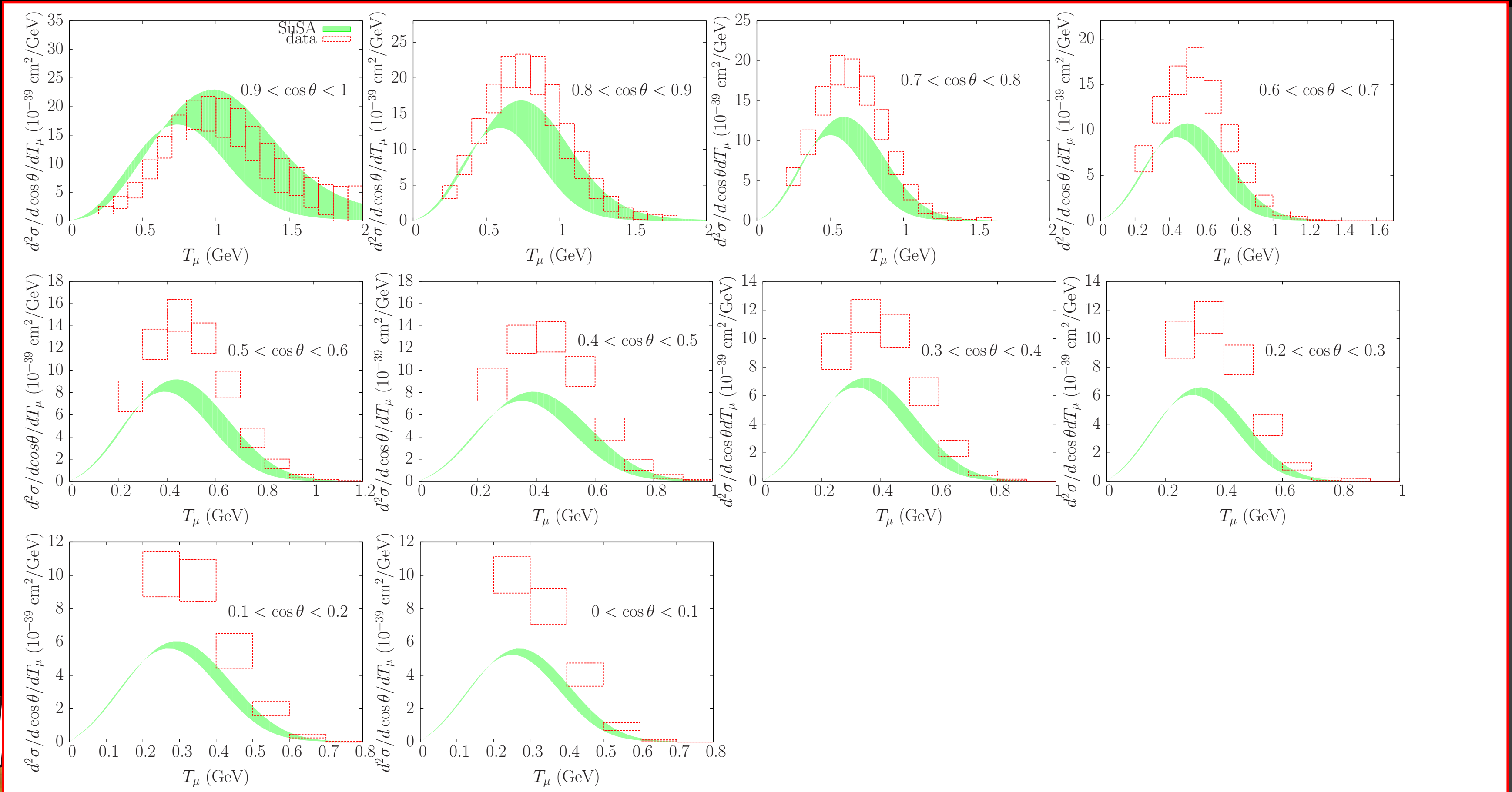

The low q, ω region - small angles

- Approaches like SuSA or the RFG should not be trusted for very forward kinematics.
- Blue band: a lower cut $\omega > 50$ MeV in the integral over neutrino flux

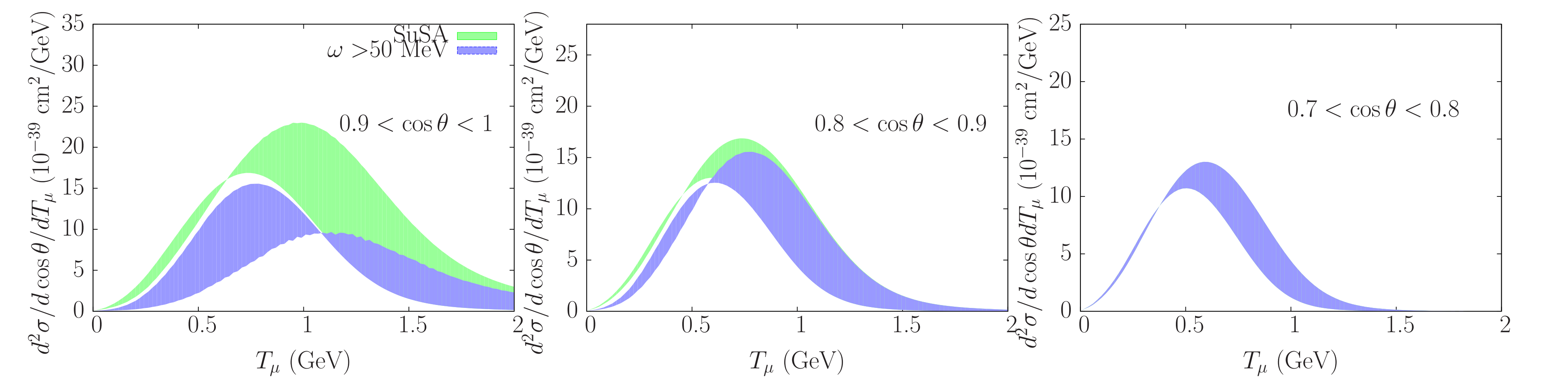

Meson-Exchange Currents (MEC)

Two-particle two-hole Meson Exchange Currents (MEC)

- Relativistic Fermi Gas two-nucleon emission channel
- Added to the SuSA results
- A. De Pace *et al.* NPA 726, 303 (2003)
- J.E. Amaro *et al.* PRC 82, 0444601 (2010)

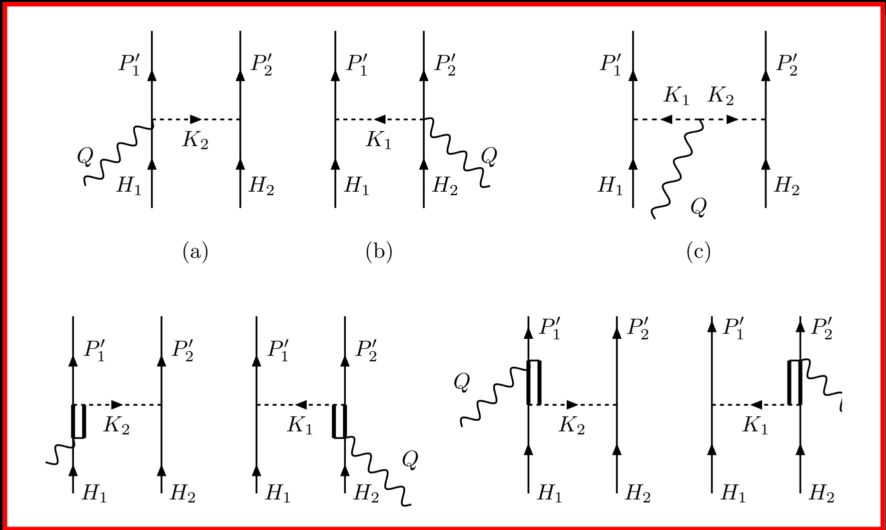

SuSA plus MEC (2p-2h)

- The MEC tend to increase the cross section
- Agreement with data out to $\cos\theta \sim 0.6$.
- At larger angles the MEC are not sufficient to account for the discrepancy

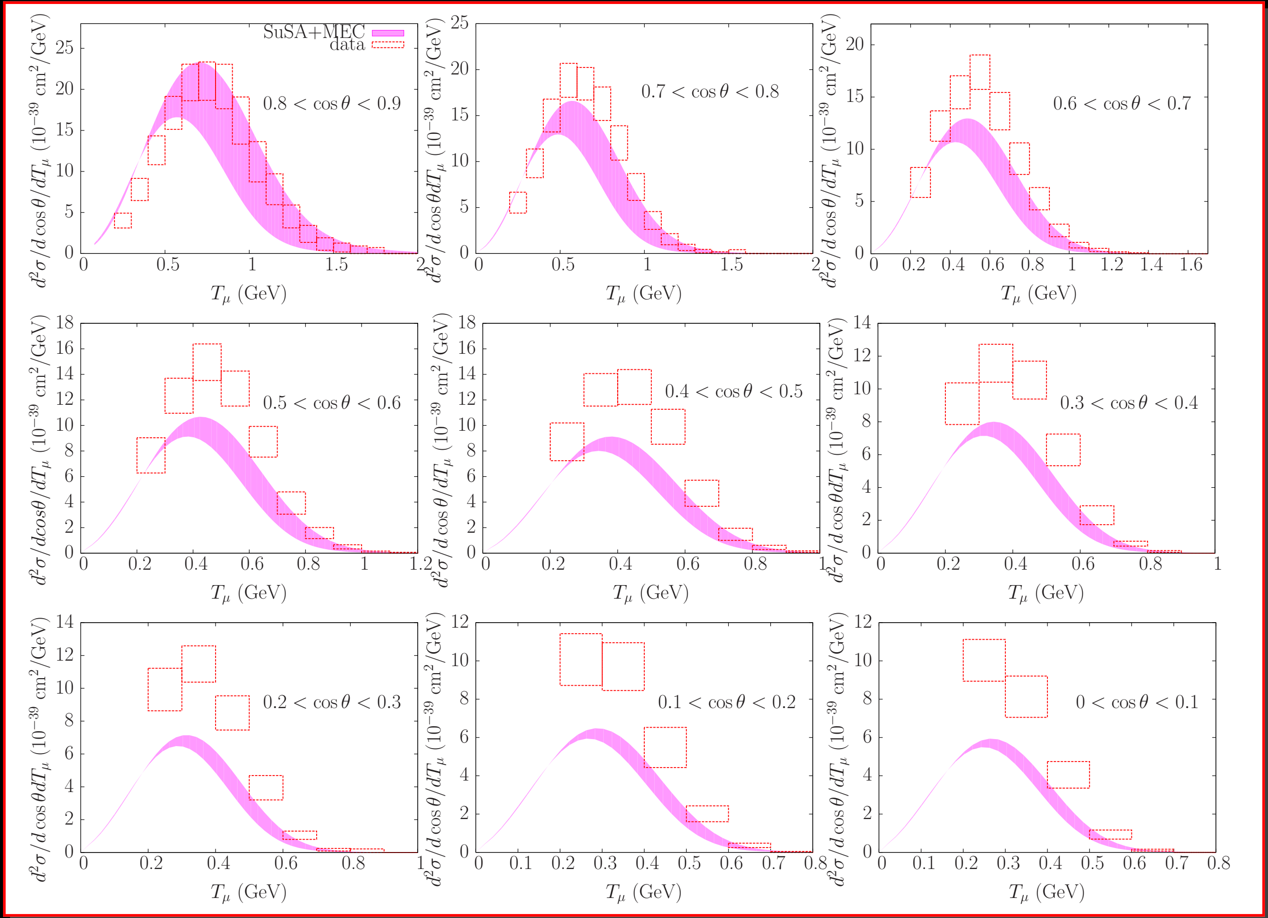

$0.8 < \cos\theta < 0.9$

Without MEC

With MEC

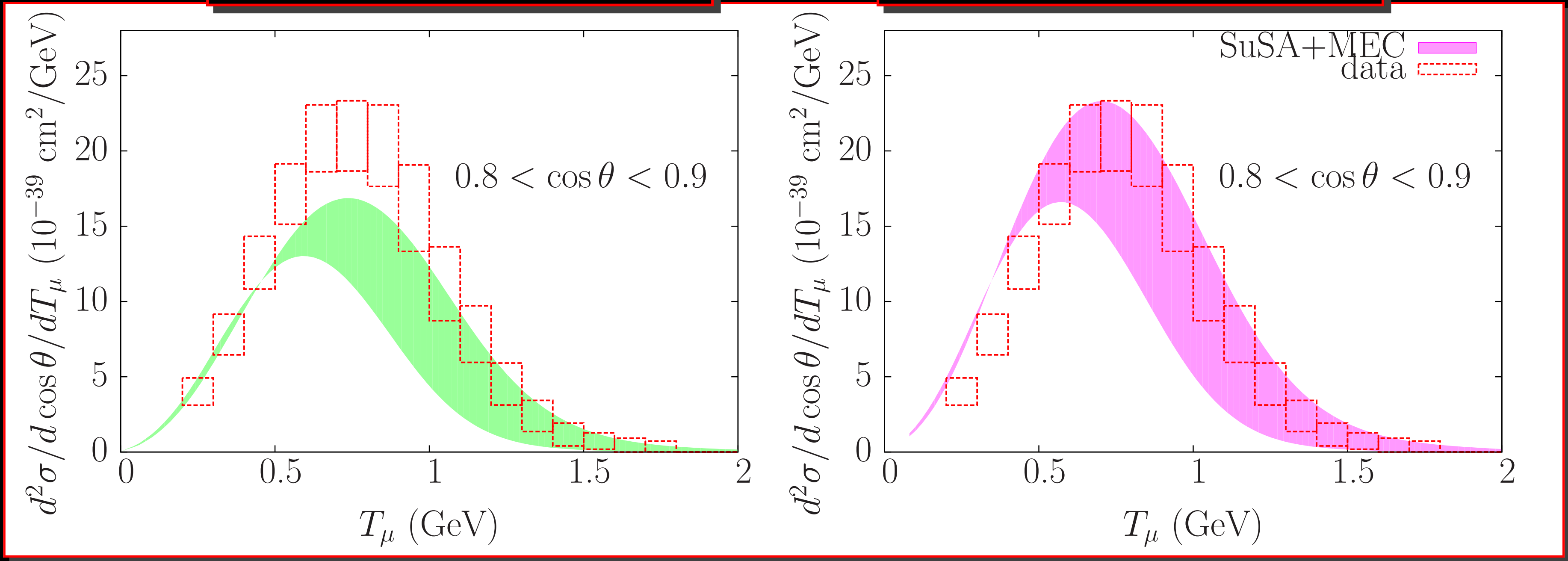

$0.7 < \cos\theta < 0.8$

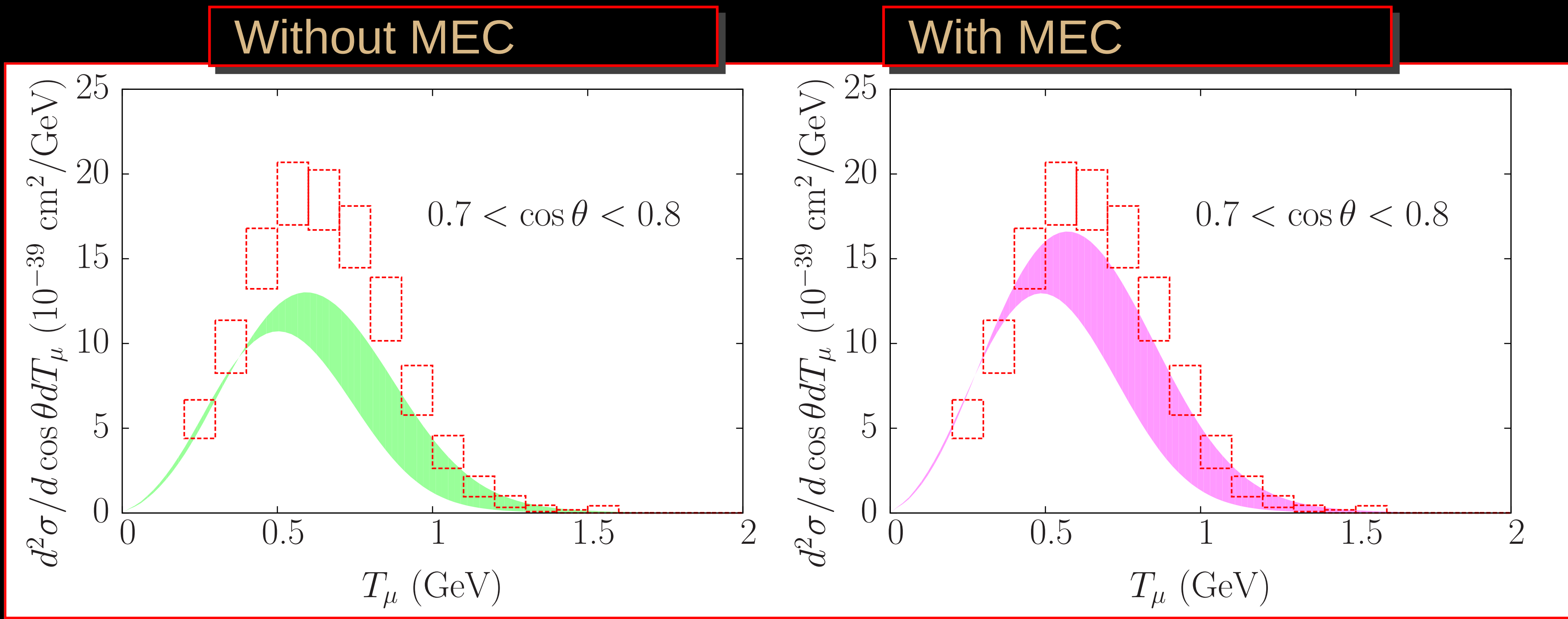

$0.6 < \cos\theta < 0.7$

Without MEC

With MEC

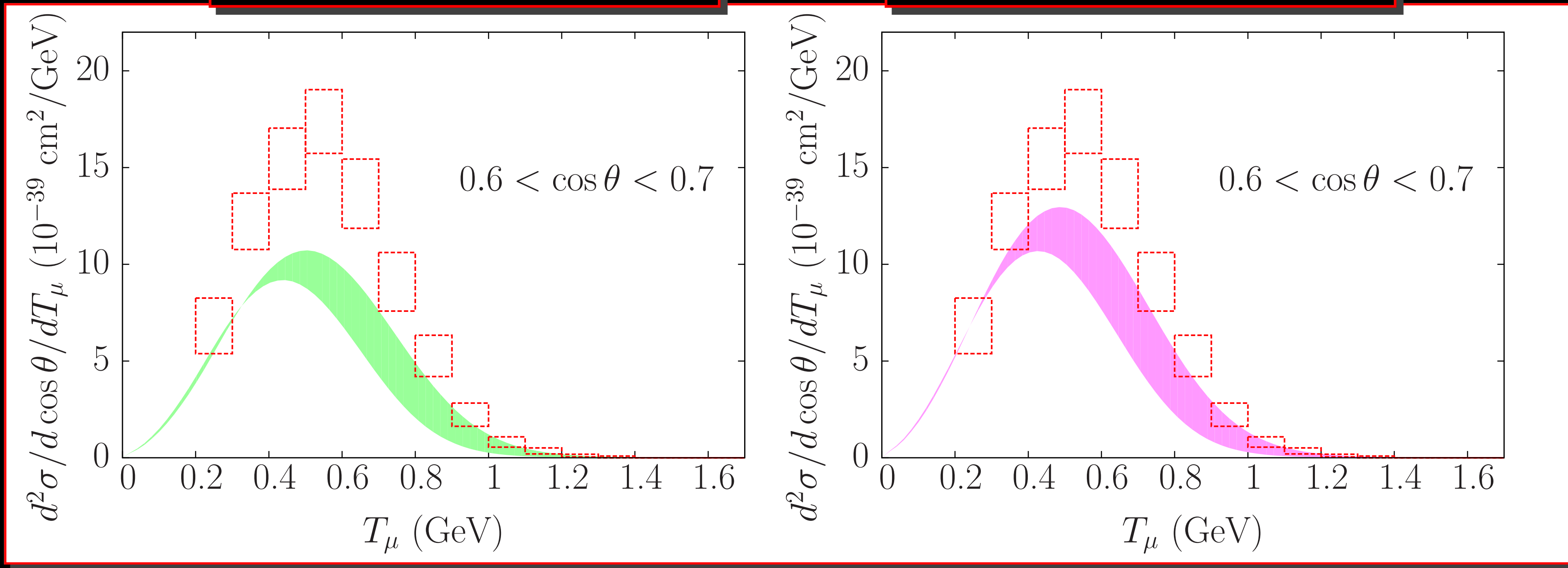

$0.5 < \cos\theta < 0.6$

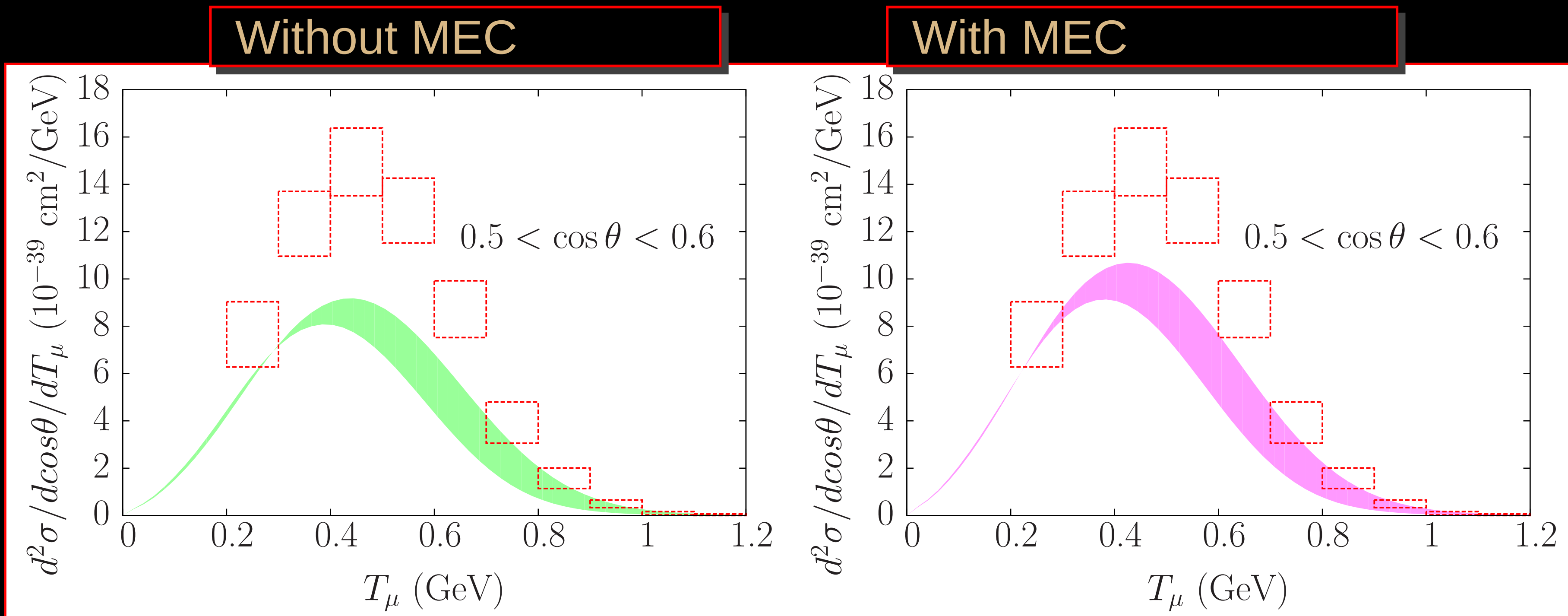

$0.4 < \cos\theta < 0.5$

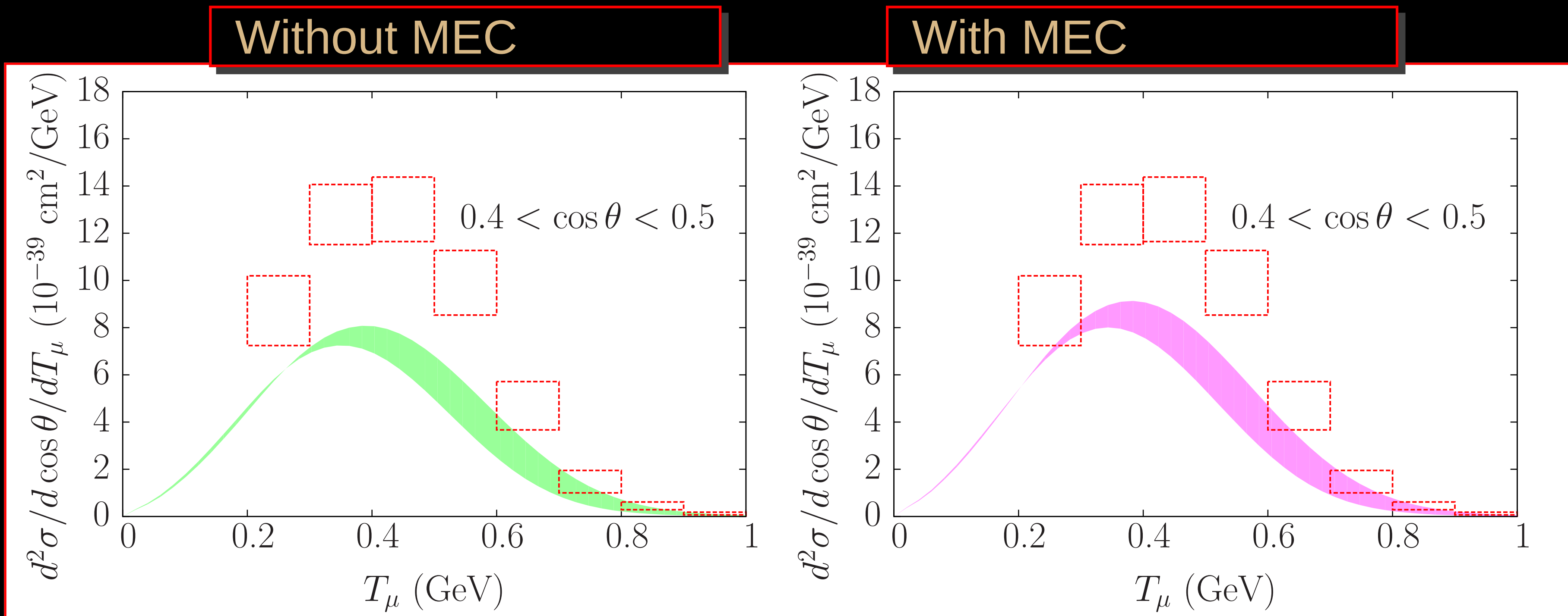

$0.3 < \cos\theta < 0.4$

Without MEC

With MEC

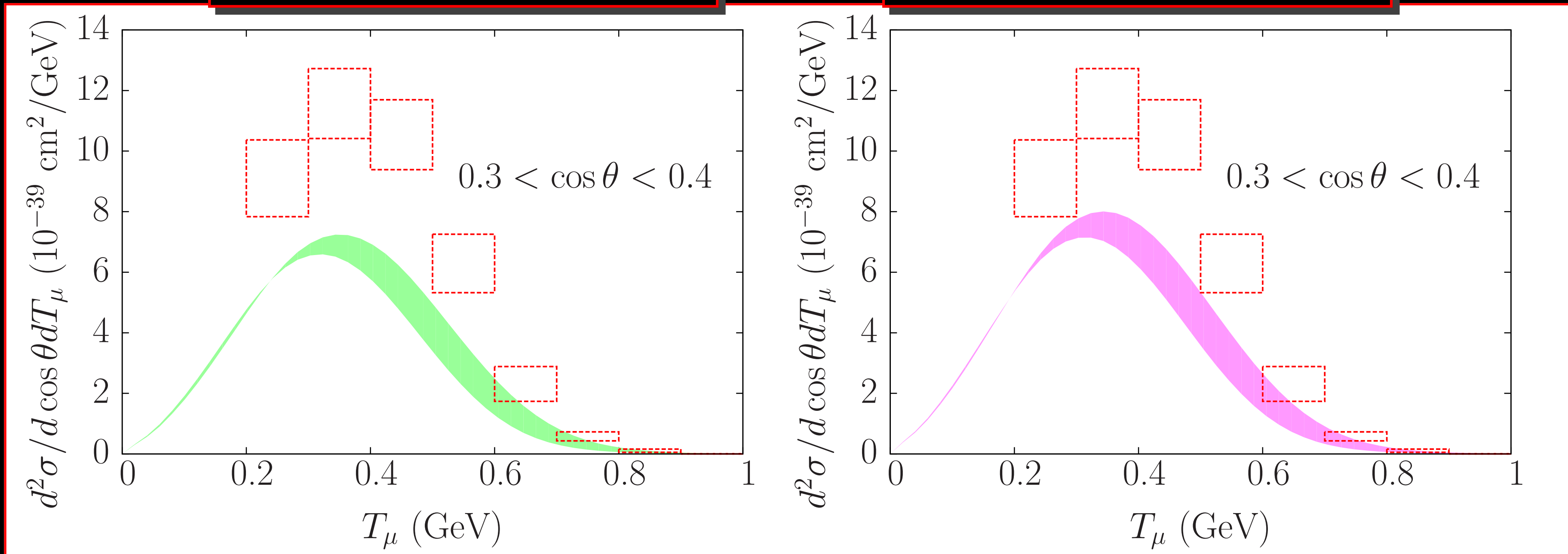

$0.2 < \cos\theta < 0.3$

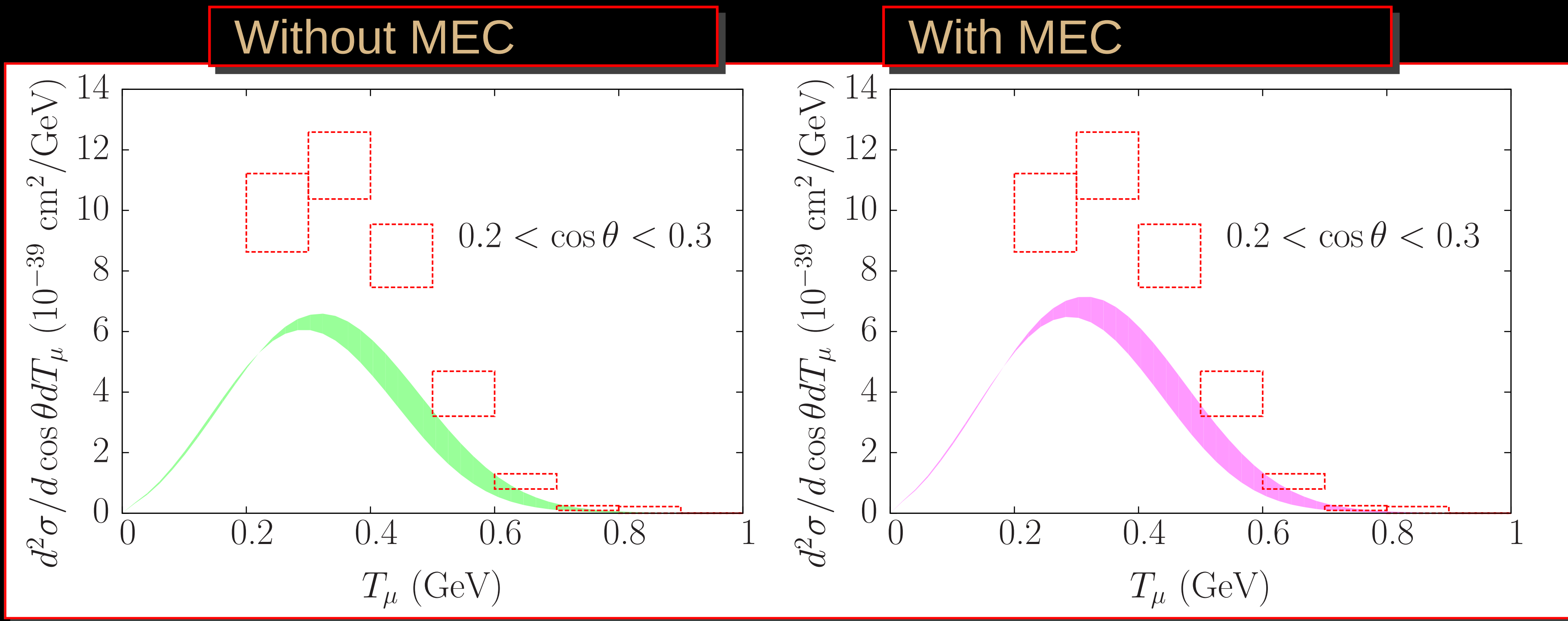

SuSA. Versus the scattering angle

Without MEC

With MEC

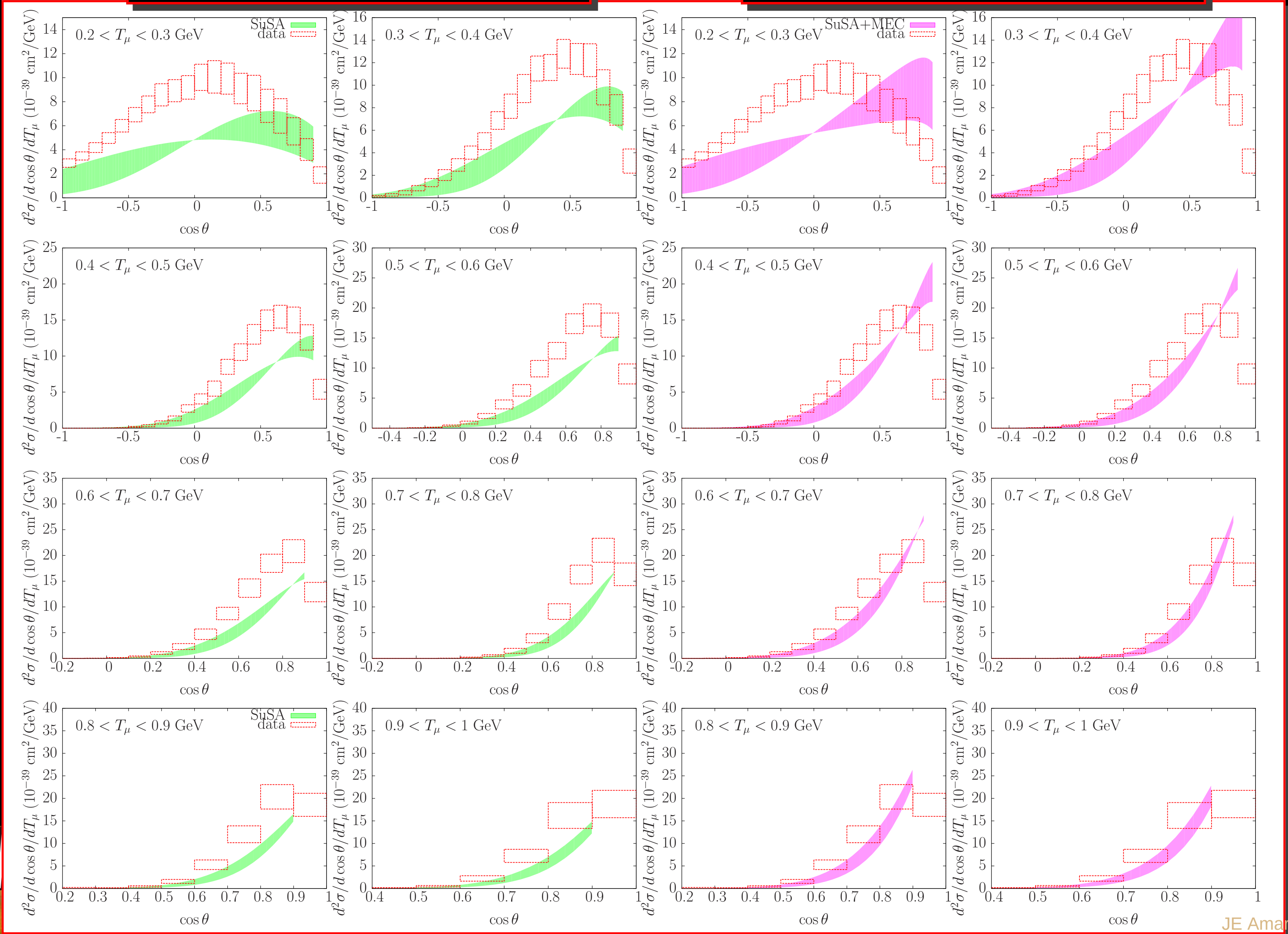

Conclusions and improvements of the model

- Strict SuSA predictions for (ν_μ, μ) QE x-section show a systematic discrepancy between data and theory
- SuSA+ MEC(2p-2h) yields results compatible with data for $\theta < 50^{\rm o}$, but lie below data
- There are indications from RMF studies and from (e, e') data that the vector transverse response should be enhanced over the strict SuSA [Caballero et al, PLB 653 (2007)]
- Contributions of nuclear strong correlations to 2p-2h excitations also enhance the cross section in RFG [Amaro et al., PRC 82 (2010)]

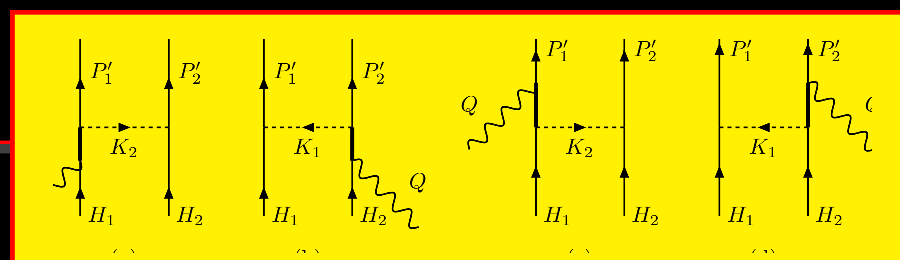

SuSA predictions for QE ν-nucleus scattering

THANK YOU

J. Enrique Amaro